

***In vitro* modulatory effects of fermented rooibos extract
(*Aspalathus linearis*) against ethanol-induced effects on the
mouse blood-brain barrier**

Shireen Mentor



*A thesis submitted in fulfilment of the requirements for the degree of
Magister Scientiae in the Department of Medical Biosciences,
University of the Western Cape.*

Supervisor: Prof. D. Fisher

Co-supervisors: Dr K. Gamielien

Dr F. Cummings

November 2014

DECLARATION

I, **Shireen Mentor**, declare that the ***In vitro* modulatory effects of fermented rooibos extract (*Aspalathus linearis*) against ethanol-induced effects on the mouse blood-brain barrier** is my own work, that it has not been submitted before for any degree or assessment in any other university, and that all the sources I have used or quoted have been indicated and acknowledged by means of complete references.

Shireen Mentor:



November 2014

Date Signed :

ACKNOWLEDGMENTS

To God, for the unmerited grace that has taught me to always remain teachable.

To my mother, Alice Mentor, for being a great example of compassion and perseverance.

Much gratitude is paid to my supervisor, Prof. D. Fisher, for his academic support and relentless reminders to take ownership of my potential, always reminding me to remain inquisitive and decisive.

To my co-supervisor, Dr K. Gamieldien for reminding me to always “empty my cup” and for her ability to motivate and inspire greatness.

To Dr. F. Cummings for meticulously guiding me and for willingly sharing his knowledge and expertise in the field of electron microscopy.

To the Department of Medical Biosciences and the Neurobiology group, at the University of the Western Cape, for being given the opportunity to grow within an environment that has helped me realize my potential.

To the Antioxidant Research Laboratory, at the Cape Peninsula University of Technology (CPUT) for the chemical analysis of the fermented rooibos extract, performed by Mr F. Rautenbach, under the supervision of Prof. J.L. Marnewick.

To the National Research Foundation (NRF), for financial support.

To my Grade 10 English teacher, Mr M. Matthews who professed that I will one day become a “mad scientist!!!”

ABSTRACT

Alcohol abuse is a growing crisis within South Africa, with severe health and socio-economic implications. Alcohol compromises the function of the blood-brain barrier (BBB), and thus its ability to regulate the homeostatic environment of the CNS is interrupted. In this study, an *in vitro* model of the BBB was utilized to study the effects of selected concentrations of alcohol (25mM-200mM) and the ameliorating effects of fermented rooibos (*Aspalathus linearis*) (0.003125%-1%), in an attempt to reverse the harmful oxidative effects of alcohol. The literature clearly states that alcohol (ethanol) compromises the BBB by reactive oxygen species (ROS) production and, therefore, rooibos, a shrub high in antioxidants and widely utilized nationally, was added to alcohol-exposed mouse brain endothelial (bEnd5) cells with the view to reverse the alcohol-induced effects on the BBB model.

Alcohol-treated (25mM-400mM) bEnd5 monolayers expressed no toxicity, however, cell numbers were significantly suppressed ($P < 0.0274$). To validate this finding, the activity of the mitochondria was investigated in order to understand if the cell's metabolism was related to the decrease in cell division. Results showed that for both acute and chronic exposure there was a decrease in mitochondrial activity (MA) for a period of 24-48 hours, thereafter, the MA of the bEnd5 cells returned to normality. However, in experiments which chronically (600mM and 800mM) exposed cells to alcohol over a period of 96 hours, MA was suppressed and did not return to normal.

Fermented rooibos caused a biphasic response to cellular proliferation at 24-72 hours, where the lower concentrations (0.0625-0.125 %) caused an increase in cellular proliferation and the higher concentrations (0.5-1%) resulted in a relative decrease in cellular proliferation. The long-term effect, after acute exposure, however, resulted in cell suppression at 96 hours ($P < 0.0073$). With respect to the MA, bEnd5 cells exposed to fermented rooibos showed that lower concentrations (0.003125-0.0125%) were suppressed at 24 hours and was elevated at 48 hours and 96 hours for all concentrations. The exception being the highest concentration (0.1%), which showed a depression in MA ($P < 0.05$). Treating cells with both alcohol and rooibos, resulted in exacerbated suppressing of the MA.

The physiological function of the BBB model was investigated by monitoring the permeability using transendothelial electrical resistance (TEER) studies and the *in vitro* model used in this study was endorsed for the first time using high resolution scanning electron microscopy. TEER indicated incidental changes in the permeability, only at 24 hours, for both acute and chronic exposure to alcohol and rooibos.

A novel finding, within this study, was the increase in electrical resistance across the formation of the cell monolayer, after treatment with alcohol. The data lead to the hypothesis for the effect of ROS on resistivity and provides a rationale to explain the effects of combinatory treatments that were expected to ameliorate the negative effect of alcohol, however, this study showed synergistically negative effects on the bEnd5 cells.

In summary the main findings in this study were: (a) alcohol was not toxic on bEnd5 cells, (b) alcohol increased the permeability across monolayers of bEnd5 cells and (c) rooibos did not significantly reverse the ROS-induced effects of alcohol, but exacerbated the effects. Rooibos treatment caused the following: (i) biphasic effect on cellular proliferation, (ii) an increase in MA, and (iii) a cyclic effect in TEER studies.

Key words: Blood brain barrier; TEER, alcohol, rooibos, mitochondrial activity, viability, proliferation.

November 2014



LIST OF SELECTED ABBREVIATIONS

Å	Angstrom
AAE	Ascorbic acid equivalents
AAPH	2,2'-Azobis (2-methylpropionamide)
ABC	ATP-binding cassette transporters
ABTS	2,2'-Azino-bis (3-ethylbenzothiazoline-6-sulfonic acid)
ABTS ⁺	ABTS radical
ADH	Alcohol dehydrogenase
AJ	Adherens junction
ALDH	Aldehyde dehydrogenase
ALDH2	Aldehyde dehydrogenase 2
<i>A.linearis</i>	<i>Aspalathus linearis</i>
AO	antioxidant
ATCC	American type culture collection
ATP	Adenosine triphosphate
AUC	Area under the sample curve
AVD	Apoptotic volume decrease
AWA	Acetone/water/acetic acid

BA	Bioavailability
BAC	Blood alcohol concentration
BALB	Albino laboratory bred strain of house mouse
β-PE	Beta fuorescein
BBB	Blood-brain barrier
BBEC	Bovine brain endothelial cell
BBMEC	Bovine brain microvascular endothelial cell
bEnd5	Mouse brain endothelium
BMVEC	Brain microvascular endothelial cell
BV	Blood vessel
CE	Catechin equivalents
CIDP	Demyelinating polyradiculoneuropathy
CNS	Central nervous system
CO ₂	Carbon dioxide
C ₂₀ H ₁₀ Na ₂ O ₅	Fluorescein sodium salt
CP	Critical point
CPD	Critical point dryer
CS	Chondroitin sulfate
CSF	Cerebrospinal fluid

CT	Connective tissue
Ctrl	control
CYP2E1	Cytochrome P450
Da	Dalton
dH ₂ O	distilled water
ddH ₂ O	double distilled water
DMACA	4-Dimethylamino-cinnamaldehyde
DMEM	Dulbecco's Modified Eagle's Media
DNA	Deoxyribnucleic acid
DOF	Depth of field
DPPH	2,2-diphenyl-1-picrylhydrazyl
EAE	Experimental allergic encephalomyelitis
EC	Endothelial cell
ELISA	Enzyme-Linked Immunosorbent Assay
ERS	Electrical Resistance System
EtOH	Ethanol
F-actin	Filamentous actin
FACS	Fuorescein-activated cell sorting
FAEE	Fatty acid ethyl ester

FAS	Fetal Alcohol Syndrome
FASD	Fetal Alcohol Spectrum Disorders
Fe ²⁺	Ferrous iron
Fe ³⁺	Ferric iron
FBS	Fetal Bovine Serum
FLK-1	Fetal liver Kinase-1
FRAP	Ferric Reducing Antioxidant Power
GAE	Gallic acid equivalents
GAG	Glycosaminoglycans
GC	Glucocorticoid
GFAP	Glial Fibrillary Acid Protein
G ₀	Quiescent/senescent phase in cell cycle
G ₁	Gap 1 check point in the cell cycle
G ₂	Pre-mitotic phase of cell cycle
HA	Hyaluronic acid
HC	Hydrocortisone
HS	Heparan Sulfate
H ₂ O ₂	Hydrogen peroxide
ICAM-1	Intercellular Adhesion Molecule-1

ICAM-2	Intercellular Adhesion Molecule-2
IL-6	Interleukin-6
JAM	Junctional Adhesion Molecule
kDa	kiloDalton
M	Mitosis
M	Molar
MA	Mitochondrial activity
mAU	milliabsorbance units
MBCEC	Mouse brain capillary endothelial cell
MDH	Mitochondrial dehydrogenous
MECA-32	Anti-mouse panendothelial cell antigen antibody
MeOH	Methanol
MEOS	Microsomal ethanol-oxidizing system
MLCK	Myosin light-chain kinase
MRC	Medical Research Council
n	sample number
NaCO ₃	Sodium carbonate
NAD ⁺	Nicotinamide adenine dinucleotide (oxidized)
NADH	Nicotinamide adenine dinucleotide (reduced)

NaH ₂ PO ₄ .H ₂ O	Sodium di-hydrogen orthophosphate-1-hydrate
Na ₂ HPO ₄ .2H ₂ O	Di-sodium hydrogen orthophosphate dehydrate
NEAA	Non-essential amino acid
NH ₃	Ammonia
ORAC	Oxygen Radical Absorbance Capacity
O ₂	Oxygen
PBCEC	Porcine brain capillary endothelial cell
PCA	Perchloric acid
PECAM-1	Platelet/Endothelial Cell Adhesion Molecule-1
pH	“Power” of hydrogen (scale for measuring acidity and basicity)
PLD	phospholipase D
pMBMEC	Primary mouse brain microvascular endothelial cell
P-value	Probability-value
QE	Quercetin equivalent
Redox	Reduction-oxidation
R _f	Fermented rooibos herbal extract
R _{fa}	Resistivity of fluid in apical compartment of bicameral model

R_{fb}	Resistivity of fluid in basolateral compartment of bicameral model
R_i	Resistance of insert membrane
R_{TJ}	Paracellular resistance of tight junctions
ROS	Reactive oxygen species
rpm	Revolutions per minute
RMCD	Randomly methylated beta-cyclodextrin
S	DNA synthesis phase of cell cycle
SA	South Africa
SARC	South African Rooibos Council
SEM	Scanning electron microscopy
SEM	Standard error of mean
SFM	Serum free media
TB	Trypan blue
TC	Tissue culture
TEAC	Trolox equivalent antioxidant capacity
TE	Trolox equivalents
TEER	Transendothelial electrical resistance
TGF- β	Tissue growth factor beta

TJ	Tight junction
TPTZ	Tripyridyl-triazine
TWSS	Total water soluble solids
V	Voltz
VCAM-1	Vascular cell adhesion molecule-1
VE-cadherin	Vascular Endothelial-cadherin
viz	Adverb for “namely”/ “that is to say”
vs	versus
v/v	volume per volume
WC	Western Cape
ZO-1	Zonula occludens-1
ZO-2	Zonula occludens-2
ZO-3	Zonula occludens-3
<	Less than symbol
Ω	Ohms

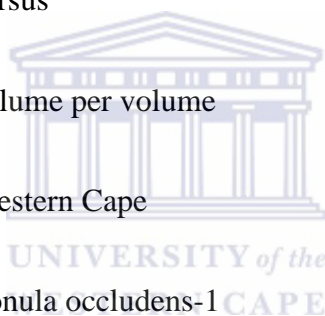
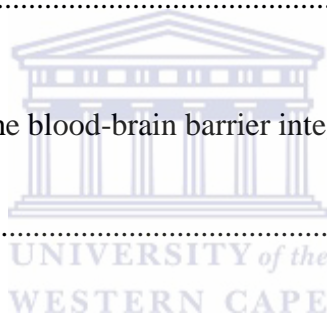


TABLE OF CONTENTS

DECLARATION.....	i
ACKNOWLEDGEMENTS.....	ii
ABSTRACT.....	iii
LIST OF SELECTED ABBREVIATIONS.....	vi
TABLE OF CONTENTS.....	xiv
LIST OF FIGURES.....	xxv
LIST OF TABLES.....	xxx
APPENDIX.....	xxxi
1. CHAPTER 1: LITERATURE REVIEW <i>of the</i>	1
1.1. Socio-economic impact of alcohol abuse- burden of disease.....	1
1.2. Maternal adverse effects of alcohol.....	4
1.2.1. Prenatal care.....	6
1.3. The chemistry of ethanol.....	8
1.3.1. Bioavailability of ethanol.....	9
1.4. The blood-brain barrier.....	10
1.4.1. The neurovascular unit.....	10
1.4.1.1. Brain endothelial cells.....	11
1.4.1.2. Astrocytes.....	11

1.4.1.3. The basal lamina.....	12
1.4.1.4. Pericytes.....	12
1.4.2. Protective properties of the blood-brain barrier.....	13
1.4.2.1. Protective surface structures of the endothelial cell membrane.....	14
1.4.3. Transport system across the blood-brain barrier.....	16
1.4.4. Mouse brain endothelial cell histology.....	18
1.4.5. Molecular basis for blood-brain barrier function.....	19
1.5. Establishing the immortalized mouse brain endothelial cell line.....	21
1.6. The proposed <i>in vitro</i> blood-brain barrier model.....	22
1.7. The <i>in vitro</i> blood-brain barrier model: Clinical problem.....	23
1.8. Physiological studies on the blood-brain barrier.....	24
1.8.1. Molecular studies.....	24
1.8.2. Permeability studies.....	25
1.9. Experimental model.....	26
1.9.1. Factors inducing cellular proliferation.....	26
1.9.2. Optimizing the cell monolayer using hydrocortisone as a blood-brain barrier enhancing glucocorticoid.....	27
1.10. Toxicological effects of Alcohol (Ethanol).....	29
1.10.1. Pertinent information on ethanol metabolism.....	29

1.10.2. Ethanol-induced pathology of the mitochondria.....	32
1.11. Rooibos - <i>Aspalathus linearis</i>	33
1.11.1. Fermentation of rooibos.....	34
1.11.2. Protective antioxidant properties of <i>Aspalathus linearis</i>	35
1.11.3. Polyphenols.....	38
1.11.4. Classification of polyphenols.....	39
1.11.5. Phenolic structure of aspalathin.....	40
1.11.6. Aspalathin.....	40
1.12. Antioxidants and the blood-brain barrier integrity.....	41
1.13. Problem statement.....	42
1.13.1. Rationale.....	43
1.14. Research aims and objectives.....	44
1.14.1. Aims.....	44
1.14.2. Objectives.....	45
1.15. Research question/ hypothesis.....	46
2. CHAPTER 2: MATERIALS AND METHODS.....	47
2.1. Preparation of an aqueous herbal infusion of <i>A.linearis</i>	47
2.2. Chemical analysis of fermented rooibos (<i>A.linearis</i>).....	48



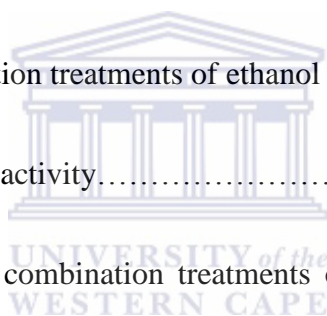
2.2.1. Measurement of polyphenols.....	48
2.2.1.1. Principle of polyphenolic measurements.....	48
2.2.1.2. Chemical requirements and sample handling for the quantification of polyphenols.....	49
2.2.1.3. Sample analysis.....	49
2.2.2. Ferric reducing antioxidant power assay.....	50
2.2.2.1. Principle of the Ferric reducing antioxidant power assay.....	50
2.2.2.2. Chemical requirements and sample handling for the FRAP assay.....	50
2.2.2.3. Sample analysis.....	51
2.2.3. Oxygen radical absorbance capacity assay.....	51
2.2.3.1. Principle of the oxygen radical absorbance capacity assay.....	51
2.2.3.2. Chemical requirements and sample handling for the ORAC assay.....	52
2.2.3.3. Sample analysis.....	53
2.2.4. ABTS (TEAC) radical cation scavenging assay.....	54
2.2.4.1. Principle of the ABTS (TEAC) assay.....	54
2.2.4.2. Chemical requirements and sample handling for the ABTS (TEAC) assay.....	54
2.2.4.3. Sample analysis.....	55
2.2.5. Measurement of flavonols.....	55

2.2.5.1. Principle of flavonol measurements.....	55
2.2.5.2. Chemical requirements and sample handling for quantifying flavonols.....	55
2.2.5.3. Sample analysis.....	56
2.2.6. Measurement of flavanols.....	56
2.2.6.1. Principle of flavanol measurements.....	56
2.2.6.2. Chemical requirements and sample handling for quantifying flavanols.....	57
2.2.6.3. Sample analysis.....	57
2.3. <i>In vitro</i> analysis of the bEnd5 cells.....	58
2.3.1. Bio-reagents.....	58
2.3.2. The immortalized mouse brain endothelial cell line.....	59
2.3.3. Tissue culturing of bEnd5 cells.....	59
2.3.3.1. Operating principle.....	59
2.3.3.2. Tissue culture procedure.....	60
2.4. Trypan blue assay.....	61
2.4.1. Operating principle.....	61
2.4.2. Experimental treatments.....	62
2.4.2.1. Treatment with ethanol and fermented rooibos (<i>A.linearis</i>).....	62

2.4.2.2. Cell count using the Neubauer hemocytometer.....	63
2.5. XTT cell viability assay.....	64
2.5.1. Operating principle.....	64
2.5.2. Experimental treatments.....	65
2.5.2.1. Treatment with ethanol and fermented rooibos (<i>A.linearis</i>).....	65
2.6. Transendothelial electrical resistance across a bEnd5 cell monolayer.....	66
2.6.1. Operating principle.....	66
2.6.2. Experimental model of the blood-brain barrier.....	66
2.6.3. The extracellular insert membrane.....	67
2.6.4. Seeding for TEER.....	68
2.6.5. Measuring the resistance across a bEnd5 cell monolayer.....	68
2.6.5.1. True resistance across an insert membrane.....	69
2.7. Optimization of TEER and experimental treatments.....	69
2.7.1. Optimization of TEER using hydrocortisone.....	69
2.7.2. Effect of ethanol on TEER.....	70
2.7.3. Effect of fermented rooibos (<i>A.linearis</i>) on TEER.....	71
2.7.4. Effect of combination treatments of ethanol and fermented rooibos (<i>A.linearis</i>) on TEER.....	71
2.8. Electron microscopy.....	72

2.8.1. Scanning Electron Microscopy.....	72
2.8.2. Operating principle.....	72
2.8.3. Resolution and Depth of Field.....	74
2.8.4. Factors affecting resolution and DOF.....	75
2.8.5. Protocol for imaging a biological specimen	
using high resolution SEM.....	76
2.8.5.1. Chemical fixation.....	76
2.8.5.2. Critical point drying.....	78
2.8.5.3. Sputter coating and SEM imaging.....	79
2.9. Statistical analysis.....	80
3. CHAPTER 3: RESULTS.....	81
3.1. Chemical analysis and determination of antioxidant capacity of fermented	
rooibos (<i>A.linearis</i>) herbal tea.....	81
3.2. Trypan blue assay.....	84
3.2.1. Effect of acute ethanol exposure on live cell count.....	84
3.2.2. The toxic effect of acute ethanol exposure on bEnd5 cells.....	85
3.2.3. Effect of acute fermented rooibos exposure on live cell count.....	86
3.2.4. The toxic effect of acute fermented rooibos exposure on bEnd5 cells.....	87

3.3 Effect of selected compounds on mitochondrial activity using the reduced formazan (XTT) assay.....	88
3.3.1. Effect of acute ethanol exposure on bEnd5 mitochondrial activity.....	88
3.3.2. Effect of chronic ethanol exposure on bEnd5 mitochondrial activity.....	89
3.3.3. Effect of acute fermented rooibos exposure on bEnd5 mitochondrial activity.....	91
3.3.4. Effect of chronic fermented rooibos exposure on bEnd5 mitochondrial activity.....	92
3.3.5. Effect of combination treatments of ethanol with fermented rooibos on bEnd5 mitochondrial activity.....	93
3.3.5.1. Effect of acute combination treatments of ethanol with 0.05% fermented rooibos on bEnd5 mitochondrial activity.....	94
3.3.5.2. Effect of chronic combination treatments of ethanol with 0.05% fermented rooibos on bEnd5 mitochondrial activity.....	95
3.3.5.3. Effect of acute combination treatments of ethanol with 0.1% fermented rooibos on bEnd5 mitochondrial activity.....	97
3.3.5.4. Effect of chronic combination treatments of ethanol with 0.1% fermented rooibos on bEnd5 mitochondrial activity.....	98
3.4. Transendothelial electrical resistance.....	100



3.4.1. Effect of chronic exposure to ethanol and fermented rooibos on transendothelial electrical resistance.....100

3.4.1.1. Effect of chronic ethanol exposure on transendothelial electrical resistance.....100

3.4.1.2. Effect of chronic fermented rooibos exposure on transendothelial electrical resistance.....101

3.4.1.3. The effect of chronic exposure to ethanol in combination with 0.05% fermented rooibos on transendothelial electrical resistance..... 102

3.4.1.4. The effect of chronic exposure to ethanol in combination with 0.1% fermented rooibos on transendothelial electrical resistance..... 104

3.5. High resolution scanning electron microscopy.....105

3.5.1. Imaging cell confluence on a 12mm insert membrane.....105

4. CHAPTER 4: DISCUSSION.....113

4.1. Introduction: Importance of the blood-brain barrier integrity.....113

4.2. Chemical analysis of fermented rooibos.....115

4.3. Effect of ethanol on cellular proliferation and mitochondrial activity.....116

4.3.1. Effect of ethanol on cellular proliferation.....116

4.3.2. bEnd5 Mitochondrial activity as an indicator of cell viability.....118

4.3.2.1. Introduction: The role of the mitochondria.....118

4.3.3. The correlation between the effects of ethanol on bEnd5 mitochondrial activity and cellular proliferation.....119

4.4. Effect of fermented rooibos on cellular proliferation, mitochondrial activity and toxicity.....121

4.4.1. Effect of fermented rooibos on cellular proliferation.....121

4.4.2. Effect of rooibos -induced changes on bEnd5 mitochondrial activity.....122

4.4.3. Combinatory effect of ethanol and fermented rooibos on the mitochondrial activity.....123

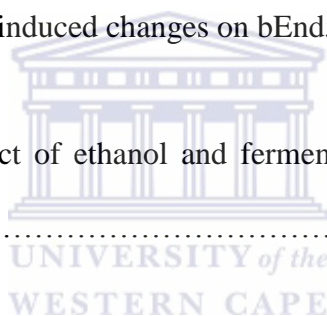
4.5 Endorsement of the BBB model.....125

4.5.1 The high resolution morphological characteristics of an endothelial cell monolayer.....125

4.5.2. Effect of cell density on characteristic cell-to-cell interaction: Comparison between high and low cell densities.....126

4.5.3. The basement membrane.....127

4.5.4. Shear stress and the glycocalyx.....128



4.5.5. Elucidating the paracellular space in the light of SEM: Tight junctions and adherens junctions.....130

4.6. Bioelectrical studies: Transendothelial electrical resistance.....132

4.6.1. Introduction: Effect of ethanol and fermented rooibos on transendothelial electrical resistance optimization of a monolayer.....132

4.6.2. Optimization of the monolayer.....132

4.6.3. The effect of ethanol on TEER.....134

4.6.4. Equivalent electrical circuit for TEER experiments.....135

4.6.4.1. True resistance of a monolayer = $R_{\text{experiment}} - R_{\text{blank}}$136

4.6.5. Effect of fermented rooibos on TEER.....137

4.6.6. Effect of ethanol and fermented rooibos in combination on TEER.....139

5. CHAPTER 5.....140

5.1. Conclusion.....140

5.2. Future perspectives.....141

6. CHAPTER 6.....142

6.1. References.....142

6.2. Web-based References.....170

APPENDIX A-F.....174

LIST OF FIGURES

CHAPTER 1:

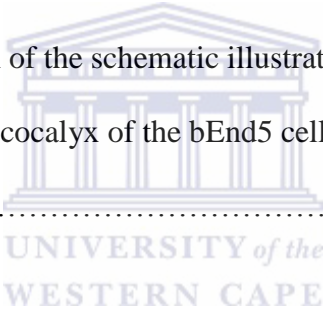
- Figure 1.** FASD as an umbrella concept (Thomas and Riley, 1998).....5
- Figure 2.** Chemical structure of EtOH
(http://medicaldictionary.thefreedictionary.com/_/viewer.aspx?path=dorland&name=formula_structural.jpg).....8
- Figure 3.** Schematic diagram of the anatomical basis of the neuro-vascular unit *in vivo* (Wilhelm et al., 2011).....13
- Figure 4.** Schematic diagram illustrating the physiological transport system across a typical brain EC monolayer (Ohtsuki and Terasaki, 2007).....16
- Figure 5.** Schematic diagram of the substances which traverse the BBB *in vivo* (Re et al., 2012).....16
- Figure 6.** Schematic diagram of a hypothetical BBB *in vitro* using the bicameral system (Siddiqui et al., 2011)26
- Figure 7.** Nonoxidative metabolic pathway for EtOH (Zakhari, 2006).....30
- Figure 8.** Oxidative metabolic pathways of EtOH in brain cells (Deitrich, 2006).....32
- Figure 9.** Polyphenolic profile
(http://www.frenchglory.com/polyphenols_classification.pdf).....39

Figure 10.	Basic chemical structure of aspalathin (http://www.chemspider.com/Chemical-Structure.26286888.html).....	40
Figure 11.	Antioxidant neutralization of ROS production (http://www.esc.rutgers.edu/publications/general/fs1065.htm)	42
CHAPTER 2:		
Figure12.	Schematic diagram of a bicameral chamber representing a confluent monolayer of the bEnd5 cells <i>in vitro</i> (http://www.pharmadirections.com/_blog/Formulation_Development_Blog/post/Bio-pharmaceutics_Classification_System_and_In-vitro_membrane_models/).....	66
Figure 13.	Schematic representation of the different signals that are generated upon interaction of the primary electron beam with the specimen surface (Yao and Wang, 2005).....	73
Figure 14.	Schematic representation of a scanning electron microscope column (Postek et al., 1980).....	73
Figure 15.	Illustration of the effects of working distance and aperture size on resolution and DOF (Cummings, 2006).....	76

CHAPTER 3:

- Figure 16.** Illustration of HPLC results illustrating polyphenols present in an R_f sample. Chromatographic analysis of the R_f sample generated a prevalent absorbance value of 16.024 mAU, confirming the presence of aspalathin.....83
- Figure 17.** 3.2.1 Effect of acute ethanol exposure on live cell count.....84
- Figure 18.** 3.2.3 Effect of acute fermented rooibos exposure on live cell count.....86
- Figure 19.** 3.3.1 Effect of acute ethanol exposure on bEnd5 mitochondrial activity.....88
- Figure 20.** 3.3.2 Effect of chronic ethanol exposure on bEnd5 mitochondrial activity.....89
- Figure 21.** 3.3.3 Effect of acute fermented rooibos exposure on bEnd5 mitochondrial activity.....91
- Figure 22.** 3.3.4 Effect of chronic fermented rooibos exposure on bEnd5 mitochondrial activity.....92
- Figure 23.** 3.3.5.1 Effect of acute combination treatments of ethanol with 0.05% fermented rooibos on bEnd5 mitochondrial activity.....94
- Figure 24.** 3.3.5.2 Effect of chronic combination treatments of ethanol with 0.05% fermented rooibos on bEnd5 mitochondrial activity.....95

Figure 25.	3.3.5.3 Effect of acute combination treatments of ethanol with 0.1% fermented rooibos on bEnd5 mitochondrial activity.....	97
Figure 26.	3.3.5.4 Effect of chronic combination treatments of ethanol with 0.1% fermented rooibos on bEnd5 mitochondrial activity.....	98
Figure 27.	3.4.1.1 Effect of chronic ethanol exposure on transendothelial electrical resistance.....	100
Figure 28.	3.4.1.2 Effect of chronic fermented rooibos exposure on transendothelial resistance.....	101
Figure 29.	3.4.1.3 The effect of chronic exposure to ethanol in combination with 0.05% fermented rooibos on transendothelial electrical resistance.....	102
Figure 30.	3.4.1.4 The effect of chronic exposure to ethanol in combination with 0.1% fermented rooibos on transendothelial electrical resistance	104
Figure 31.	Comparison of bEnd5 cell confluence. (A) Semi-confluent (20%) bEnd5 cells distally located (1×10^4 cells/well/insert) and (B) represented a confluent (100%) bEnd5 monolayer with cells in close proximity (1×10^6 cells/insert/well) grown on a 12mm diameter mixed cellulose insert.....	106
Figure 32.	100% Confluent bEnd5 cell monolayer seeded at a density of 1×10^6 cells/well/insert (insert=12mm diameter) after 24 hr exposure to DMEM-F12.....	107

Figure 33.	Establishment of the bEnd5 cell basement membrane after 24 hrs bEnd5 cells were grown in supplemented DMEM-F12 at a cell density of 1×10^4 cells on a 12mm mixed cellulose esters insert.....	107
Figure 34.	bEnd5 cell division in one cell grown on a mixed cellulose esters insert membrane.....	109
Figure 35.	Cell-to-cell protein interactions between adjacently located bEnd5 cells grown on a mixed cellulose ester insert membrane.....	110
Figure 36.	Cytoplasmic projections on the lateral border in the cleft between adjacent bEnd5 cells seeded at a density of 1×10^6 cells/well/insert.....	111
Figure 37.	Formation of the schematic illustration of an EC glycocalyx (Yao et al., 2007) (A) and the glycocalyx of the bEnd5 cell membrane surface <i>in vitro</i> (B).....	112
		
CHAPTER 4:		
Figure 38.	The micrograph in A. is a paracellular area between 2 cells and depicts the molecular interaction between two adjacent cells, SEM looks at the cell from a surface perspective (see XX on diagram A); B. is a schematic diagram of the tight junctional protein complexes between two adjacent cells (http://www.pharmacology.arizona.edu/images/faculty/davisfig2.gif).....	131
Figure 39.	Effective/true resistance of a monolayer using an equivalent circuit.....	136
Figure 40.	Directly proportional relationship between antioxidant (AO) concentration's and ROS production.....	138

LIST OF TABLES

Table 1.	Comparison between brain and peripheral endothelial cells (Reese and Karnovsky, 1967; Ballabh et al., 2004; Pekny et al., 1998; Begley, 2004).....	15
Table 2.	The composition of a typical cup of R _f (amount of flavonoids in aqueous extract of <i>A.linearis</i>) (mg/g ± SD) (Bramati et al., 2002).....	37
Table 3.	Detection of the maximum quantity of unchanged flavonoids within the plasma of volunteers (in nM) and % recovery rates of these respective flavonoids after the ingestion of 500ml of an aqueous extract of R _f (Breiter et al., 2011).....	38
Table 4.	Polyphenolic composition of an aqueous extract of fermented <i>A.linearis</i>	82
Table 5.	Effect of acute EtOH exposure on % toxicity using the Trypan blue assay.....	85
Table 6.	Effect of acute R _f exposure on % toxicity using the Trypan blue assay.....	87

APPENDIX

APPENDIX A:	174
Table 1. Breakdown of provincial drug related crime trends for the past 5 years (SAPS) (Modernisation programme, 2010).....	174
Table 2. Summary of FAS prevalence in various U.S. and selected foreign studies by methodology (May et al., 2001).....	175
APPENDIX B:	177
Table 1. Standard series of gallic acid prepared for the measurement of polyphenols.....	177
Table 2. Standard series of ascorbic acid prepared for the FRAP assay.....	177
Table 3. Standard series of Trolox prepared for the ORAC assay.....	178
Table 4. Standard series of Trolox prepared for the ABTS (TEAC) radical cation scavenging assay.....	178
Table 5. Standard series of quercetin prepared for the measurement of flavonols.....	179
Table 6. Standard series of the catechin prepared for the measurement of flavanols.....	179
Table 7. Plate layout for antioxidant assays (96-well plate).....	180

APPENDIX C:.....181

Table 1. Effect of acute exposure to selected concentrations of EtOH on bEnd5 live cell numbers, using the Trypan blue assay at selected time intervals (mean±SEM; n=5).....181

Table 2. Effect of acute exposure to selected concentrations of EtOH on bEnd5 mitochondrial activity, using the XTT assay at selected time intervals (mean±SEM; n=5).....182

Table 3. Effect of chronic exposure to selected concentrations of EtOH on bEnd5 mitochondrial activity, using the XTT assay at selected time intervals (mean±SEM; n=5).....183

Table 4. Effect of acute exposure to selected concentrations of R_f on bEnd5 live cell numbers, using the Trypan blue assay at selected time intervals (mean±SEM; n=5).....184

Table 5. Effect of acute exposure to selected concentrations of R_f on bEnd5 % live cell number, using the Trypan blue assay at selected time intervals (mean±SEM; n=5).....185

Table 6. Effect of acute exposure to selected R_f concentrations on bEnd5 mitochondrial activity, using the XTT assay at selected time intervals (mean±SEM; n=5).....186

Table 7. Effect of chronic exposure to selected R_f concentrations on bEnd5 mitochondrial activity, using the XTT assay at selected time intervals (mean±SEM; n=5).....187

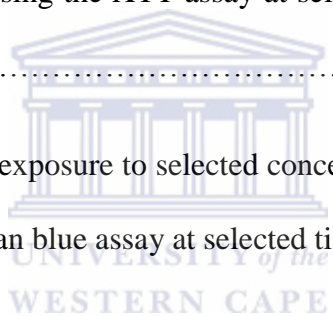


Table 8A. Effect of acute combination treatments of selected EtOH concentrations with 0.05% R _f concentrations on bEnd5 mitochondrial activity, using the XTT assay at selected time intervals (mean±SEM; n=5).....	188
Table 8B. Effect of chronic combination treatments of selected EtOH concentrations with 0.05% R _f concentrations on bEnd5 mitochondrial activity, using the XTT assay at selected time intervals (mean±SEM; n=5).....	189
Table 8C. Effect of acute combination treatments of selected EtOH concentrations with 0.1% R _f concentrations on bEnd5 mitochondrial activity, using the XTT assay at selected time intervals (mean±SEM; n=5).....	190
Table 8D. Effect of chronic combination treatments of selected EtOH concentrations with 0.1% R _f concentrations on bEnd5 mitochondrial activity, using the XTT assay at selected time intervals (mean±SEM; n=5).....	191
APPENDIX D:	192
Table 1. Effect of chronic exposure to selected concentrations of EtOH on bEnd5 cell monolayer permeability, using TEER measurements at selected time intervals (mean±SEM; n=4).....	192
Table 2. Effect of chronic exposure to selected concentrations of R _f on bEnd5 cell monolayer permeability, using TEER measurements at selected time intervals (mean±SEM; n=4).....	193
Table 3. Effect of chronic exposure to selected concentrations of EtOH in combination with 0.05% R _f on bEnd5 cell monolayer permeability, using TEER measurements at selected time intervals (mean±SEM; n=4).....	194

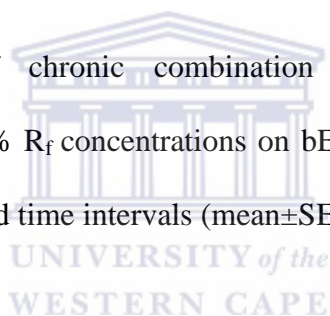


Table 4. Effect of chronic exposure to selected concentrations of EtOH in combination with 0.1% R _f on bEnd5 cell monolayer permeability, using TEER measurements at selected time intervals (mean±SEM; n=4).....	195
APPENDIX E:	196
1. Optimization of the TEER across the bEnd5 cell monolayer.	
1.1. Fig. 1 Effect of acute treatment with HC (500nM) on the TEER in the absence or presence of serum.....	196
1.2. Fig. 2 Effect of chronic treatment with HC (500nM) in the absence or presence of serum.....	197
APPENDIX F:	199
Cape Times Articles:	
“Cape’s rooibos dops pioneer new way to make a drink.”.....	199



CHAPTER 1: Literature Review

The chapter aims to provide substantial evidence on the national health concern related to alcohol abuse and to provide an overview on the adverse effects of alcohol in the disruption of the blood-brain barrier (BBB) integrity. Furthermore, the antioxidant (AO) properties of the indigenous South African herb, *Aspalathus linearis* (rooibos) as a potential therapeutic agent for the amelioration of the adverse effects of alcohol on the BBB is reviewed.

1.1 Socio-economic impact of alcohol abuse-burden of disease

Official provisional statistics reported findings on elevated substance abuse, within the Western Cape (WC) over the past 5 years. The South African police services has reported the province to have the highest number of cases in drug-related crime in 2008/2009 which was reported at 52 000 cases, four times higher than the Kwazulu Natal (KZN) province, with 1000 per 100 000 in the WC in comparison to 235 per 100 000 in KZN. The WC, therefore, accounts for almost half of the drug-related ills in South Africa (SA) (See **Appendix A, Table 1**). The modernisation programme (2010), conducted by the SA police services (SAPS), brought several pertinent factors to light. For example, the WC has one of the highest rates of fetal alcohol spectrum disorders (FASD) in the world (Modernisation programme, 2010). It has been reported that in WC, 75 out of every 1000 children suffered from fetal alcohol syndrome (FAS). This data is supported by FAS statistics for Cape Town, WC; which was reported as occurring in 1 per 282 live births (Modernisation programme, 2010).

The aforementioned data are supported by research conducted by Viljoen et al. (2005), of a community secondary primary school in SA. It was found that the rates of FAS being reported were of the highest in the overall global community, with 65.2-74.2 per 1.000 children. Comparatively, rates in the United States (U.S.) ranged between 0.33-2.2 per 1.000 children, making FAS prevalence, within a local community in SA, 33-148 times greater than estimates in the U.S. Within regional context, in the U.S, clinic-based African Americans of low socio-economic status from inner-city areas showed rates of 2.29 per 1000 children, while FAS rates within American Indian reservation communities very rarely exceeding 10 per 1000 children (Viljoen et al., 2005; Abel 1995; Abel, 1998; Abel and Sokol, 1987; May 2001) **(See Appendix A, Table 2.)**

Survey studies conducted by the Modernisation programme, (2010) have shown alcohol to be the most commonly abused substance in the WC province. Research conducted between the years 2002 to 2004, for annual prevalence studies and lifetime prevalence studies, found the WC to be the second highest (7.1%) for annual prevalence studies and the highest ranked (18.5%) for lifetime prevalence studies. In addition the province is reported to have the greatest incidence in alcohol abuse at 16%, while rural areas appear to have higher rates in binge drinking as opposed to urban regions (Modernisation programme, 2010).

Prevalence studies conducted in the Northern Cape and WC, SA, found incidences of FASD, in high risk areas, and according to a policy brief on FASD in Cape Town, SA, numbers reached as high as 119 per 1000 children (Modernisation programme, 2010; Policy brief on FASD, 2008).

According to the FASD policy brief, (2008) farm-based women, in the WC, are at higher risk of being affected by alcohol exposure than their urban counterparts. Despite the governmental measures to minimize possible alcohol misuse by women and children, researched evidence has shown that cheap wine sold on the market contains unacceptable levels of chemical contaminants such as: mercury, phthalates, and ochratoxin. The addition of a combination of these chemicals to alcohol in wine may exacerbate the damage observed in the developing fetus (Modernisation programme, 2010).

The increase in FASD in the WC, in particular, made it important to characterize and classify vulnerable groups, such as women at risk of alcohol exposure during pregnancy. In support of the national health system in SA, the Medical Research Council (MRC) has established the Burden of Disease and The Alcohol and Drug Abuse Unit. The primary aims of these units were to incorporate drug discovery tools for developing drug treatments and the integration of African natural products. According to these units, national statistics for FAS for the year 2000 estimated the incidence rates to range from 11.8 per 1000 births to 103 per 1000 births. The estimated national incidence rate is 14 per 1000 births. This figure is based on a FAS incidence of 11.8 per 1000 births occurring in 92% births in the year 2000 in SA and is contrasted against the highest incidences of 40 per 1000 in 8% births occurring in the coloured population (Schneider et al., 2007).

1.2 Maternal adverse effects of alcohol

Alcohol is characterized as a teratogen and as a result, it has the ability to induce abnormal prenatal development by exerting its effects on the biological system (Hannigan, 1996; Tsai et al., 2007). It readily crosses the placenta, resulting in blood alcohol levels of the fetus reaching levels similar to that of its mother. The degree to which a developing fetus is affected as a result of alcohol exposure depends on a range of factors such as: time, pattern, socio-economic status and the dose (the absolute amount of alcohol consumed) (Brocardo et al., 2011; Gil-Mohapel et al., 2010; Hannigan, 1996; Tsai et al., 2007).

Excessive use of alcohol damages most, if not all bodily tissues, and may result in an array of abnormalities, including fetal origins of adult disease which will progress and become a major public health concern. In the context of this study, at issue, is the damage of cells which cannot recover from this alcohol insult, causing long-term injury to the brain tissue, impacting on children's ability to learn and free themselves from social shackles.

Legalistic measures are being implemented to create awareness amongst the general population by the incorporation of warning labels on alcoholic beverages, informing the consumer about the deleterious effects of alcohol on the development of the fetus. Such measures are significant, since it has been shown that women, who are inclined to excessive drinking habits during pregnancy, place themselves at higher risk of giving birth to children with alcohol-associated deficits, as opposed to women who are pregnant and are not abusing alcohol (Thomas and Riley, 1998).

Chronic maternal drinking results in a cluster of characteristic anomalies termed FASD (Thomas and Riley, 1998).

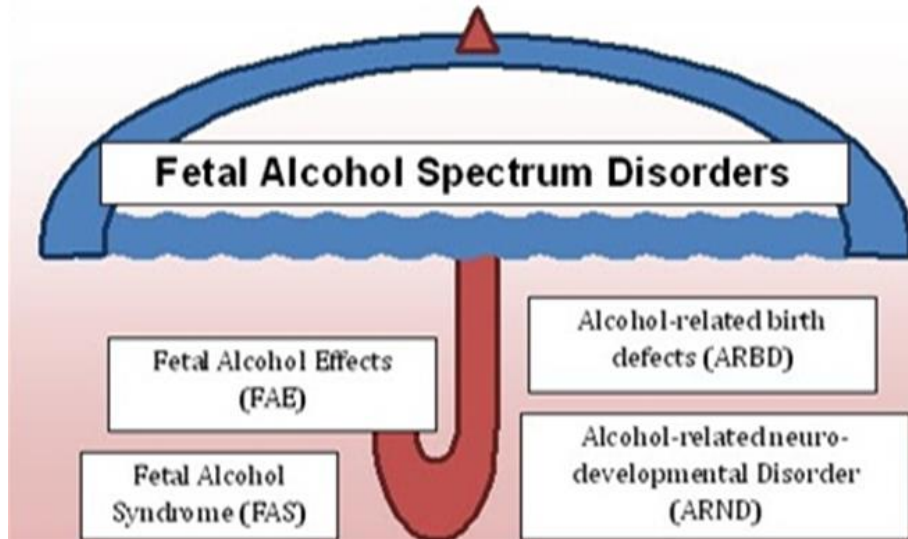


Figure 1. FASD as an umbrella concept (Thomas and Riley, 1998)

FASD is a broad concept incorporating an array of permanent pathological conditions within the developing fetus as a result of maternal alcohol exposure. It is one of the most common preventable causes of developmental disability and is, to date, one of the most critical public health concerns in SA (Floyd et al., 2007).

FAS, a subset of FASD, was found to be the most severe condition, occurring upon the exposure of alcohol to the developing fetus, *in utero*. FAS is associated with a pattern of cranio-facial dysmorphologies that results from alcohol-induced damage, during the formation of the facial bones, growth retardation and central nervous system (CNS) anomalies. Symptoms also include: an abnormally small head (microcephaly) and behavioral problems, such as attention deficits, hyperactivity, motor dysfunction, mental retardation and learning and social skills deficits. (Brocardo et al., 2011; Manning and Hoyme, 2007; Thomas and Riley, 1998, Gil-

Mohapel et al., 2010). These physical anomalies are said to be closely related to intelligence quotient (IQ) and development (Viljoen et al., 2005).

1.2.1 Prenatal care

Women, who have acquired insufficient information regarding prenatal care, are prone to inadequate practicing of such prenatal care (Salihu, et al., 2011). Maternal consumption of alcohol, involves the entry of alcohol into the mothers' bloodstream and subsequent circulating directly to the fetus. The developing fetus has a lower metabolic rate than an adult, causing the half-life exposure to alcohol in the blood to occur over a longer period of time. Alcohol has the ability to kill off brain cells and subsequently retard primordial cell growth as the brain is very susceptible to the alcohol during gestation (Floyd et al., 2007). Alcohol has been found to contribute to an array of conditions; such as the development of vascular lesions leading to adverse pregnancy outcomes as it has the ability to readily cross the placenta, causing dose-dependent placental vasoconstriction and decrease in placental weight (Khong, 2004; Burd et al., 2007; Salihu et al., 2011).

Prenatal alcohol exposure (PAE) has also been shown to increase oxidative stress in developing organs, including the brain. Brief exposure to alcohol during gestation is able to produce an imbalance in the brains intracellular reduction-oxidation (redox) state (Brocardo et al., 2011; Dong et al., 2010). The pattern of exposure, developmental timing of the exposure, epigenetics, maternal characteristics, and synergistic reactions with other drugs (Riley and McGee, 2005) are associated with determining the nature and the extent of the effects of PAE (Rendall-Mkosi et al., 2008).

Within the context of the above, research on animals has demonstrated that the times prior to and after pregnancy are both critical periods for alcohol exposure. Paternal and maternal alcohol consumption, occurring even before pregnancy and alcohol consumption by lactating mothers will influence the health of the offspring (Hannigan, 1996).

Buske, (2013) investigated the effects of embryonic alcohol exposure; in order to better elucidate the cause of FASD was conducted on the eggs of the zebrafish (*Danio rerio*). The alcohol was administered in a petridish, containing the *D. rerio* eggs and system water, as these eggs are able to develop externally from its mother. The research findings further validated that minute amounts of alcohol can penetrate the chorion. The alcohol doses used in the study ranged from as small as 0-1% v/v of which only 1/30th was able to penetrate the chorion (Fernandes and Gerlai 2009). Behavioral changes were evident within the embryonic *D. rerio* exposed to EtOH, without finding any morphological changes in the phenotype of the brain itself. A single treatment with the alcohol, at low concentrations, showed changes in the social habits of the *D. rerio*. No real distinction could be made between the alcohol groups. When compared to controls, however, the whole brains of alcohol treated *D. rerio* were reduced in comparison to the controls, demonstrating reduced levels of dopamine and serotonin, two vital neurotransmitters associated with social behaviour (Buske, 2013; Fernandes and Gerlai, 2009).

1.3 The chemistry of ethanol

Alcohol is described as a compound composed of carbon, hydrogen and oxygen. The three common alcohols are methyl alcohol (methanol/MeOH), isopropyl alcohol (isopropanol) and ethyl alcohol (ethanol/EtOH). All alcohols have similar structure containing an hydroxyl group, "OH", attached to a carbon molecule (Brick, 2005).

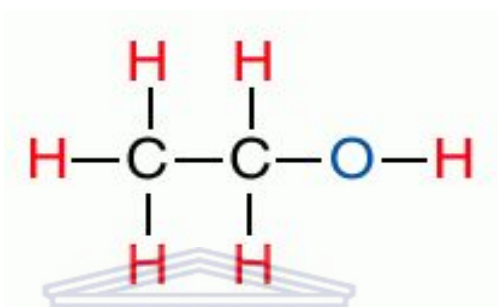


Figure 2. Chemical structure of EtOH (http://medical-dictionary.thefreedictionary.com/_/viewer.aspx?path=dorland&name=formula_structural.jpg)

EtOH or grain alcohol, which is the subject of this research, has a melting point of -114°C , boils at 78.5°C , with a density of 0.789 g/mL at 20°C and a molecular weight of 46.07 g/mol . It has a vapour pressure of 57.3 hPa at 20°C and a flash point of $13-14^{\circ}\text{C}$ (Li et al., 2005; OECD SIDS, 2004). EtOH, is the form of alcohol found in alcoholic beverages consumed by many people and will be referred to as EtOH in the text.

1.3.1 Bioavailability of ethanol

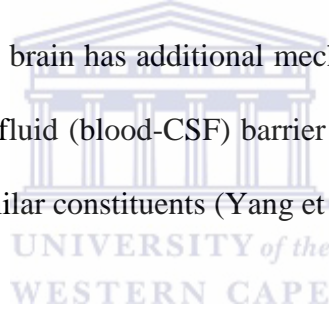
The bioavailability (BA) refers to the availability of a drug substance in the nervous system, which refers to its ability to cross over into the BBB (Hoheisel et al., 1998). Irrespective of exogenous alcohol consumption, it is also naturally found within the body. Its' endogenous presence is due to the metabolism of intestinal microflora, producing blood alcohol concentrations (BACs) of between 0.062mg/L to 0.73mg/L (Sprung et al.,1981; OECD SIDS, 2004).

EtOH levels in the brain are difficult to measure, therefore, BACs are used to assess the degree of intoxication. Most people show measurable mental impairments at 0.05% ($\pm 8.6\text{mM}$) blood alcohol. Above 0.5% (86mM) the breathing center of the brain or the heart rate is suppressed, which could result in death and according to the BAC laws implemented by the Center for Public Health Excellence (Killoran et al., 2010), there exists strong evidence that any one person's ability to drive is impaired if they have any trace of alcohol in their blood system. An individual with BAC of between 0.02% (3.4mM) and 0.05% (8.6mM) has greater risk of dying in a vehicle accident as opposed to an individual who has not consumed alcohol (Killoran et al., 2010). BACs, even after moderate consumption of alcohol (2-3 drinks/day) (International Drinking Guidelines, 2010), are considered to fall within the range of 0.046% (8mM) and 0.092% (15.8mM). The normal blood alcohol range which people have consumed is between 10-20mM (Zakhari, 2006). In addition, BAC's of chronic alcoholics are able to reach 50mM (Dietrich and Harris, 1996). Based on the aforementioned data, it can be deduced that the physiologically relevant levels of alcohol fall within the range of 0-50mM (Barnes and Singletary, 2000; Dietrich and

Harris, 1996). Anything above these values would be considered supraphysiological concentrations of alcohol (Cofan et al., 2000).

1.4 The blood-brain barrier

The blood-brain barrier (BBB) is described as being the interface regulating the exchange of substances between cerebral microvasculature and brain parenchymal tissue, and, in so doing, maintaining homeostasis of the CNS (Gumbleton and Audus 2001; Wilhelm et al., 2011; Cardoso et al., 2010). This is crucial for the functioning of the neurons of the CNS in that a change in the homeostatic milieu of the brain microenvironment could cause impaired thought processing and motor function. In addition to the BBB, the brain has additional mechanisms of defense. These include the blood cerebrospinal fluid (blood-CSF) barrier and the arachnoid barrier with all three barriers having similar constituents (Yang et al., 2007; Cardoso et al., 2010).



1.4.1 The neurovascular unit

The establishment and maintenance of the BBB is supported by a complex cellular system denoted as the neuro-vascular unit (Weiss et al., 2008). The principle cellular components are: brain microvascular endothelial cells (BMVECs), which are ensheathed by tubular astrocytic end-feet (Janzer, 1993; Yang et al., 2007; Wilhelm et al., 2011). Other important cellular constituents, which contribute the neuro-vascular unit and subsequent structural integrity of the BBB, include pericytes, perivascular microglia, the basal lamina, proteins and cytoskeletal elements (Yang et al., 2007; Cardoso et al., 2010).

1.4.1.1 Brain endothelial cells

The brain capillary endothelium forms the anatomical basis of the BBB and is comprised of brain endothelial cells (ECs). These cells lack fenestrations and have extensively distributed intercellular, protein tight junction (TJ) complexes and minimal pinocytosis. The brain EC TJs limit the paracellular transport of an array of hydrophilic molecule across the BBB (Ballabh et al., 2004) and, therefore, possesses properties which accomplish barrier functions between both the apical and luminal interstitium (See Fig 3.). This barrier ensures a chemically stable brain environment, with respect to vertebrates (Weidenfeller et al., 2005; Cardoso et al., 2010). This is crucial for the functioning of the neurons of the CNS.

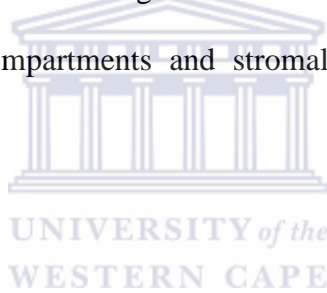


1.4.1.2 Astrocytes

The astrocytes, which are extended, foot-like projections, ensheath the cerebral capillary endothelial vessels and play an important role by inducing the expression of barrier specific properties in ECs (Yang et al., 2007). During development, astrocytes modulate angiogenesis and endothelial TJ formation by releasing growth and neurotrophic factors and in an adult brain participates in maintaining BBB integrity (Zhao et al., 2006). In addition the astrocyte makes provision for essential modulatory factors such as tissue growth factor beta (TGF- β), interleukin-6 (IL-6), and glial fibrillary acidic protein (GFAP). Astrocytes with insufficient GFAP are reported to have an inability in enhancing BBB properties (Pekny et al., 1998; Wilhelm et al., 2011). Thus, astrocytes' role is collective, since it is involved in the induction, maintenance and repair of the BBB and in the angiogenesis of the brain microvasculature (Janzer, 1993; Weiss et al., 2008).

1.4.1.3 The basal lamina

In vivo, the EC's are orientated to sit on a base known as the basement membrane, also referred to as the basal lamina. This membrane consists of three layers comprised of a complexity of proteins. The ECs produce one layer made up of laminin 4 and 5, the second layer derived by the astrocytes, containing laminin 1 and 2; and the middle layer which contains collagen type IV. Other complex proteins include fibronectin and heparin sulfate (HS) proteoglycans, found within the basement membrane of the brain (Weiss et al., 2008). The basement membrane is essentially a product of the epithelium and its underlying stroma. The stromal factors serve to differentiate the regulated function of the cell as well as provide a barrier between cell compartments and stromal compartments (Freshney et al., 2002).



1.4.1.4 Pericytes

Embedded between the basement membrane and the EC membrane are pericytes. The pericyte covers an estimated 22-32% of the brain endothelium. Its role is to regulate EC proliferation, angiogenesis and inflammatory processes and for the synthesis of most elements of the basement membrane (a considerable amount of proteoglycans) (Dore-Duffy, 2008, Cardoso et al., 2010). Without the pericyte the brain will undergo various alterations in its normal functioning, resulting in abnormal vasculogenesis, endothelial hyperplasia and increased permeability (Armulik et al., 2010).

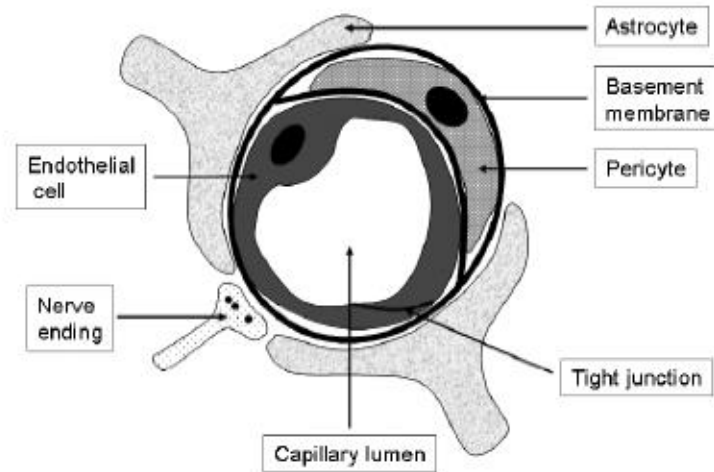


Figure 3. Schematic diagram of the anatomical basis of the neuro-vascular unit *in vivo* (Wilhelm et al., 2011)

1.4.2 Protective properties of the blood-brain barrier

The BBB serves as protection of the brain from an array of toxic substances within the circulatory milieu. It also affects selective transport and modulates blood and/or brain borne substances (Ribatti et al., 2006).

The BBB is comprised of four different restrictive barriers, which enable it to regulate the movement of foreign substances: (1) the first protective barrier is the paracellular restriction provided by the endothelial junctions, such as the TJs and the adherens junctions (AJs), which assists in TJ formation. This barrier prevents the movement of water soluble compounds between adjacent ECs', (2) the transcellular barrier, which serves to inhibit cytoplasmic transport of substances, is characterized by a low rate of transcytosis and endocytosis, (3) the enzymatic barrier, comprised of an array of enzymes such as: acetylcholinesterase, alkaline phosphatase, gamma glutamyl transpeptidase, monoamine oxidase and a variety of other drug metabolizing enzymes. The last protective measure of the BBB is the EC membrane transporters, which are efflux transporters serving as a means to pump drugs out of

the CNS, namely: the ATP-binding cassette (ABC) transporters: ABC1 (P-glycoprotein)/ BCRP, ABCC1, ABCC4 and ABCG2 (Wilhelm et al., 2011). These efflux protein transporters are abundant and highly expressed in the luminal compartment of the EC (Passeleu-LeBourdonnec et al., 2013) (See Fig 4 and Fig 5).

The BBB is, therefore, impenetrable by hydrophilic molecules, as well as, hydrophobic low molecular weight organic solutes, demonstrating restrictive properties of the BBB which inhibit the crossing over of foreign molecules into the CNS (Ballabh et al., 2004; Omid et al., 2003).

1.4.2.1 Protective surface structures of the endothelial cell membrane

The cell membrane carbohydrates make up approximately 3% of the cell membrane weight (Martini, 2006). Based on the literature, the cell membrane surface of the brain EC cells presents with a network of structures. These structures appear to span the entire surface of the EC. The EC membrane comprises of a diversity of membrane bound macromolecules. The carbohydrate proteins of these molecules have been shown to extend toward the outer surface (luminal) of the cell membrane establishing the structure known as the glycocalyx (Weinbaum et al., 2007). The glycocalyx is associated with transport properties which influences the flux of molecules, sized between water (approximately 3Å) and molecules the size of albumin, which equates to 69,000 Daltons (Da). The glycocalyx is, however, unable to regulate permeability in the event of TJs being compromised, due to the size of the junctions, thus, permeability as a result of the glycocalyx structure is little to none. Solutes which traverse this layer are usually much smaller than its fiber spacing (Tarbell et al., 2010).

The features of the brain ECs compared to the peripheral ECs were reported by (Reese and Karnovsky, 1967; Ballabh et al., 2004; Pekny et al., 1998; Begley, 2004), and have been described in the table below:

Table 1. Comparison between brain and peripheral endothelial cells

Characteristics of membrane permeability	Brain endothelium	Peripheral endothelium
1. Fenestrations and pinocytic vesicles	Absent	Present
2. Tight junctions	Reinforced	Absent
3. Mitochondria	High prevalence	Low prevalence
4. Enzymes: γ-glutamyl-transpeptidase (γ-GT), monamine oxidase (MAO) and alkaline phosphatase (AP)	High prevalence	Low prevalence
5. Efflux pumps	Present	Absent

1.4.3 Transport system across the blood-brain barrier

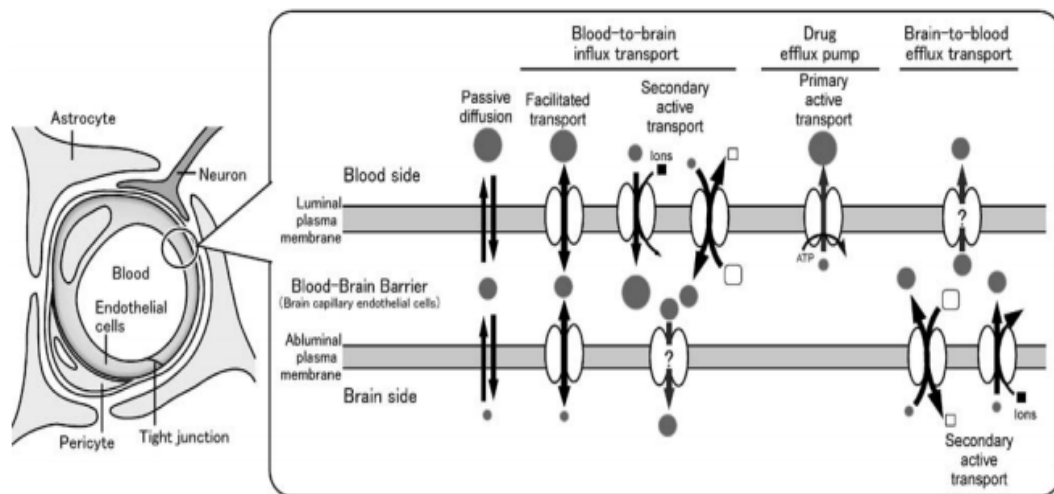


Figure 4. Schematic diagram illustrating the physiological transport system across a typical brain EC monolayer (Ohtsuki and Terasaki, 2007)

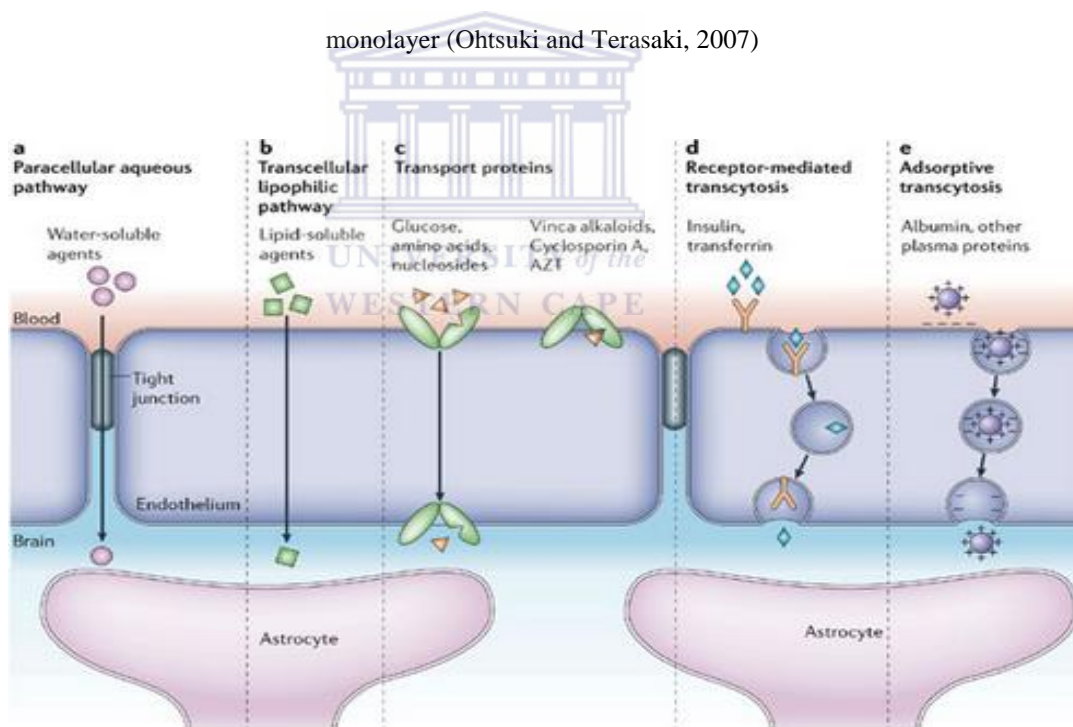


Figure 5. Schematic diagram of the substances which traverse the BBB *in vivo* (Re et al., 2012)

A transport barrier exists across the brain EC membrane. This barrier system consists of a very low rate of receptor-mediated transcytotic vesicular transport, absorptive transcytosis and transport proteins such as enzymes, carrier systems and

brain EC-specific molecules of unknown function (Janzer, 1993). Specialized TJs of the CNS endothelia are the main structures establishing barrier properties and are locally found on the apical region of the brain EC (Cardoso et al., 2010). Apart from these structures, the brain EC exhibits a specific distribution pattern of unique receptors, transporters and non-selective drug export pumps on its apical and basolateral surfaces. These transport mechanisms serve to protect the CNS from a plethora of toxic/harmful hydrophobic compounds found within the blood (Perrière et al., 2007). As a result, a very low rate of transcytosis is prevalent across the cerebral capillary endothelium (Tuma et al., 2003). The mechanism with which a compound crosses the BBB depends on its polarity, size and lipophilic nature. Possible pathways of passage across the BBB are: saturable transport systems, passive diffusion (across the membrane along a concentration gradient), leakage (extracellular pathways) and endocytosis or diapedesis (Banks, 2009), which involves the extravasation of blood cells, particularly white blood cells, across intact vascular endothelium (Petri and Bixel, 2006). The molecules allowed to cross the BBB can be classified into three distinct categories: (1) Lipid soluble compounds (Lipophilic solutes), namely, carbon dioxide (CO₂), oxygen (O₂), (Ballabh et al., 2004); ammonia (NH₃), morphine and nicotine; (2) small alcohols, namely, EtOH; (3) lipids, namely, steroids and prostaglandins (Banks, 2009), all of which are able to diffuse across the endothelial cell membrane into the brain interstitium.

The transport of water and water-soluble compounds, namely: sodium, hydrogen, potassium and chloride are, however, controlled by channels in both the apical and basolateral cell membrane surfaces. These compounds are either actively or passively transported across the cell (Martini, 2006).

1.4.4 Mouse brain endothelial cell histology

Based on research conducted by Navone et al. (2013), findings on brain microvascular ECs (BMVECs) expressed phenotypical and morphological cell monolayers which expressed a cobblestone-like appearance. In addition light phase contrast and scanning electron microscopy (SEM) expressed cultured human ECs in monolayers of large cells in close proximity (Jaffe et al., 1973). Research conducted by Jaffe et al. (1973), using high resolution SEM, showed cultured ECs exhibiting large (30x50µm), flat cells growing within a monolayer with definite boundaries and an array of cytoplasmic projections and pits on its surfaces (Jaffe et al., 1973).

Technology has elucidated the cytoskeleton structure of the EC. The literature reports that the mouse brain endothelial (bEnd5) cells show a longitudinal type pattern of filamentous-actin (F-actin) distribution compared to the more organized orientation of apical rings in the primary mouse brain microvascular ECs (pMBMECs), throughout the entire cell body (Steiner et al., 2011). The bEnd5 cells expressed a more spindle-shape cell morphology when compared to the pMBMECs (Steiner et al., 2011).

Structural and surface morphological studies are imperative for elucidating the brain EC as the anatomical basis of the BBB. It has been firmly established that the malfunctioning and pathology of brain ECs has led to the increasing need to establish effective *in vitro* BBB model systems (James, 1992; Kalaria, 1992; Navone et al., 2013).

1.4.5 Molecular basis for blood-brain barrier function

A technique, such as immunocytochemistry, has further endorsed the hypothetical model of the BBB by allowing for the investigation of the internal structures of the brain ECs, and has shed light on the molecular structures from a histological point of view. The TJs are composed of a combination of transmembrane and cytoplasmic proteins interconnected with an intracellular-based actin cytoskeleton. This allows for it to form a barrier while functioning as a rapid modulator and regulator of permeability. The paracellular permeability of the BBB depends on the arrangement of the TJs, which is a process that involves the intricate interaction between an array of protein complexes (Chen et al., 2009).

The transmembrane proteins complexes forming these TJs include: occludins and claudins. In addition, there are cytoplasmic proteins, which are classified as plaque proteins, namely, the zonula occludin-1, 2 and 3 (ZO-1, ZO-2 and ZO-3), which are among the molecules that are important to the TJ structure and play a critical role in the maintenance of BBB function (Wilhelm et al., 2011; Passeleu-LeBourdonnec et al., 2013).

In the BBB, the expressed proteins: claudin-3, claudin-5, and claudin-12 are associated with increased transendothelial electrical resistance (TEER) readings, with claudin-5 being an essential component in the establishment of the BBB as it restricts small molecules up to 800 Da (Schreibelt et al., 2007). The claudin-5 has been shown to be the main adhesion protein molecule involved in the maintenance of a functional BBB (Nitta et al., 2003). It is the most abundantly expressed subtype among claudins in mouse brain capillary ECs at the mRNA level (Ohtsuk et al., 2008; Kashiwamura et al., 2011).

Occludin shows high prevalence and is present in a distinct, continuous pattern along cellular margins in the cerebral endothelium (Hawkins and Davis 2005). The occludin is a 60-65 kDa protein with a carboxy(C)-terminal domain and joins to associate recruiting proteins of the ZO-1 protein (Schreibelt et al., 2007).

While the claudin-5 is important for the formation of TJs, occludin maintains the tightness of the TJ. The ZO serve as anchoring proteins which interact with the cytoplasmic domains of the claudins, occludin and adhesion molecules which link these proteins to the actin cytoskeleton (Colgan et al., 2008; Fashori and Kachar 1999, Haorah and Heilman et al., 2005).

Other transmembrane proteins include: Junctional Adhesion Molecules (JAM), namely: JAM-A, JAM-B and JAM-C and the vascular-endothelial-cadherin (VE-cadherin) proteins. These proteins are present on the lateral surfaces of brain ECs and are essential for the stabilization of the paracellular space between brain ECs, but do not play a role in the paracellular permeability between adjacent brain ECs. They are, however, a prerequisite for the formation and maintenance of TJ proteins. (Colgan et al., 2008; Fashori and Kachar, 1999; Haorah and Heilman et al., 2005).

TJ integrity is greatly dependent on an elevated occludin/claudin-5 expression and intracellular signaling processes that control the phosphorylation state of the TJ proteins (Rubin and Staddon, 1999; Haorah and Heilman et al., 2005). With respect to the *in vitro* situation, the transmembrane TJ, claudin-5, appeared to be confined to the cell-to-cell junctions in both primary and immortalized cell lines. In addition, the distribution of ZO-1 and ZO-2 showed junctional localization, and was also expressed in both models, whereas the occludin proteins, which were overly

expressed in the pMBMECs, were poorly expressed in the immortalized cell line (Steiner et al., 2011).

The disruption of the BBB can, therefore, result in a range of autoimmune disorders linked to the peripheral nervous system, including: Guillain-Barré Syndrome, Chronic Inflammatory Demyelinating Polyradiculoneuropathy (CIDP) and Paraproteemic neuropathy (Kanda et al., 2000; Kanda et al., 2004; Lach et al., 1993).

1.5 Establishing the immortalized mouse brain endothelial cell line

The immortalized mouse brain endothelium (bEnd5) is a cell line that has been transfected with a polyoma middle-T-oncogene. This particular cell line expresses specific EC proteins such as the vascular cell adhesion molecule (VCAM)-1, specific for T-cell adhesion and the intercellular cell adhesion molecules: (ICAM)-1 and ICAM-2 which are role players in T-cell diapedesis (Reiss et al., 1998).

The bEnd5 cells simulate the barrier properties of the BBB, similar to the pMBMECs. Both pMBMECs and bEnd5s are associated with the establishment of a highly restrictive barrier which minimizes the permeability across the *in vitro* BBB model. The bEnd5 cells have been carefully profiled and express an array of EC specific proteins, such as VE-cadherin, von Willebrand factor, platelet endothelial cell adhesion molecule-1, endoglin, ICAM-2 and claudin-5. In addition, the bEnd5s have also been found to show an upregulation in cytokine-induced expression of VCAM-1 and ICAM-1 (Coisne et al., 2005; Reiss et al., 1998; Rohnelt et al., 1997; Steiner et al., 2011). A disadvantage of the bEnd5 cell line is its inability to express the TJ protein, occludin, in its intercellular junctions and for this reason lacks in its barrier integrity compared to the pMBMECs (Steiner et al., 2011). The immortalized

bEnd5s are, however, more readily available in sufficient quantities, with less time-consuming isolation procedures (Steiner et al., 2011).

1.6 The proposed *in vitro* blood-brain barrier model

An *in vitro* model is utilized in an attempt to better elucidate physiological and morphological mechanisms in order to make inferences about the *in vivo* BBB. It is a basic tool which allows for the study of BBB functionality and can be utilized for monitoring drug delivery across the BMVECs (Yang et al., 2007).

In vitro models of the BBB are composed of EC culture systems retrieved from BMVECs. The model requires specific conditions whereby primary brain ECs are isolated by enzymatic digestion, making use of different sets of enzymes such as collagenase or dispase. Alternatively, brain capillary ECs are retrieved by the use of mechanical homogenization and filtration (Cecchelli et al., 1999).

In vitro BBB models rely on cell cultures of ECs. This is advantageous in that it allows for repeatability of experiments and control of factors which are found to be more complex within an *in vivo* location, namely: stress conditions, illness and behavior of the animal. The *in vitro* model is useful in that it reduces animal usage in experiments and is able to retrieve useful information about the transport mechanisms of a particular drug in a timeous manner, because of its ability to provide information on basic mechanisms that establish the BBB with less administration of the concentration of specific compounds under investigation which allows for quick and greater drug profiling (Weidenfeller et al., 2005; Lundquist et al., 2002).

Primary cultures of the bEnd5 cells are limited since they are inclined to grow slowly, have lower passage numbers and are very sensitive to contamination.

With reference to the immortalized bEnd5 cell line, not only does it express cellular prominent markers of ECs of the *in vivo* BBB markers of humans, but that of the mouse BBB and is, therefore, in alignment with our laboratory *in vivo* model. It is for this reason that the immortalized cell line has been selected for this research study. With respect to the morphological and histological characteristics of the bEnd5 cells, there is a lack of morphological evidence for what is known about the cellular morphology in theory. Morphological research evidence, therefore, needs to be generated in order to support its functionality as an *in vitro* BBB model.

1.7 The *in vitro* blood-brain barrier model: Clinical problem

The model allows for many clinical problems to be evaluated. Most disease pathologies are in many ways related to the formation and/or the regeneration of blood vessels (BVs), and as a result there is a particular demand to investigate the brain ECs, which line the inner surface of the brains' microvascular capillaries. These ECs are pivotal role players in the development and progression of neurodegeneration and neuroinflammation, due to it being the main cellular constituent forming the restrictive barrier between blood and the brain tissue (Navone et al., 2013; Xu et al., 2012).

In the event of a pathological condition, such as chronic exposure to narcotics, namely, alcohol and methamphetamine, the production of ROS is likely to follow. If produced in excess, ROS is able to significantly contribute to BBB dysfunction and inflammation in the brain by enhancing cellular migration. There is, however, a lack

of research conducted, with respect to the molecular mechanism by which ROS alters BBB integrity. Studies have demonstrated that ROS causes alterations in BBB integrity, which is paralleled by cytoskeleton rearrangements and redistribution and disappearance of the TJ proteins, claudin-5 and occludin (Schreibelt et al., 2007). EtOH studies conducted by Xu et al. (2012), found that EtOH was associated with morphological changes in the EC, which was confirmed by the formation of intercellular gaps in the EC monolayer by the disruption of the cell-to-cell contacts between adjacent ECs (Xu et al., 2012).

1.8 Physiological studies on the blood-brain barrier

1.8.1 Molecular studies

Research conducted by Haorah and Heilman et al. (2005) deduced that exposure to 10-50mM EtOH could result in the activation of myosin light-chain kinases (MLCK) within the bovine brain microvascular EC (BBMEC). The expression of the EtOH-metabolizing enzyme, cytochrome P-450-2E1 (CYP₄₅₀) was reported in studies conducted on the human coronary ECs (Borlak et al., 2003; Kapucuoglu et al., 2003), in human umbilical vein-derived cell lines (Hoebel et al., 1998; Farin et al., 1994) and in porcine or bovine ECs (Farin et al., 1994). It was found that CYP450-2E1 results in acetaldehyde (AA) and ROS production, which activated MLCK mediated phosphorylation, consequently mediating the phosphorylation of the claudin-5 TJ protein. In the literature, it is clearly stated that claudin-5 is a major part of the TJs in the BBB (Nitta et al., 2003), thus, a decrease in the expression of this particular protein and increases in its phosphorylation could result in the BBB loosening after EtOH exposure (Haorah and Heilman et al., 2005).

1.8.2 Permeability studies

BBB permeability to drugs that are needed for treating CNS disease is becoming increasingly important in order to treat diseases by way of transcellular and paracellular drug diffusion processes, metabolism and active transport (Gumbleton and Audus, 2001). Transendothelial electrical resistance (TEER) is a measure of the integrity across a cell monolayer in culture and is a tool by which to determine the permeability across it. This bioelectrical measurement qualitatively measures cell monolayer health and quantitatively measures changes in the permeability across an *in vitro* BBB.

In vivo, the BBB exhibits high TEER and is impermeable to charged particles, proteins, ions and hydrophilic molecules and hormones that could mimic specific neurotransmitters (Tanobe et al., 2003; Colgan et al, 2008). Unlike peripheral endothelium, cultures of brain ECs show high TEER *in vitro* (Weidenfeller et al., 2005). The literature has reported on narcotics, such as alcohol, to be a major factor influencing the onset of neurodegenerative disorders via the loss of BBB integrity (Haorah and Knipe et al., 2005). According to research conducted by Haorah and Heilman et al. (2005), it was found that at physiological concentrations of EtOH (50mM) resulted in significant increases in permeability of a BBMEC monolayer, whereas, the lower concentrations had no effect on permeability. In addition, after a 50mM EtOH exposure (0.5-2 hrs) the expression of TJ proteins (ZO-1, claudin-5 and claudin-3) decreased in its intensity.

1.9 Experimental model

The experimental model (*in vitro*) was incorporated to further understand complications which occur within a clinical setting.

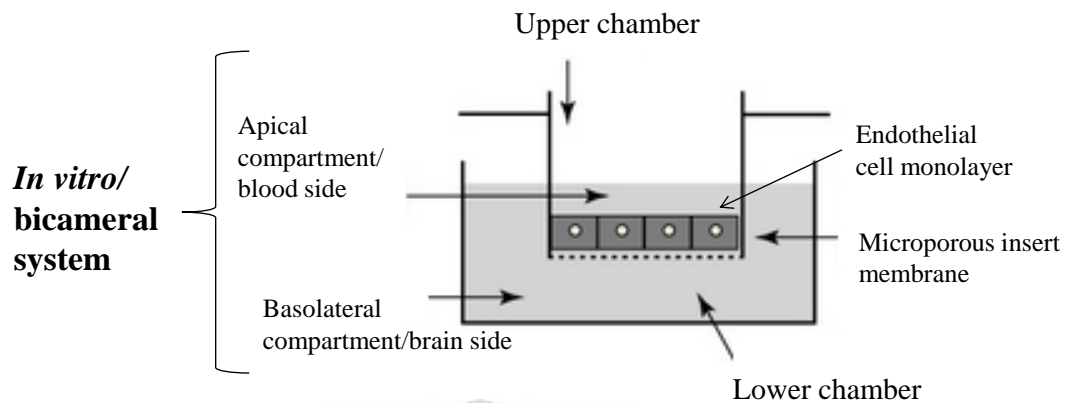


Figure 6. Schematic diagram of a hypothetical BBB *in vitro* using the bicameral system (Siddiqui et al., 2011)

1.9.1 Factors inducing cellular proliferation

The close proximity of the cells in deep brain regions make up the functional unit, denoted as the neuro-vascular unit, as was previously mentioned earlier in the text. During normal and pathological development this unit secretes various neurotoxic peptides and bioactive factors, triggering changes in the homeostasis of the cerebral microenvironment. The brain microcapillaries, as the anatomical foundation for the BBB, provide the BBB with nutritive support. These capillaries are mainly comprised of the single layer of ECs which are in close proximity (approximately 2 μ m). The ECs of the BBB modulate the molecular transport between brain interstitial fluid and the systemic circulation, with perivascular neurons and glia (astrocytes, microglia and oligodendrocytes). The vascular ECs are functionally

connected and are able to secrete multiple neurotoxic peptides and bioactive factors, which triggers changes in brain homeostasis (Zhao et al., 2006).

Intercellular signaling, inevitable among cell populations in culture, are influenced by cell density as well as its surrounding environment. Cell growth or proliferation, in turn, is strongly influenced by surface area, which accelerates the process of cellular attachment and contact inhibition between adjacent cells. In order to manage intercellular paracrine signalling, distance can be achieved by altering the density of the cells and subsequently altering the paracrine distance between neighboring cells. Signaling expression of growth factors is, thus, enhanced by autocrine or paracrine signal transduction. These are critical parameters involved in the controlling of subsequent cell proliferation (Kim and Dean, 2009).

1.9.2 Optimizing the cell monolayer using hydrocortisone as a blood-brain barrier enhancing glucocorticoid

Glucocorticoids (GCs) have been used effectively to improve the BBB *in vitro*. (Förster et al., 2008). Barrier tightening effects of GC treatment have been demonstrated for cerebral endothelial cells *in vitro* (Hoheisel et al., 1998; Förster et al., 2008). Reports demonstrate GC's ability to up-regulate TJ proteins and increase barrier properties of human and mouse microvascular EC lines (Förster et al., 2005; Förster et al., 2008; Kashiwamura et al., 2011). Based on research performed on swine, porcine *in vitro* cultures of BMVECs had modified electrical properties of its monolayer of brain ECs after being treated with the GC, hydrocortisone (HC). Physiological concentrations of HC (500nM) have thus been found to significantly enhance the barrier properties of porcine brain capillary endothelial cells (PBCEC)

in serum-free culture conditions (0% Fetal Bovine serum) (Hoheisel et al., 1998; Weidenfeller et al., 2005). Studies performed by Hoheisel et al (1998), showed that TEER was in fact elevated after the withdrawal of serum while in the presence of physiologically relevant levels of HC.

The functional differentiation of EC by the flow-induced forces as well as by the presence of HC has been found to improve the mouse brain capillary EC (MBCEC) barrier properties and the tightness of the EC monolayer to the existing *in vivo* model, rendering it an ideal *in vitro* model for human BBB research (Cardoso et al., 2010; Weidenfeller et al., 2005).

In addition, very few studies have been performed on the human brain microvasculature. One particular study conducted, using the human cell line consisting of hCMEC/D3 cells, strongly proposed the stabilization of BBB function as a mode of GC action on a molecular level (Förster et al., 2008).

This particular study proved the administration of GCs to induce the expression of the targets occludin 2.75±0.04-fold and claudin-5 up to 2.32±0.11-fold, which most likely contributed to the more than three-fold enhancement of TEER, reflecting barrier integrity (Förster et al., 2008).

Filamentous actin (F-actin) is one of the main constituents of eukaryotic cytoskeleton. Globular actin (G-actin) polymerizes to form the F-actin (Glogauer et al., 1998; Gardel, 2004). F-actin is linked to TJs and integrins and takes part in the regulation of cell-cell and cell-substrate contacts. *In vitro* studies performed on MBCEC in the presence of serum-containing media and HC-supplemented media showed that with serum withdrawal, actin delocalizes within the cell body and demonstrates a filamentous distribution in the longitudinal direction of the cells.

Along with these changes are a modulation of the cytoskeleton and changes in the mechanical properties of cells. The HC, thus, enhanced the barrier properties after its effect on the actin (Weidenfeller et al., 2005).

Reduced TEER, correlating to increased paracellular permeability, occurs when the basolateral surface of the brain endothelia, usually subjected to serum-free interstitial fluid *in vivo*, is exposed to serum (Nitz et al., 2003; Hoheisel et al., 1998). This is endorsed by research conducted on PBCEC where it has been established that serum, within normal concentrations of 10% v/v, weakens the barrier of PBCEC, especially when exposed to the basolateral side (Nitz et al., 2003).

TEER, can be indicative of the restrictiveness of the paracellular pathway to solute transport and may be influenced by variables, such as the extent to which cell-to-cell interaction occurs at the TJs, the type of culture environment to which the basolateral surface is exposed and the accumulation of F-actin in the cytoplasmic margins which ultimately affects TEER readings (Rist et al., 1997).

1.10 Toxicological effects of Ethanol

1.10.1 Pertinent information on ethanol metabolism

For the purpose of this study, the scope of the research investigations is limited to the effects of EtOH. The metabolism of the EtOH within the brain endothelium generates oxidative and nitrosative byproducts which play a strong role in oxidative damage to the BBB, thereby, increasing the permeability of toxic substances (Haorah and Heilman et al., 2005; Haorah and Knipe et al., 2005). The literature has reported that the moderate consumption of alcohol/EtOH (in the range of 10-20mM) can have transient effects on cell function by way of interacting with certain proteins

and cell membranes. EtOH, as discussed previously, is able to produce damaging molecules as a result of its metabolism which results in the formation of ROS, namely super oxide radicals (O_2^-), hydroxyl radicals (OH^\cdot), single oxygen (O_2) or peroxy radicals (RO_2^\cdot) (Munin and Edwards-Lévy, 2011).

EtOH metabolism occurs via two pathways, namely the oxidative and nonoxidative pathways. The oxidative pathways involve either the addition of oxygen or the removal of hydrogen, via the enzymes alcohol dehydrogenase (ADH), CYP₄₅₀ and catalase (Zakhari, 2006). The nonoxidative metabolism involves two pathways, the first is a reaction catalyzed by the enzyme fatty acid ethyl ester (FAEE) synthase to form FAEE molecules and the second is a reaction governed by the enzyme phospholipase D (PLD), which forms a phospholipid known as phosphatidyl ethanol (Zakhari, 2006).

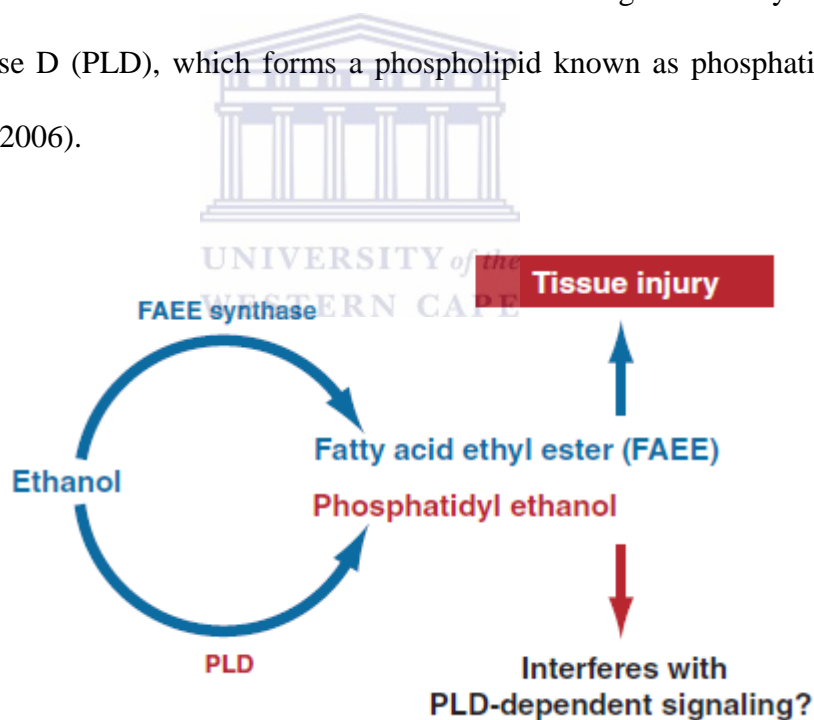


Figure 7. Nonoxidative metabolic pathway for EtOH (Zakhari, 2006)

The first and primary oxidative pathway of EtOH metabolism occurs via ADH, which is a cytosolic enzyme catalyzing the conversion of alcohol to acetaldehyde. Associated with the reaction are intermediate electron carriers namely: Nicotinamide

adenine dinucleotide (NAD^+), reduced by two electrons to form NADH. The CYP2E1 prevalent in the cells' microsomes metabolize alcohol to acetaldehyde at increased concentrations of alcohol (Gemma et al., 2006; Zakhari, 2006; Manzo-Avalos and Saavedra-Molina, 2010). Acetaldehyde, a metabolite of EtOH, is further metabolized in the mitochondria, primarily by aldehyde dehydrogenase 2 (ALDH2) forming acetate and NADH and catalase, found within peroxisomes. These metabolic reactions require the use of hydrogen peroxide (H_2O_2) for the oxidation of alcohol (Manzo-Avalos and Saavedra-Molina, 2010; Zakhari, 2006)

A second pathway, known as the microsomal ethanol-oxidizing system (MEOS), assists in removing toxins through CYP2E1 and functions similar to ADH by converting the alcohol to aldehyde. The reaction is aerobic and requires reduced NADPH for the formation of NADP and water (Manzo-Avalos and Saavedra-Molina, 2010; OECD SIDS, 2004).

The third pathway for the metabolizing of EtOH involves catalase found within the cellular organelle, the peroxisome. It is capable of causing the oxidation of minute amounts (2%) of EtOH in the presence of an H_2O_2 -generating system, forming acetaldehyde in the absence of NAD as a co-factor (Weiner, 1987; Manzo-Avalos and Saavedra-Molina, 2010).

EtOH metabolism in non-liver tissues does not possess alcohol dehydrogenase (ADH), such as brain and brain regions (Zakhari, 2006). The enzymes involved in the EtOH metabolism of the brain and its associated areas are CYP₄₅₀ and catalase.

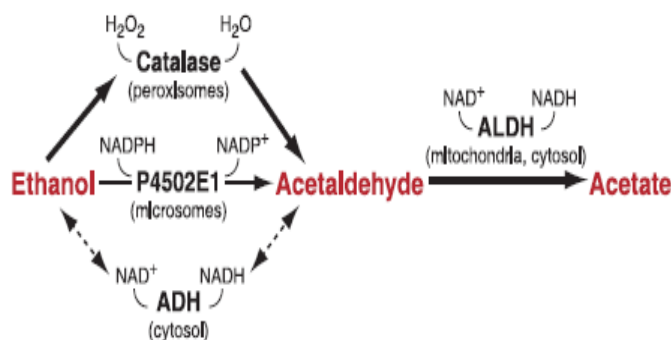


Figure 8. Oxidative metabolic pathways of EtOH in brain cells

(Deitrich, 2006)

The brain cell metabolizes EtOH, producing acetaldehyde by the breakdown of H₂O₂ to H₂O via the enzyme catalase, which is found within the subcellular, peroxisomes (See Fig 8.). This catabolic process requires the presence of H₂O₂. CYP2E1 is present within the cytosol of brain cells and the enzyme aldehyde dehydrogenase (ALDH), present in both the mitochondria and cytosol, functions in the conversion of acetaldehyde to acetate (Deitrich, 2006).

WESTERN CAPE

1.10.2 Ethanol-induced pathology of the mitochondria

The mitochondrion plays a pivotal role in cellular metabolism via ALDH, which involves the catalysis of acetaldehyde into acetate, as mentioned above. Upon the dissemination of this particular enzyme, acetaldehyde begins to leak into the vascular system, leading to biomolecular damage of lipids, proteins and nucleic acids. This may result in the intoxicative effects related to alcohol consumers (Manzo-Avalos and Saavedra-Molina, 2010).

Thus, alcohol consumption affects the mitochondria's ability to function. This will have a direct effect on the metabolic activity of the cell and its overall viability (Agarwal, 2001; Manzo-Avalos and Saavedra-Molina, 2010). Elevated levels of

acetaldehyde have been found to induce toxic effects by the inhibition of mitochondrial functioning and subsequent reactivity (Manzo-Avalos and Saavedra-Molina, 2010).

Microvessels, which are the main components of the BBB, are vulnerable to oxidative damage, during alcohol-induced stress, resulting in oxidative damage within the vessels of the brain (Alikunju et al., 2011). The EtOH-metabolizing enzymes, such as the ADH and CYP2E1 as well as catalase were found to localize within brain microvascular endothelial cells (Haorah and Knipe et al., 2005).

Chronic abusers of alcohol are at risk of suffering from neurocognitive deficits, neuronal injury and neuronal loss. The literature has reported on alcohol-elicited BBB damage and its involvement in the progression of neuroinflammation and neuronal loss (Harper 1998; Parsons 1998; Abdul Muneer et al., 2011).

There is, therefore, a desperate need to develop novel therapeutic strategies in which potential antioxidant candidates may be used in the treatment and/or prevention of BBB associated disorders. Furthermore, identification of indigenous, natural compounds which are easily accessible and financially viable to the general population of a developing country, such as South Africa, is always a critical factor to consider when identifying such candidates.

1.11 Rooibos - *Aspalathus linearis*

Aspalathus linearis (*A.linearis*), commonly known as “rooibos” or “red-bush” is a leguminous shrub, indigenous to the Cederberg mountains and within a regional context, involves areas such as Citrusdal, Clanwilliam and Nieuwoudtville in the WC of SA (Joubert et al., 2008). It is used for the manufacture of fermented rooibos

herbal tea which is derived from the leaves and stems of the fynbos plant, *A.linearis* (Marnewick, 2011). For the purpose of this research study fermented rooibos herbal extract/tea will be denoted as R_f .

1.11.1 Fermentation of rooibos

Most of the teas produced globally, are fermented. The fermentation process involves the enzymatic oxidation of polyphenols and other components found in the tea leaves. The initial step for the processing of non-fermented tea, involves an enzymatic inactivation process carried out by way of heat (Joubert et al., 2005). The rooibos is harvested during hot summer months by topping whole bush to approximately 45cm, with active growth not being more than 50cm - without flower growth - in order to avoid producing poor quality/weak tea. The leaves turn red-brown when the shredded plant material becomes “fermented,” which occurs in ambient temperatures, followed by sun drying between 38-42°C (Joubert and De Villiers, 1997). The age of the rooibos and the cultivation areas are major factors influencing the fermentation time (Joubert, 1994) and the shredding of the leaves is what causes the enzymatic oxidation of the polyphenols, resulting in the browning of the plant (Joubert, 1996).

R_f is a unique beverage since it is rich in volatile components, minerals and ascorbic acid, it is caffeine-free and has low tannin content (such as gallic acid) (Rabe et al., 1994). R_f has consequently gained much popularity for its anecdotal remedies and medical value with respect to its antioxidant (AO) activity, attributed to its high polyphenolic content (Joubert et al., 2008).

1.11.2 Protective antioxidant properties of *Aspalathus linearis*

Recent reports have shown that consumption of R_f noticeably improved the lipid profile as well as the redox status - both relevant to heart disease - in adults at risk for developing cardiovascular disease. The AO properties are attributed to the polyphenolic factors found within the herbal tea (Marnewick et al., 2011). It is for this reason that the health benefits of rooibos are directly attributed to its phenolic content (Niwa and Miyachi, 1986; von Gadow et al., 1997).

A. linearis, contains a variety of bioactive phenolic compounds such as dihydrochalcones, flavonols, flavones and flavanols particularly the unique C–C linked dihydrochalcone glucoside, aspalathin (Koeppen and Roux, 1966). Numerous studies have reported on the *in vitro* AO activity of rooibos, (Yoshikawa et al., 1990; Ito et al., 1991; Lamosová et al., 1997; von Gadow et al., 1997; Joubert et al., 2004), as well as *in vivo* activity in experimental rats (Marnewick et al., 2003). Studies show that rooibos treatment resulted in inhibition of lipid peroxidation in rat liver (Kucharska et al., 2004).

The polyphenol AOs identified in R_f include: the monomeric flavonoids aspalathin, nothofagin, quercetin, rutin, isoquercitrin, luteolin, vitexin, isovitexin and chrysoeriol. Currently, rooibos is the only natural source of aspalathin (Erickson, 2003) used as a therapeutic compound.

More specifically, aspalathin, and nothofagin, similar in structure to aspalathin and, therefore, has similar AO capabilities, are present in relatively large amounts in unfermented rooibos and are the most abundant monomeric flavonoids. Some of the aspalathin and nothofagin are, however, oxidized to other substances during

fermentation; thus, R_f contains less of these polyphenols than the unfermented form. The change in polyphenol composition is the reason why the tea changes color with fermentation (Erickson, 2003). Aspalathin seems to contribute to the AO capabilities of rooibos, but it is not as well studied as quercetin and luteolin. (Erickson, 2003).

Prior research carried out on *A.linearis*, has demonstrated its ability to reduce deleterious effects of agents of oxidation on human health, as a result of the presence of the flavonol, quercetin, the flavone, luteolin, with their antispasmodic properties and five additional glycosides, the dihydrochalcone, aspalathin, the flavones, orientin and isorientin, and the flavonols, isoquercitrin and rutin (Rabe et al., 1994).

A typical cup of rooibos tea contains an array of polyphenols (**See Table 2.**), but in order to make more clinically appropriate inferences about physiological effects of R_f , plasma concentrations of selected flavonoids need to be identified after a cup of tea is consumed. Consumption of a typical cup of R_f is a good source of AOs. This is supported in work carried out by Breiter et al. (2011) where traces of flavonoids were detected within the blood plasma, after the consumption of 500ml of R_f .

Table 2. The composition of a typical cup of R_f (amount of flavonoids in aqueous extract of *A.linearis*) (mg/g ± SD)

Flavonoid	mg/g±SD
*Aspalathin	1.234 ± 0.010
Isoorientin	0.833 ± 0.007
Orientin	1.003 ± 0.010
Vitexin	0.330 ± 0.002
Rutin	1.269 ± 0.006
Isovitexin	0.265 ± 0.002
Isoquercitrin and Hyperoside	0.429 ± 0.002
Luteolin	0.029 ± 0.001
Quercitrin	0.107 ± 0.002
Chrysoeriol	0.022 ± 0.003
Total	5.521 ± 0.003

***Note:** Extracts were prepared by pouring 60ml of hot distilled water on 1g of R_f and steeping it for 10 min. The solution was cooled and filtered (Bramati et al., 2002).

Table 3. Detection of the maximum quantity of unchanged flavonoids within the plasma of volunteers (in nM) and % recovery rates of these respective flavonoids after the ingestion of 500ml of an aqueous extract of R_f (Breiter et al., 2011).

Flavonoid	Peak amount of flavonoids (nM)	Plasma concentration (% recovery rate in nM)
*Aspalathin	1.9719	0.17
Isoorientin	0.0639	0.18
Orientin	0.7243	1.00
Vitexin	0.2892	2.25
Rutin	0.4686	1.49
Isovitexin	0.0611	0.69

***Note:** The sample of tea was prepared by pouring 500ml of boiling water on 10g of R_f and steeping it for 10 min. The % recovery rate displays the actual recovered amounts of flavonoids (in nM), found within the plasma, relative to the ingested amount (Breiter et al., 2011).

1.11.3. Polyphenols

Polyphenols are a diverse class of chemicals found in various plants, fruits, vegetables, wines and an array of teas. It is a term used to characterize a compound which presents with one or more benzene rings which can be subdivided into flavonoids, stilbenes (resveratrol) and tannins (See Fig. 9 and Fig. 10) (Hagerman et al., 1998). Polyphenolic compounds, ubiquitous in plants, have gained much popularity for its antioxidative action and modulation of several protein functions

and its role as an anti-inflammatory agent (Joubert and Ferreira, 1996). In addition, it is well known for its epidemiological influence in the prevention of neurodegenerative disorders and chronic diseases including cancers (Vanzour et al., 2010). The free radical scavenging mechanisms by which polyphenols neutralize ROS involve the breaking of free radical chain reactions. In addition, polyphenols function in the suppression of free radical formation by the regulation of enzyme activity and chelating metal ions which are role players in free radical formation. These metals include: copper and iron, and are chelated through multiple hydroxyl groups and carbonyl moieties (Fraga et al., 2010; Perron and Brumaghim, 2009; Vladimir et al., 2012).

1.11.4 Classification of polyphenols

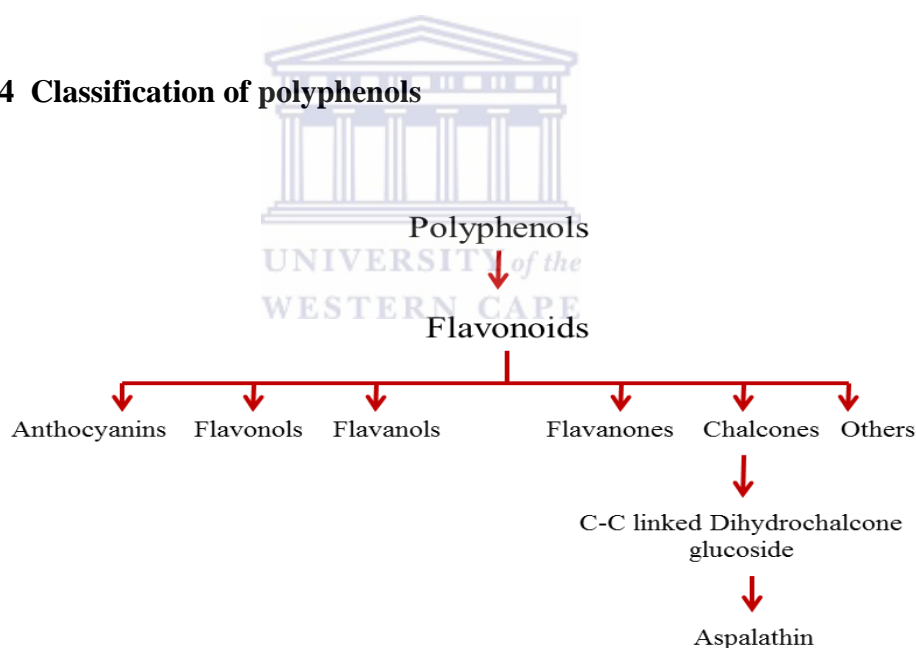


Figure 9. Polyphenolic profile (http://www.frenchglory.com/polyphenols_classification.pdf)

Polyphenols are common in plants, functioning as pigments and sunscreens, as insect attractants and repellants and as antimicrobials and AOs. A polyphenol group is subdivided into smaller groups such as flavonoids and phenolic acids (See **Fig. 9**). The polyphenols may also be classified as monomeric (molecules containing a

single unit) or polymeric (larger molecules containing more than one unit) (Erickson, 2003).

1.11.5 Phenolic structure of aspalathin

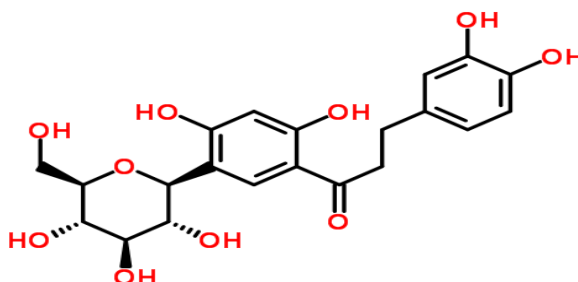


Figure 10. Basic chemical structure of aspalathin (<http://www.chemspider.com/Chemical-Structure.26286888.html>)

1.11.6 Aspalathin

Aspalathin, constitutes the major flavonoid of R_f , however, most of its polyphenolic nature is attributed to flavanones and unknown polymeric substances (Marais, 1996; von Gadow et al., 1997; Joubert, 1996). Aspalathin undergoes cyclization during oxidation to form the flavanones: dihydro-orientin and dihydro-isoorientin, of which the dihydrochalcones are more effective as AOs than the aforementioned flavanones. R_f was reported to possess significant AO activity, with inhibition activity of 83.43%. Thus, this AO activity can be attributed to the oxidation products of aspalathin in R_f (Dziedzic et al., 1985; von Gadow et al., 1997).

While the AO capacity of green and black tea is well documented, more studies need to be conducted on the rooibos tea. Due to the oxidative process involved in the

fermentation of rooibos, it contains lower amounts of flavonoids, such as aspalathin in comparison to the unfermented rooibos and, therefore, has a lower AO capacity (Stanley et al., 2001). *In vitro* studies, have however, reported on the AO activity within the R_f, which was comparable to both green and black tea (Snijman et al., 2009; Breiter et al., 2011). R_f expresses a polyphenolic profile which has the potential to aid in the recovery of a negative change in the bEnd5 cell's metabolic status as a result of oxidative stress, based on its AO capacity (See Table 3.). Thus, it possesses the potential to ameliorate the effect that generic narcotics have on a biological system and more specifically on the bEnd5 cell line.

1.12 Antioxidants and the blood-brain barrier integrity

The reduction-oxidation (redox) state of cells is known to impact strongly on cellular functions such as the glutathione s-transferase mediated elimination of electrophilic xenobiotics and some serve as the end-products of lipid peroxidation (Rebrin et al., 2005; Marnewick, 2011). Redox activity within a cell is used as an important indicator of the oxidative status of the brain parenchyma *in vivo*.

The body employs three main phases of protection against free radical attack: preventative AOs, scavenging AOs and repair enzymes. In addition, nonenzymatic AOs are involved in the neutralization of ROS (Rahman, 2007). The preventative AOs are associated with the inhibition of free radical production such as metal binding proteins, albumin, transferrin, myoglobin and ferritin, which bind metals such as iron and copper (Leopoldini et al., 2011; Rahman, 2007). The scavenging enzymatic AOs remove the ROS upon formation. These include enzymes such as, superoxide dismutase, glutathione, peroxidase and catalase, The repair enzyme

functions in DNA repair enzymes which function in the repairing of damaged biomolecules. In addition, the nonenzymatic AOs, include, carotenoids and polyphenols, namely, flavonoids (Rahman, 2007).

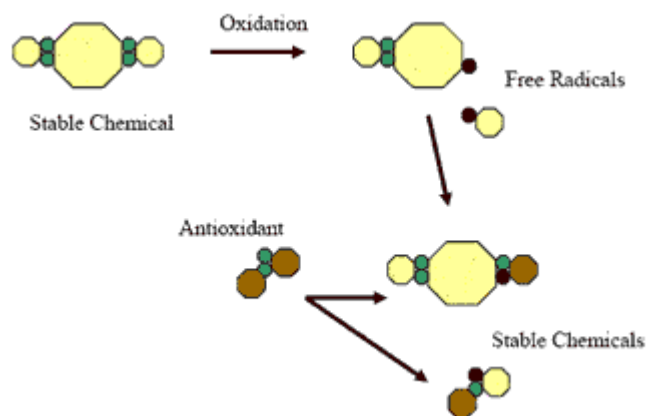


Figure 11. Antioxidant neutralization of ROS production

(<http://www.esc.rutgers.edu/publications/general/fs1065.htm>)

1.13 Problem statement

The high rate of alcohol abuse and prevalence of FASD, with its effect on the South African socio-economic status, is a problem that simply cannot be ignored. This study, therefore, aims to produce a body of scientific knowledge that will support and improve on the existing awareness of the detrimental effects of alcohol abuse, from an occasional and long-term perspective - on the BBB, and the advocating of therapeutic mechanisms to ameliorate these effects.

The research focused on investigating the compromising effects of selected alcohol concentrations on the BBB and how these effects can be reduced or eradicated by using rooibos, a plant known for its high AOs and is widely used and cheaply available to all sectors of the South African population.

Although research has been conducted on rooibos, none focuses on its effects on the BBB and little is known about clinical interventions reversing the alcohol-induced effects on the BBB. Given the devastating socio-economic impact of alcohol abuse on SA, much research is required not just to understand mechanisms of BBB disruption by alcohol, but to reverse or neutralize the effect of this adverse outcome.

1.13.1 Rationale

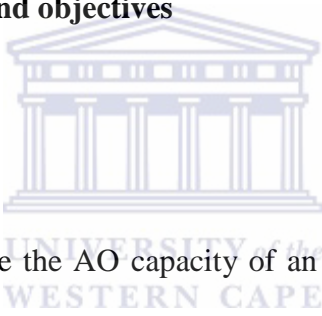
The highly selective BBB is crucial to the brain as it maintains the homeostatic milieu of the brain microenvironment. The role of the BBB should never be underestimated, as the very function of the brain's neurons, depend on the strict regulation and management of the extracellular environment. Should the BBB become compromised by primary or secondary alcohol effects, it could result in the disruption of the normal functioning of neurons, resulting in spontaneous action potentials, irregular motor, sensorial and psychological function. The ECs form the anatomical basis of the BBB and constitute the route by which the transport of substances (which may be toxic), viruses or bacteria within the plasma, are regulated and controlled (Nitta et al., 2003; Rubin and Staddon, 1999).

Literature has stated, emphatically, that EtOH affects the brain by means of ROS production (Dietrich, 2006; Zakhari, 2006). This supports the research findings on alcohol's association in BBB impairment as being strongly correlated to oxidative stress (Haorah and Knipe et al., 2005). Trolox, which has high AO potential, has been shown to reverse certain detrimental effects of EtOH on the BBB (Ramirez et al., 2009). This study investigated whether the AOs present in rooibos and widely used in South African communities, is able to reverse these harmful effects.

There is a desperate need to develop novel therapeutic strategies in which potential AO candidates may be used in the treatment and/or prevention of alcohol-related diseases and conditions such as FASD associated disorders. Furthermore, identification of indigenous, natural compounds which are easily accessible and financially viable to the general population of a developing country such as SA, is therefore, a critical factor to consider when identifying such candidates in an effort to ameliorate the negative physiological effects that alcohol abuse has on the integrity of the BBB. Rooibos herbal tea extract, high in AOs, fulfills all the criteria as a suitable candidate.

1.14 Research aims and objectives

1.14.1 Aims

- 
- (i) To chemically analyse the AO capacity of an aqueous extract of *A.linearis*. (ii) To analyse the *in vitro* effect of EtOH and fermented *A. linearis* aqueous extract separately and in combination on physiological parameters of the bEnd5 cells line model of the BBB.

1.14.2 Objectives

(i) Chemical analysis of fermented *A. linearis* to determine:

- The total polyphenol content
- The total flavonol content
- To analyse the oxygen radical scavenging properties of fermented *A. linearis*

(ii) *In vitro* analysis on bEnd5 cells:

Control and experimental (alcohol exposed, rooibos exposed and combination of alcohol and rooibos exposed) groups analysed in order to determine:

- Cell viability by measuring the % mitochondrial activity for selected concentrations of alcohol and fermented rooibos and combinations of the compounds at selected intervals.
- The effect of selected concentrations of alcohol and fermented rooibos on cellular proliferation at selected time intervals.
- The effect of alcohol and fermented rooibos and combinations of the compounds at selected time intervals on TEER.

(iii) In an attempt to morphologically characterize the BBB bicameral model system, investigation of the growth of bEnd5 monolayers and its development on mixed cellulose inserts using high resolution SEM was performed in a sequential manner. The addition of electron microscopy would further endorse the ultrastructural characteristics of the bEnd5 cells of the *in vitro* BBB model.

1.15 Research question/ hypothesis

The hypothesis for this study is that selected concentrations of fermented *A.linearis* will modulate the adverse alcohol/EtOH-induced changes to the *in vitro* mouse BBB physiology.



CHAPTER 2: Materials and Methods

The *in vitro* analysis was carried out in order to investigate generic responses of bEnd5 cells to acute (24 hrs) and chronic (daily: 24-144 hrs) exposure to EtOH and an aqueous extraction of fermented rooibos (*A. linearis*/ R_f), separately, as well as in combination, on the bEnd5 cells. Selected physiological parameters were investigated – namely, mitochondrial activity (MA), cellular proliferation, permeability and morphological studies - to investigate the functional and morphological characteristics of the bEnd5 cells. The initial phase of the study was to chemically analyze an aqueous extract of *A.linearis* in order to determine its polyphenol content and antioxidant (AO) capacity.

2.1 Preparation of an aqueous herbal infusion of *A.linearis*

A.linearis (harvested in the WC, in the Cederberg Mountains of Clan William) was prepared by steeping the dried leaves in boiling water for 30 min. A 20% aqueous extract was pre-filtered through cheesecloth and subsequently through whatman no.4 followed by no.1 (Sigma, South Africa) filter paper. The filter extract was stored at - 20°C, protected from light. The R_f aqueous extract was used directly after dilution with distilled water to a specified concentration of 20%. Sample precipitates were removed by centrifugation for 3 min at 4000rpm and the supernatant was used for the chemical analysis. Stock standard series were prepared and the selected amount of standard stock solutions were added to the diluents in the respective tubes (See **Appendix B, Table 1-6.**)

2.2 Chemical analysis of fermented rooibos (*A.linearis*)

Analysis was carried out by the Cape Peninsula University of Technology (CPUT), Oxidant Research Laboratory, Bellville, Cape Town, SA. R_f was obtained from the South African Rooibos Council (SARC, batch no. P06-02KK) and the total polyphenol, flavonol and flavanol content of R_f was determined. AO assays included: ferric reducing AO power (FRAP) assay (Benzie and Strain, 1996), oxygen radical absorbance capacity assay (ORAC) assay, the ABTS (2, 2'-azinobis (3-ethyl-benzthialozine-6- sulphonic acid) (TEAC-Trolox equivalent AO capacity) assay (Thaipong et al., 2006).

2.2.1 Measurement of polyphenols

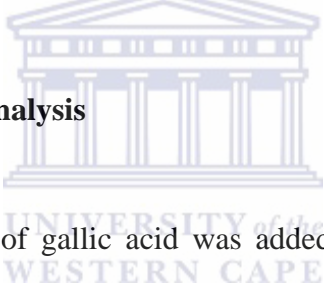
2.2.1.1 Principle of polyphenolic measurements

The analysis utilized the Folin Ciocalteu reagent, with gallic acid as the standard to measure total polyphenol content in a sample. The principle of the Folin Ciocalteu method involved the oxidation of polyphenolics in alkaline medium with molybdenum and tungsten. This formed a blue chromophore complex. The blue-coloured complex together with the polyphenols was measured spectrophotometrically at 750nm (Bajčan et al., 2013).

2.2.1.2 Chemical requirements and sample handling for the quantification of polyphenols

The chemicals utilized in the quantification of polyphenols included: 10% EtOH and Folin Reagent (Merck, Cat no.109001) and 7.5% sodium carbonate (NaCO_3) (Sigma-Aldrich, Cat no.223530) which was stored at room temperature (RT). Gallic acid (Sigma-Aldrich, Cat no.G7384) was prepared by dissolving 40mg in 50ml of 10% EtOH to give a stock concentration of 800mg/L. The control was prepared by dissolving 10mg of the gallic acid into 50ml of 10% EtOH solution to give a final concentration of 200mg/L. All solutions were prepared on the day of analysis. The sample was prepared on ice and all samples were held in storage at -40°C .

2.2.1.3 Sample analysis



For the standards, 25 μl of gallic acid was added to each well of a clear 96-well microtiter plate (Lasec SA, Cat no.PGRE655180). For the controls, 25 μl of the control was added to wells while 25 μl of the sample was added to the designated experimental wells, in triplicate (**See Appendix B, Table 7. Plate layout and concentrations**). 125 μl Folin reagent was added to all wells. The plate was left for 5 min at RT, prior to the addition of 100 μl Na_2CO_3 to each well. The plate was left for 2 hrs at RT in the dark. The plate was read using a MultiskanTM plate reader at 760-765nm.

2.2.2 Ferric reducing antioxidant power assay

2.2.2.1 Principle of the Ferric reducing antioxidant power assay

The FRAP assay was used for assessing AO power. The AOs were used as reductants in a redox-linked colorimetric method, employing an easily reduced oxidant present in excess. At low pH values, reduction of a ferric tripyridyltriazine (Fe^{3+} -TPTZ) complex to the ferrous (Fe^{2+}) form, which has an intense blue colour, can be monitored by measuring the change in absorption at a wavelength of 593nm. The reaction is non-specific, in that any half-reaction that has a lower redox potential than that of the ferric or ferrous half-reaction will drive the ferric (Fe^{3+}) to ferrous (Fe^{2+}) reaction. The change in absorbance is, therefore, directly related to the reducing power of the electron donating AOs present in the reaction mixture (Benzie and Strain, 1996; Benzie and Szeto, 1999).

2.2.2.2 Chemical requirements and sample handling for the FRAP assay

The chemicals required for the FRAP assay included: 300mM acetate buffer, pH 3.6 which was comprised of 1.627g sodium acetate and 16ml glacial acetic acid (Saarchem, Cat no.1021000) made up to 1L with distilled water (dH_2O). A 40mM of HCl and 10mM TPTZ (2, 4, 6-tri [2-pyridyl]-s-triazine) (Sigma-Aldrich, Cat no.T1253) comprised of 0.0093g TPTZ and 3ml of 40mM HCl. A 20mM iron (III) chloride hexahydrate (Sigma-Aldrich, Cat no.F2877) solution was made up with 0.054g $\text{FeCl}_3 \cdot 6\text{H}_2\text{O}$ and 10ml dH_2O . For the measurement of FRAP, L-ascorbic acid (Sigma-Aldrich, Cat no.A5960) was used as a standard. A stock concentration of 1mM L-ascorbic was prepared by dissolving 0.0088g of ascorbic acid in 50ml dH_2O . 400 μM of a control stock of L-ascorbic acid was prepared by dissolving 0.00352g of

ascorbic acid in 50ml dH₂O. All solutions were prepared on the day of the chemical analysis. All samples were stored at -40°C.

2.2.2.3 Sample analysis

The FRAP solution (straw-coloured) was prepared in a 50ml conical tube. The following reagents were added: 30ml acetate buffer, 3ml TPTZ solution, 3ml FeCl₃ solution, and 6.6ml dH₂O. For the standards, 10µl of ascorbic acid was added to each well of a clear 96-well microtiter plate. For the controls, 10µl of the control was added to wells while, 10µl of the sample was added to the designated experimental wells in triplicate. (See Appendix B, Table 7. Plate layout and concentrations). 300µl of the FRAP reagent was added to all wells with a multichannel pipette. The final volume of the assay was 310µl. It was not necessary for all the wells to be used on the plate at one time. The plate was incubated for 30 min in the incubating oven, set at 37°C and was read using a Multiskan™ plate reader at a wavelength of 593nm.

2.2.3 Oxygen radical absorbance capacity assay

2.2.3.1 Principle of the oxygen radical absorbance capacity assay

The ORAC method was used to analyze the lipid-soluble AO samples by introducing randomly methylated beta-cyclodextrin (RMCD) in a 50% acetone water mixture. The mixture made lipid-soluble AOs soluble in phosphate buffer. The assay was both reliable and sensitive and was based on the inhibition of the peroxy-radical (free radical) induced oxidation and, thereby, measured the peroxy radical absorbance capacity of AOs and serum or other biological fluids using Trolox as a

standard (Prior et al., 2003). This method can be performed with a fluorometry plate reader, using a 96-well microtiter plate to perform simultaneous kinetic analysis of many samples and to reduce the amount of sample required. The excitation wavelength was set at 485nm and the emission wavelength was set at 520nm (Prior et al., 2003).

2.2.3.2 Chemical requirements and sample handling for the ORAC assay

The chemicals required for the ORAC assay included: hexane (Saarchem, Cat no.2868040 LC) stored at RT, acetone/water/acetic acid solution (AWA) solution which consisted of 700ml acetone (Saarchem, Cat no.1022040 LC), 295ml dH₂O and 5ml glacial acetic acid. A 75mM, pH 7.4, phosphate buffer was prepared and consisted of two solutions.

Solution 1 was prepared by weighing out 1.035g sodium di-hydrogen orthophosphate-1-hydrate (NaH₂PO₄·H₂O) (Sigma-Aldrich, Cat no.S9638) and dissolving it in 100ml of double distilled water (ddH₂O). Solution 2 was prepared by weighing out 1.335g di-sodium hydrogen orthophosphate dehydrate (Na₂HPO₄·2H₂O), (Merck, Cat no.5822880EM) and dissolving it in a 100ml of ddH₂O. The pH was rechecked before each assay in order to maintain consistency. 18ml of solution 1 was mixed with 82ml of solution 2, in order to obtain 75mM, pH 7.4 phosphate buffer. The stock solution of fluorescein sodium salt (C₂₀H₁₀Na₂O₅) was stored at 4°C in a dark container (Sigma-Aldrich, Cat no.F6377). A 0.0225g of C₂₀H₁₀Na₂O₅ was weighed and dissolved in 50ml phosphate buffer. The 25mg/ml peroxy radical, denoted as AAPH (2, 2'-Azobis (2-methylpropionamide) dihydrochloride (Sigma-Aldrich, Cat no.440914). 0.5M Perchloric acid (PCA)

(Saarchem, Cat no.494612) consisted of 195ml dH₂O mixed with 15ml 70% PCA. For the measurement of ORAC, Trolox (Sigma-Aldrich, Cat no.238831) was used as a standard. A 500 μ M of Trolox standard concentration was prepared by dissolving 0.00625g of 6-Hydroxy-2,5,7,8-tetra-methylchroman-2-carboxylic acid (Sigma-Aldrich, Cat no.238831) in 50ml phosphate buffer and was mixed until dissolved. A 250 μ M of Trolox control was prepared by dissolving 0.00312g of 6-Hydroxy-2,5,7,8-tetra-methylchroman-2-carboxylic acid in 50ml phosphate buffer. All solutions were prepared on the day of analysis. All samples were prepared on ice and were stored at -40°C.

2.2.3.3 Sample analysis

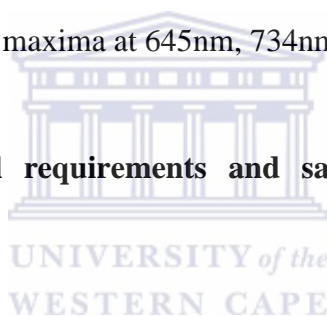
For the standards, 12 μ l of Gallic acid was added to each well of a clear 96-well microtiter plate. For the controls, 12 μ l of the control was added to wells, while 12 μ l of the sample was added to the designated wells in triplicate (See **Appendix B, Table 7. Plate layout and concentrations**). From the fluorescein stock solution, 10 μ l was added into 2ml phosphate buffer (in an Eppendorf tube), diluted as follows: 240 μ l of this solution was added to 15ml phosphate buffer using a 15ml screw cap tube. 138 μ l of the fluorescein/buffer solution was added to all wells of a black 96-microwell plate. 6ml of the phosphate buffer was added to the weighed AAPH and mixed well until dissolved. 50 μ l of this solution was transferred to each well. The final volume of the assay was 200 μ l. The plate was read using a MultiskanTM plate reader with an excitation wavelength set at 485nm and the emission wavelength at 530nm.

2.2.4 ABTS (TEAC) radical cation scavenging assay

2.2.4.1 Principle of the ABTS (TEAC) assay

The ABTS radical cation scavenging assay was based on the capacity of a sample to inhibit the ABTS radical ($ABTS^+$) (Zulueta et al., 2009). It was developed for the determination of the total AO status of body fluids and in food extracts. AOs added to this system could either scavenge the ABTS formed or interfere with the radical generating process. Measurement of the absorbance at a specific time after addition enables the calculation of a percentage scavenging (RE and Pellegrini et al., 1999). The radical cation ($ABTS^+$) can be monitored by measurement of one of its characteristic absorption maxima at 645nm, 734nm and 820nm.

2.2.4.2 Chemical requirements and sample handling for the ABTS (TEAC) assay



The chemicals required for the ABTS assay included: 7mM ABTS diammonium salt (Sigma-Aldrich, Cat no.A1888) and 140mM potassium-peroxodisulphate, both prepared fresh (Merck, Cat no.105091). The ABTS solution was prepared 24 hrs before starting the assay. The potassium-peroxodisulphate solution was added to the ABTS solution and left in the dark at RT. Trolox was used as a standard for the ABTS assay. 1mM of the standard was prepared by dissolving 0.0125g of Trolox (Sigma-Aldrich, Cat no.238831) in 50ml of EtOH. In addition, 200 μ M of the control was prepared by dissolving 0.0025g of Trolox in 50ml of EtOH. All samples were prepared on ice and were stored at -40°C.

2.2.4.3 Sample analysis

For the standards, 25 μ l of Trolox was added to each well of a clear 96-well micotiter plate. For the controls, 25 μ l of the controls was added to wells, while 25 μ l of the sample was added to the designated wells, in triplicate (See **Appendix B, Table 7. Plate layout and concentrations**). The ABTS solution was diluted with EtOH by adding 1ml of ABTS to 20ml of EtOH. The absorbance was read at approximately 2 (\pm 0.1) nm. From the ABTS solution, 300 μ l was added to each well. The plate was left for 30 min at RT and was read using a MultiskanTM plate reader at 734nm with a temperature set to 25°C.

2.2.5 Measurement of flavonols

2.2.5.1 Principle of flavonol measurements

The flavonol analysis made use of quercetin as the standard for determining total phenolics at a wavelength of 360nm. All solutions were prepared on the day of analysis.

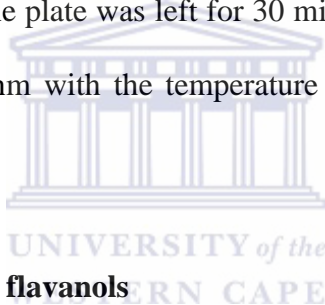
2.2.5.2 Chemical requirements and sample handling for quantifying flavonols

The chemicals required for the measurement of flavonols included: 10% EtOH, 95% EtOH, 0.1% HCl (Saarchem, Cat no.100319 LP) mixed in 95% EtOH and 2% HCl. For the measurement of flavonols, quercetin was used as a standard. The standard solution consisted of 4mg quercetin (Sigma-Aldrich, Cat no.Q0125) which was dissolved in 50ml of 95% EtOH. The control was made by dissolving 1.5mg

quercetin in 50ml 95% EtOH. All samples were stored at -40°C between subsequent analysis steps.

2.2.5.3 Samples analysis

For the standards, 12.5µl of quercetin was added to each well of a clear 96-well microtiter plate. For the controls, 12.5µl of the control was added to wells, while 12.5µl of the sample was added to the designated wells, in triplicate (**See Appendix B, Table 7. Plate layout and concentrations**). A 12.5µl solution which consisted of 0.1% HCl and 95% EtOH was added to each well, followed by the addition of 225µl 2% HCl to each well. The plate was left for 30 min at RT. The absorbance was read at a wavelength of 360nm with the temperature set to 25°C using a Multiskan™ spectrum plate reader.



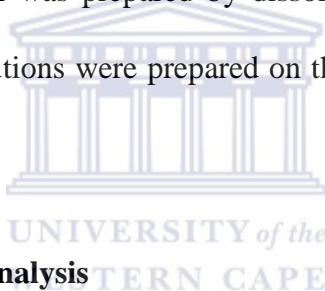
2.2.6. Measurement of flavanols

2.2.6.1 Principle of flavanol measurements

Flavanol analysis was carried out by using 4-dimethylaminocinnamaldehyde (DMACA) which reacts with flavanols to form a characteristic light blue colour and is measured at a wavelength of 640nm. The DMACA assay is an efficient technique which quantifies proanthocyanidins, which are condensed forms of tannins, in foods and beverages (McMurrough and McDowell, 1978; Kelm et al., 2005). The DMACA method used acid (acid butanol). The acid hydrolyzed the proanthocyanidins into their carbocation unit (extension unit) and the flavan-3-ol unit (terminal unit). The proanthocyanidin is largely ubiquitous in nature and highly prevalent in staple diets (Hummer and Schreier 2008; Wallace and Giusti 2010).

2.2.6.2 Chemical requirements and sample handling for quantifying flavanols

The chemicals utilized in the quantification of flavanols included: 32% HCl-methanol (HCl-MeOH), 250ml HCl (Saarchem, Cat no.100319 LP) which was added to 750ml MeOH (Saarchem, Cat no.4164080 LC) and mixed well. A 0.25g of DMACA (Merck, Cat no.822034) was weighed and 500ml HCl-MeOH mixture was added and mixed until dissolved. Catechin was used as a standard for the measurement of flavanols. A 1mM of catechin hydrate standard (Sigma-Aldrich, Cat no.C1251) was prepared by dissolving 0.0145g of catechin hydrate in 50ml MeOH. A 200 μ M of the control was prepared by dissolving 0.0029g catechin hydrate in 50ml of MeOH. All solutions were prepared on the day of analysis and all samples were stored at -40°C.



2.2.6.3 Sample analysis

For the standards, 50 μ l of catechin was added to each well of a clear 96-well microtiter plate. For the controls, 50 μ l of the control was added to wells, while 50 μ l of the sample was added to the designated wells, in triplicate (**See Appendix B, Table 7. Plate layout and concentrations**). 250 μ l of DMACA was added to all the wells to initiate the reactions. The plate was left for 30 min at RT and absorbance was read at a wavelength of 640nm using a MultiskanTM spectrum plate reader. If any of the flavanol values did not fit to the scale of the standard curve range, after the initial absorbance readings were taken, samples were diluted by pipetting 100 μ l of the sample supernatant into a new Eppendorf and 900 μ l of MeOH was added to

effect a 10-fold dilution. The flavanol assay with the diluted sample was then repeated.

2.3 *In vitro* analysis of bEnd5 cells

2.3.1 Bio-reagents

The following reagents were required for *in vitro* analysis: EtOH (Sigma-Aldrich, Cat no.E7023) and R_f (SARC, Batch no.P06/02/KK), which was prepared as an aqueous extract. The bio-reagents for culturing cryopreserved cells were analytical grade. The standard cell culture medium utilized was Dulbecco's modified eagles media (DMEM-BioWhitaker/Lonza[®], Cat no.12-604-F) supplemented with 1% anti-biotic-*Penicillin/ Streptomycin Amphotericin B* mixture (Whitehead Scientific (Pty) Ltd, Cat no. 17-745E), 1% sodium pyruvate (GIBCO[®], Cat no.11360), 1% non-essential amino acids (NEAA) (BioWhitaker/Lonza[®], Cat no.13-114E) and 10% fetal bovine serum (FBS) (GIBCO[®], Cat no.10500), Trypsin (0.25%) (Whitehead Scientific (Pty) Ltd, Cat no.BE 02-007E), phosphate buffer saline (PBS) (Sigma-Aldrich, cat no.D8662), Trypan blue (Sigma-Aldrich, Cat no.T-8154) The transwell inserts used for the TEER/ bioelectrical studies were purchased from MERCK (Millipore/MERCK, cat no.PIHA01250), cellular proliferation assay kit XTT II was purchased from Roche products (Pty) Ltd (Cat no.11465015001), hydrocortisone (Sigma-Alrich, Cat no.H0888), Dimethyl Sulphoxide (Whitehead Scientific (Pty) Ltd, Cat no.sc-358801) High resolution SEM studies utilized gluteraldehyde (Fluka, Cat no.49626), carbon tape (PELCO Tabs[™], Cat no. 16084-1), and aluminium stubs (Agar Scientific, Cat no. AGG301).

2.3.2 The immortalized mouse brain endothelial cell line

The immortalized mouse brain endothelioma (bEnd5) cell line (Highveld Biologicals – agents from American Type Culture Collection (ATCC)) was derived from brain endothelial cells of BALB/c mice. Immortalization was done by transfecting the primary cells with the retrovirus coding for the polyoma middle T-antigen. The bEnd5 cells expressed endothelial specific proteins: PECAM-1, Endoglin, MECA-32, Flk-1 which was determined by fluorescein-activated cell sorting (FACS). The bEnd5 cells possessed an adherent mode of growth and were able to maintain their endothelial-like morphology (Reiss et al., 1998).

2.3.3 Tissue culturing of bEnd5 cells

2.3.3.1 Operating principle

Tissue culture is based on establishing a tissue construct for use in studies pertaining to cell-cell and cell-matrix interaction. Subculture and/ or tissue culture is employed in order to populate cells by applying selective nutrients within a selective medium in order to generate an elevation in cell growth and for the generation of replicate cultures of a particular cell type (Freshney et al., 2006).

The *in vitro* model of the BBB used in this study mimicked the *in vivo* situation in that the EC is the central component of the *in vivo* BBB and the experimental model employed in this study used an established cell line (bEnd5 cell line). The cells in the BBB model displayed both morphological and functional characteristics of the ECs in an *in vivo* condition, with the expression of TJ proteins together with a plethora of intercellular junctional proteins acting as a seal between the paracellular

compartments of adjacent ECs, characteristic of ECs in the *in vivo* state (Nits et al., 2003).

2.3.3.2 Tissue culture procedure

Cryopreserved bEnd5 cells were removed from the -80°C freezer and thawed in a 37°C water bath. Quick thawing assisted with the removal of water crystals which could potentially damage cells. The bEnd5 cells were grown in DMEM, supplemented with 10% FBS, 1% anti-biotic: *Penicillin* and *Streptomycin*, 1% sodium pyruvate and 1% NEAA (Reiss et al., 1998; Steiner et al., 2011).

Cells were centrifuged at RT for 5 min at 1000rpm and the top of the cryovial was wiped with 70% EtOH, to prevent contamination and the supernatant was discarded. The cell pellet was re-suspended in 1ml medium and transferred to a 25cm² (50ml) tissue culture (TC) flask containing the desired amount of supplemented DMEM. A desired amount of bEnd5 cells (µl) were pipetted into the 50ml TC flask. Cells were incubated and cultures were maintained in an incubator set at 37°C and 5% carbon dioxide (CO₂) for 24 hrs until the cell culture expanded to confluence. After 24 hrs the cells were checked for attachment, a media colour change and cell confluence, using standard light microscopy (Inverted-phase microscope).

At 80-90% confluence, the bEnd5 cells, grown in a TC flask, were trypsinated. The media was decanted and 2-3ml PBS was used to rinse cells in order to remove any residue of media (DMEM) and remove unattached cells. The PBS was aspirated and decanted as waste. A 1ml of trypsin (0.25%) was added to the TC flask and incubated at 37°C and 5% CO₂ for 10-15 min. Trypsin (a proteolytic enzyme) dislodged the anchored cells by digesting the protein bonds that attached cells to the

floor of the TC flask (Huang and Hsing et al., 2010). If cells did not dislodge, further incubation for 1-2 min was carried out. In order to neutralize the solution, containing trypsinated cells, an equivalent amount (1ml) of media (DMEM) was added to the trypsinating cells. The detached cells were aspirated into a 15ml conical centrifuge tube (Biosmart Scientific, Cat no.PBIOT15) and centrifuged at RT for 5 min at 2500rpm. After centrifugation the supernatant was decanted and the appropriate amount of media was added to the cell pellet and resuspended until the pellet was dissolved. The required volume of cell suspension was added to TC flasks containing the appropriate amount of media.

A cell count, using Trypan blue (TB), proceeded after resuspension of the cell pellet, if necessary. This was carried out in order to seed an accurate amount of cells, specified for a particular assay/study. Cells were exposed to selected concentrations of EtOH, R_f and combinations of the two compounds. The concentrations were made up using v/v dilutions with supplemented DMEM, a 20% R_f stock and a 800mM EtOH stock, made from 99.9% EtOH.

2.4 Trypan blue assay

2.4.1. Operating principle

TB is a carcinogenic dye used for staining and identifying non-viable cells with compromised membranes. This assay differentiates between live and dead cells and is, therefore, able to determine both cell viability and cell toxicity. Non-viable cells absorb and retain the TB due to their non-selective permeability, whereas viable cells do not absorb the dye. Non-viable cells were stained blue and the viable cells

luminesced when viewed using standard light microscopy (Freshney et al., 2006; Mascotti et al., 2000).

2.4.2 Experimental treatments

2.4.2.1 Treatment with ethanol and fermented rooibos (*A.linearis*)

After a cell count, a cell density of 5×10^4 cells was seeded in 30, 35x10mm petri dishes (Cell Star, Cat no.627 160), using a sample number of 5 ($n=5$; day=0). The selected, physiologically relevant (25mM) (Barnes and Singletary, 2000) and supraphysiological (50mM, 100mM, 200mM and 400mM) concentrations of EtOH were utilized and R_f concentrations (%) (1, 0.05, 0.025, 0.0125, 0.0625) were utilized. At 24 hrs, after seeding cells, all treatments of the particular compounds were acutely exposed (once-off), including controls (exposed to standard supplemented DMEM). The cells were incubated at 37°C and 5% CO₂. After the respective time intervals of exposure to the compounds lapsed, the bEnd5 cells were trypsinated to get cells into suspension in order to perform the TB assay to determine live cell number, % live cell number and % cell toxicity was determined for 24, 48, 72, 96, 120 and 144 hrs.

800mM of an EtOH stock solution was prepared and filtered using a 0.45µm filter and selected concentrations made up by the use of 2-fold serial dilutions. The selected concentrations were added to the respective cell-containing petri dishes and after 24, 48, 72, 96, 120 and 144 hr exposure to the compound the bEnd5 cell number was determined.

R_f was filtered using a 0.45µm filter and selected concentrations were carried out by making 2-fold dilutions in a v/v ratio. The selected concentrations of % R_f were

exposed to the respective cell-containing petri dishes and after 24, 48, 72 and 96 hr exposure the bEnd5 cell number, % cell viability and % cell toxicity was determined.

2.4.2.2 Cell count using the Neubauer hemocytometer

An established ratio was used to score viable and non-viable cells, for the purpose of the counting method employed, using the Neubauer hemocytometer. A 0.4% TB solution was prepared using an isotonic solution (i.e. PBS, pH 7.2). The TB cell suspension was made up of 10 μ l cells, 30 μ l TB and 60 μ l DMEM. The bEnd5 cells were added to the solution last as TB would cause cell death after prolonged exposure. A 10 μ l of the TB cell suspension was added onto the respective sections of the hemocytometer and was observed under an inverted-phase contrast microscope (Zeiss). Cells were scored and changes in cellular proliferation were determined.

The percentage cell viability and cell toxicity was determined using the following equations:

- 1) The % cell viability was determined using the following equation:

$$\text{Cell Viability (\%)} = \frac{\text{No. unstained cells}}{\text{Total no. cells}} \times 100$$

- 2) The % cell toxicity was determined using the following equation:

$$\text{Cell Toxicity (\%)} = \frac{\text{No. stained cells}}{\text{Total no. cells}} \times 100$$

2.5 XTT cell viability assay

2.5.1 Operating principle

The 2,3-bis (2-methoxy-4-nitro-5-sulphophenyl)-2H-tetrazolium-5-carboxanilide (XTT) assay is a colorimetric cell assay used to determine the mitochondrial activity (MA), for the non-radioactive quantification of cellular proliferation in response to growth factors, cytokines and nutrients (Roche Applied Science, 2005) and the mitochondrial dehydrogenase (MDH) activity, which is only active in viable cells. The assay was based on the cleaving/reduction of the yellow tetrazolium salt (XTT) to an orange water-soluble formazan dye by metabolically active cells. This conversion only occurred in viable cells. The formazan dye formed was soluble in aqueous solutions and can be directly quantified using a scanning multi-well spectrophotometer-ELISA plate reader (Roche Applied Science, 2005; Biotium, Inc., 2011; Smith and Hunter, 2008).

An increase in the number of cells resulted in an increase in the overall activity of MDH in the cell sample. This increase was directly proportional to the amount of orange formazan product formed, as monitored by the absorbance (nm). For the purpose of this study, the assay focused on investigating the mitochondrial activity of the bEnd5 cell. Cells were incubated with XTT (2.5mg/ml in DMEM) for 4 hrs at 37°C and 5% CO₂. The remaining formazan crystals were formed and quantified by determining absorbance readings at a wavelength of 450nm, using a colorimetric 96-well microtiter plate reader.

2.5.2 Experimental Treatments

2.5.2.1 Treatment with ethanol and fermented rooibos (*A.linearis*)

The bEnd5 cells were seeded at a density of 2×10^3 cells/well ($n=5$; day=0) in 100 μ l of supplemented DMEM, in a 96-well TC microtiter plate. The cells were allowed to attach to the wells overnight (24 hrs). Culture media (supplemented DMEM) was removed and the cells were treated with selected concentrations of % R_f using a range of: 0.05, 0.025, 0.0125, 0.00625 and 0.003125 and EtOH (mM) using a range of: 25, 50, 100, 200, 400 and 800 mM. In combination, cells were exposed using 0.05% and 0.1% R_f with 25mM, 50mM and 100mM EtOH. A 24, 48, 72 and 96 hr incubation period was carried out for both R_f and EtOH and combination treated cells. The cells were treated both daily (chronic) and once-off (acute) for each treatment. 50 μ l of yellow, reconstituted-XTT solution was added to the compound-treated cells making up a final volume of 150 μ l/well, followed by incubation for 4-24 hrs at 37°C and 5% CO_2 . Orange formazan product was formed, which was spectrophotometrically quantified using an ELISA plate reader. Absorbance was read at a wavelength of between 450-500nm and % MA was determined using the following equation:

$$\% \text{ MA} = \frac{\text{Experimental absorbance abs} - \text{Media abs}}{\text{Control abs} - \text{Media abs}} \times 100$$

***Note:** Care was taken by refraining to check cells before a 24 hr time lapse, as it could disturb the cells and ultimately disturb attachment.

2.6 Transendothelial electrical resistance across a bEnd5 cell monolayer

2.6.1 Operating principle

Transendothelial electrical resistance (TEER) was based on measuring the membrane potential and resistance across an EC monolayer as a model of the BBB *in vitro*. It was used to assess the integrity of the cell membrane by quantitatively measuring cell confluence and qualitatively measuring cell monolayer health. These are important measurements required for studying bioelectrical changes in transendothelial permeability.

(www.gbo.com/bioscience; www.millipore.com/millicell) .

2.6.2 Experimental model of the blood-brain barrier

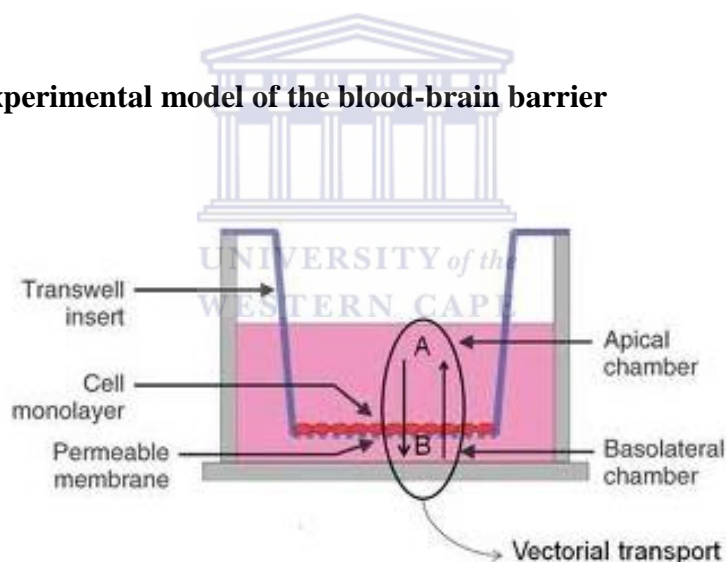


Figure12. Schematic diagram of a bicameral chamber representing a confluent monolayer of the bEnd5 cells *in vitro*

(http://www.pharmadirections.com/_blog/Formulation_Development_Blog/post/Biopharmaceutics_Classification_System_and_In-vitro_membrane_models/)

The laboratory model of the BBB *in vitro* employed the use of a bicameral chamber, illustrating a tridimensional architecture, comprised of a hollow, fiber, filter insert-substrate membrane scaffolding (Millicell[®], Cat no. PIHA 012 50). The insert was

designed so that it simulated the physiological structure of the basement membrane. Thus, it is made up of mixed cellulose esters and closely mimics the basement membrane.

The BBB model mimicked the *in vivo* BBB in that ECs constitute the main component of the BBB. This bEnd5 cell line, utilized in this model, effectively represented these conditions as these cells expressed polarized morphology and TJs, as in the *in vivo* situation. The bioelectrical resistance across the bEnd5 monolayer was investigated as an inversely proportional indicator of changes in transendothelial permeability, thus, changes in resistances were directly related to a change in permeability and subsequently affected changes in paracellular seals which could have indicated whether TJs were compromised or not (Nitz et al., 2003). The cells were grown on the mixed cellulose esters membrane (transwell filter insert) which mimicked the *in vivo* basement membrane. It displayed distinct apical and basolateral compartments which simulated the luminal (blood/plasma) and abluminal (brain) compartments of the physiological conditions which exist within the *in vivo* brain microenvironment surrounding the BBB.

2.6.3 The extracellular insert membrane

TEER was assessed post-treatment across the confluent bEnd5 cell monolayer, using an Ohm Millicell-ERS[®] (Electrical Resistance System/Volt-Ohm meter) (Millipore[™], Cat no. MERS 000 01). The Millicell[®] 24-well tissue culture inserts (Millicell[®], Cat no.PIHA012) with a pore size of 0.45 μ m, filtration diameter of 12mm and an effective filtration area of 0.6cm² was used. The filter membrane of the insert contained mixed cellulose esters, according to the manufacturers'

specifications. Millicell[®]-inserts were placed in 24-well TC microtiter plates (Adcock Ingram, Cat no.3524). High resolution SEM was used to elucidate the structure of this extracellular membrane support.

2.6.4 Seeding for TEER

The bEnd5 cells were seeded on non-coated culture inserts (Millicell[®], Cat no. PIHA012) at a cell density of 1×10^6 cells/well/insert, at 37°C and 5% CO₂ (n=4; day=0). The bEnd5 cells were allowed to attach to the bottom of the filter insert overnight, until the cells expanded to confluence. The bioelectrical effect of 500nM hydrocortisone (HC), EtOH, R_f and combinations of the compounds was bioelectrically investigated for 24, 48, 72, 96, 120 and 144 hrs, by recording TEER readings.

2.6.5 Measuring the resistance across a bEnd5 cell monolayer

The 24-well TC plates containing bEnd5 cells, seeded on the membrane insert, were removed from the 37°C incubator and were allowed to acclimatize to ambient temperatures for 20-30 min. Aseptic techniques were employed to maintain culture sterility. The electrodes were placed in EtOH for 15 min, followed by exposure to PBS for 15 min which served as an electrolyte solution for the stabilization of the electrode interface.

The mode of the epithelial Volt-Ohm meter was switched to resistance (“R”) and the power switched on. The electrode was immersed in the 24-well plates, positioning the probe such that the shorter electrode was immersed in the media inside the filter, which represented blood and the longer electrode placed through the basolateral

access hole in the media within the growth plate/well, which represented the brain. Resistance was measured, holding the electrode static for 5min or until the meter indicated a stable resistance reading for the respective solution, thereafter, the resistance reading was recorded. All readings were taken in duplicate, thrice per day for conclusive results.

Care was taken to ensure that the shorter electrode did not make contact with cells growing on the membrane to prevent the risk of piercing the cell monolayer and the thin insert membrane. Which, in the event of breakage, would create an open circuit between the apical and basal compartments.

2.6.5.1 True resistance across an insert membrane

TEER baseline resistance (true resistance) readings, (a Millicell® insert “without” cells) was subtracted from the resistance reading for each condition “with” cells (Millipore™) using the following equation:

$$\text{True resistance} = (\text{Experimental reading} - \text{Blank reading}) \times 0.6\text{cm}^2$$

2.7 Optimization of TEER and experimental treatments

2.7.1 Optimization of TEER using hydrocortisone

EC monolayers were treated in a time-dependent manner in the presence of a physiologically relevant level of hydrocortisone (HC) (500nM) (Sigma-Aldrich, Cat no.H0888-5G) (Weidenfellar et al., 2005; Hoheisel et al., 1998) in combination with DMEM containing: 10% FBS or 0% FBS (serum free media-SFM). This was done in order to determine which culture conditions generated optimal TEER readings. The

bEnd5 cells were subjected to daily exposure of HC-treated media (chronic treatment). For optimal TEER conditions a cell culture environment containing 500nM HC-supplemented SFM was established.

***Note:** Media was replaced every morning for 24-144hours (6 days) before TEER measurements were recorded to prevent the influence of pH changes in the media to affect resistance readings across the bEnd5 cell monolayer.

With respect to %R_f concentrations: 0.1, 0.05, 0.025, 0.0125 and 0.00625 was used. After 24 hrs, media was replaced as follows: The blank always contained SFM (DMEM with 0% FBS), the control was replaced with SFM supplemented with 500nM HC. R_f and EtOH concentrations were replaced with the same, respective R_f and EtOH concentrations made up with SFM supplemented with 500nM HC.

2.7.2 Effect of ethanol on TEER

The bEnd5 cells were seeded at a density of 1×10^6 cells/well/insert (n=4; day=0) using supplemented DMEM (with 10% FBS). Upon cell confluence, after 24 hrs, supplemented-DMEM was removed and the EC monolayers were treated by daily (chronic) exposure to EtOH, within an optimized TEER system. The EtOH range used was both within physiological (25mM) and a supraphysiological range (50mM, 100mM and 200mM) (Barnes and Singletary, 2000) in the presence of 500nM HC-supplemented SFM. TEER was measured using the MilliporeTM electrical resistance apparatus (Millicell-ERS[®] epithelial Volt-Ohm meter -MilliporeTM).

2.7.3 Effect of fermented rooibos (*A.linearis*) on TEER

The bEnd5 cells were seeded at a density of 1×10^6 cells/well/insert (n=4; day=0) using supplemented DMEM. Upon cell confluence, the culture media was removed and the EC monolayers were treated by daily (chronic) exposure to %R_f, within an optimized TEER system. The % R_f range used was: 0.1, 0.05, 0.025, 0.0125 and 0.0625 in the presence of 500nM HC-supplemented SFM. TEER was measured using the Millicell-ERS[®] epithelial Volt-Ohm meter -Millipore[™].

2.7.4 Effect of combination treatments of ethanol and fermented rooibos (*A.Linearis*) on TEER

The bEnd5 cells were seeded at a density of 1×10^6 cells/well/insert (n=4; day=0) using supplemented DMEM (with 10% FBS). Upon cell confluence, supplemented-DMEM was removed and the EC monolayers were treated by daily exposure to %R_f concentrations (0.05% and 0.1%) in combination with EtOH concentrations of 25mM, 50mM and 100mM, within an optimized TEER system, in the presence of 500nM HC-supplemented SFM. TEER was measured using the Millicell-ERS[®] epithelial Volt-Ohm meter -Millipore[™].

2.8 Electron Microscopy

2.8.1 Scanning Electron Microscopy

The use of the high resolution scanning-electron microscope (SEM) has become very advantageous as a result of its ability to produce images using both high magnification and great depth of field (DOF). Since SEM is able to make use of high levels of magnification, it aids in bridging the gap between the light microscope, which produces more superficial images and the transmission electron microscope (TEM). The micrographs of a typical SEM contain a substantial amount of information addressing the morphological and topographical information about a specimen (Postek et al. 1980). In recent years SEM has become widely employed by various fields of study, from the physical to biological sciences. During analyses of biological specimen, SEM imaging generates a three-dimensional image which provides useful information about the cell membrane's surface morphology and topography.

2.8.2 Operating principle

A typical SEM includes an electron gun which emits electrons, which are then accelerated to high kinetic energy (in excess of 20 keV) by means of an electron high tension tank – this generates an electron beam. The beam passes through a series of electromagnetic lenses, apertures and coils which aid in focusing the thin primary electron beam onto a specimen. The primary electron beam moves through a vacuum within the microscope and scans over the surface of the specimen. Upon interaction of the primary electrons (i.e. the electron in the beam) with the specimen, secondary electrons are emitted from the specimen surface, which are then collected

by a detector, which processes these to form an electronic image (Postek et al., 1980; Ayache et al., 2010) (See Fig. 13 below). In this work, only the secondary electrons generated from the specimen surface were used to form an image. Figure 14 shows a cross-sectional schematic of the lay-out of a typical SEM, in which the components as discussed above are shown.

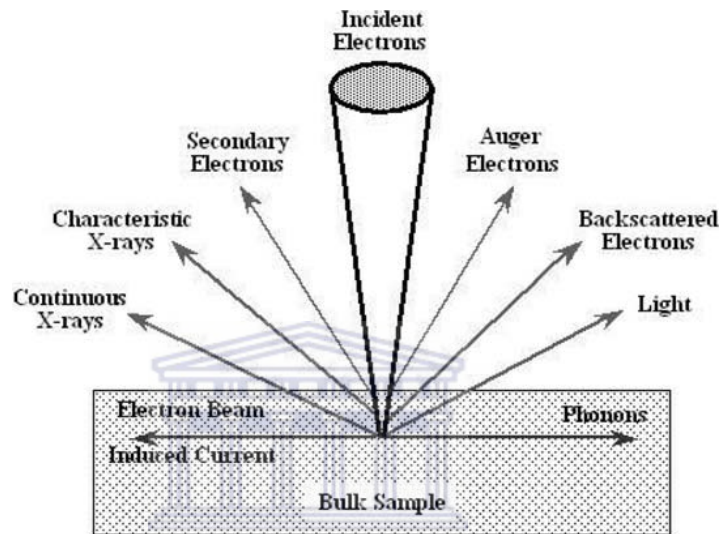


Figure 13. Schematic representation of the different signals that are generated upon interaction of the primary electron beam with the specimen surface (Yao and Wang, 2005)

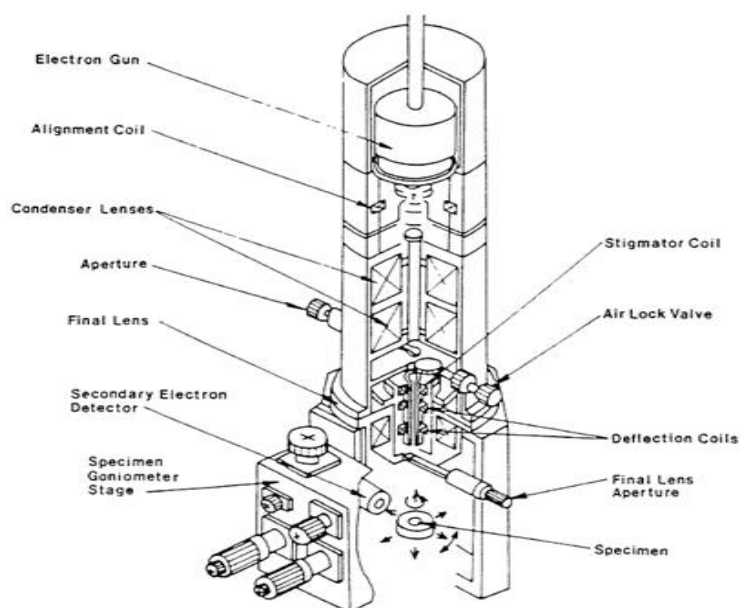
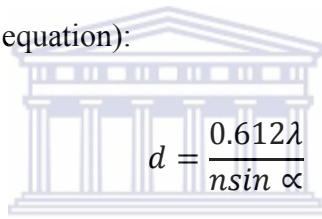


Figure 14. Schematic representation of a SEM column (Postek et al., 1980)

2.8.3 Resolution and Depth of Field

The limit of resolution of the standard light microscope is a limiting factor in better understanding the BBB. SEM enables the investigation of the cell membrane surface structures and in so doing, enables distinguishing between healthy cell structures in relation to altered cell morphology. For the purpose of this study images of the bEnd5 cell monolayer was observed at a resolution of approximately 1nm.

The resolution of any given image is referred to as a measure of the distance at which the two objects/entities are observed, such that a distinction can be made between the two different entities. The limit of resolution can be determined by the follow equation (Abbe's equation):



$$d = \frac{0.612\lambda}{n \sin \alpha}$$

where d = limit of resolution

λ = wavelength of the energy source

n = refractory index of the medium through which the energy source travels

α = aperture angle

Another important factor during analyses using SEM is the DOF, which refers to the extent of the zone on a specimen which appears acceptably in focus (Postek et al., 1980). A good quality SEM image will contain a large DOF so that an appreciable portion of the specimen is in focus.

Mathematically the relationship for the DOF is given by:

$$DOF = \frac{0.612\lambda}{n \sin \alpha \tan \alpha}$$

2.8.4 Factors affecting resolution and DOF

The first affecting factor is the aperture size. An aperture is a minute hole in a strip of metal that is placed in the path of the electron beam. It functions in restricting electron progress down the machine column. The aperture plays a role in stopping off-axis or off-energy electrons. An additional influencing factor is the working distance, which is referred to as the distance between the final lens and the upper portion of the specimen as shown in **Fig. 15** below. The working distance has been found to influence the DOF as shown in **Fig. 15**. At low working distances, a large aperture angle is found, which results in a small DOF. Conversely, at large working distances, small aperture angles are created, resulting in larger DOFs. In addition, a reduced working distance has been found to decrease spherical aberration (a defect of the electromagnetic lens system) resulting in a more focused beam and subsequently an image with higher resolution (Postek et al., 1980)

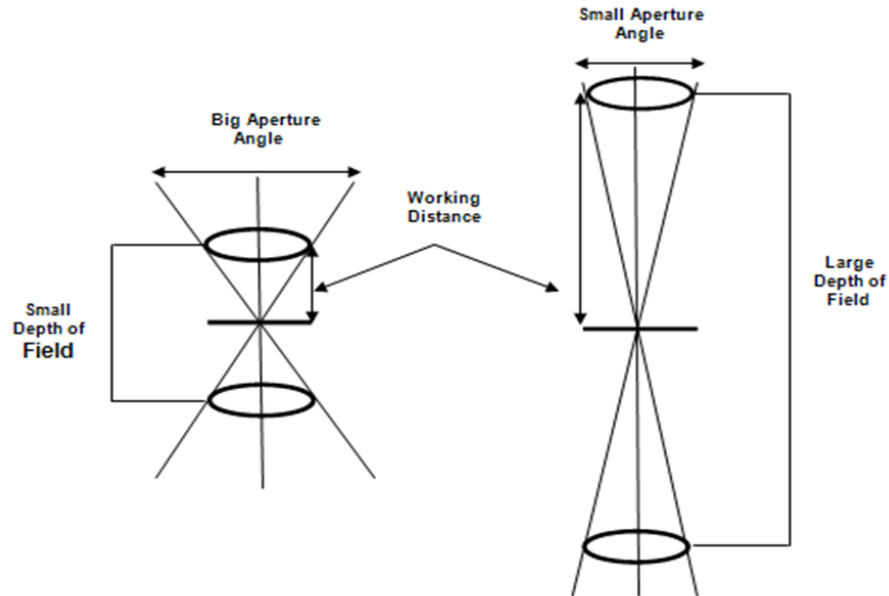


Figure 15. Illustration of the effects of working distance and aperture size on resolution and DOF (Cummings, 2006)

2.8.5 Protocol for imaging a biological specimen using high resolution SEM

2.8.5.1 Chemical fixation

A large amount of biological samples tend to be delicate in its native state and as a result they are prone to damage with excessive handling during sample preparation procedures. For the basis of microscopical studies, two means of fixation may be carried out, namely, chemical fixation and/or cryofixation (Ayache et al., 2010). However, for the purpose of this study we have employed chemical fixation procedures. Chemical fixation involves the stabilization and preservation of strongly hydrated biological samples such as, cells and tissue in their native state; this is achieved by the formation of new chemical bonds within the sample, making its proteins insoluble. These proteins become bridged and transformed into a cross-linked network and this new network formation reduces specimen distortion during the process of dehydration (Ayache et al., 2010).

Chemical fixation typically involves the use of aldehydes such as, paraformaldehyde or glutaraldehyde or the oxidant, osmium tetroxide, which is generally used for post-fixative purposes. Fixatives are usually made up within a concentration range of 0.5-4% in a buffer with suitable pH of balanced salts (Postek et al., 1980; Ayache et al., 2010).

For the purpose of this research study, the bEnd5 cells were grown on a support (12mm Millicell[®] transwell insert). The cells were seeded using densities of 1×10^4 and 1×10^6 cells/well (day = 0; n = 3) and incubated at 37°C and 5% CO₂ overnight. After 24 hrs, cells were exposed to complete culture medium (supplemented DMEM) for 24, 48, 72, 96, 120 and 144 hrs.

A 2.5% solution of glutaraldehyde (BioChemika/Fluka- Sigma-Aldrich, Cat no. 49626) was prepared in standard buffer- PBS solution (pH 7.2) (Faso et al., 1994) on the day of sample preparation. After exposure to standard DMEM-F12, at the respective time intervals, the mixed cellulose ester insert membrane, containing bEnd5 cell growth, was removed using forceps. The insert was inverted and the fibrous filter removed using a lancet. The specimen was placed in the 2.5% glutaraldehyde solution and after an hr lapsed the specimen was removed and washed in PBS (without glutaraldehyde) for 5 min (x2) and, thereafter, washed in dH₂O for 5 min (x2)

The cell specimens were removed from the dH₂O and placed in: 50%, 70%, 90%, 95% and in 100% EtOH for 10 min each. The specimen was removed from the 100% EtOH after 10 min and placed in a fresh solution of 100% EtOH before drying (Faso et al., 1994).

***Note:** All EtOH solutions were made up by diluting it in dH₂O/de-ionized H₂O

2.8.5.2 Critical point drying

Critical point drying (CPD) was performed on the fixated, dehydrated cells using an Hitachi HCP-2 CPD. CPD is conceptualized when liquid is placed in a container (sealed) leaving some vapor space and the container is heated; the vapor pressure would become greater and at the same time the liquid would expand and become less dense. The combination of temperature and pressure at which the density of the vapor is the same as the liquid, is the critical density also known as the critical point (CP). At this point the surface tension is zero and there is no difference between liquid and gas. The pressure at which the distinction between liquid and vapor disappears is the critical pressure (73.8 kg/cm^2). The temperature is denoted as the critical temperature, at this point (Bozzola and Russell, 1999).

The dehydrated cells, grown on top of the cellulose supports, were removed from the 100% EtOH solution and placed inside a 10mm diameter aluminium basket, whose bottom was covered with filter paper. These baskets were then placed inside the CPD chamber. This process was done as quickly as possible to prevent drying of the sample in air. For the injection of CO_2 , the valve of the Hitachi CPD was slowly opened and the chamber was filled with CO_2 within 50-80% of the chamber capacity. Injection of CO_2 was done gently in order to prevent specimen damage. The amount of liquid nitrogen injected is important. It must be between 50% and 80% of the total chamber volume, as the chamber would not reach the CP with inadequate liquid. Once filled, the inlet valve and the CO_2 cylinder valve were closed. The temperature control dial was set to 20°C . The power lamp glowed red and the fan switched off if the chamber reached 20°C . The chamber was allowed to

reach the respective temperature for a 10-20 min time lapse (depending on the hardness of the sample).

The purpose of CPD was to rid the biological specimen of EtOH without distortion of the specimen. The CP of CO₂ is (31°C, 73.8 kg/cm²) – at this temperature and pressure the supercritical CO₂ replaces the 100% EtOH without disturbing the native state of the cells. The temperature control dial of the Hitachi CPD was set to 37°C and the pressure was monitored carefully, ensuring that it increases to the CP (73.8kg/cm² or more). If the pressure increased to more than 180kg/cm² the exhaust valve was opened gently, in order to discharge liquid. Thereafter, a time lapse of 3-5 min was allowed, until the power lamp glowed red and the fan switched off, indicating that the chamber had reached 37°C. The temperature was kept at 37°C and the leak valve was opened. As the gas steadily discharged, the pressure gauge decreased down to a zero. This completed the drying process of the cells.

2.8.5.3 Sputter coating and SEM imaging

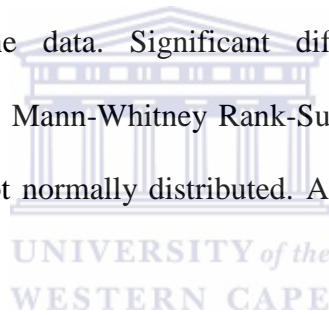
After CPD, the biological specimens were placed onto double-sided sticky carbon tape (PELCO TabsTM, Cat no. 16084-1), which covered aluminium stubs with a diameter of 12.5mm and 8mm pin size (Agar Scientific, Cat no. AGG301). Carbon was used to avoid spurious readings which occur with a metal. Thereafter, the stub, containing the specimen was placed in a Quorum Q150T ES sputter coater for the coating of the biological specimen. The sample was coated with gold-palladium at a ratio of 60:40, Au: Pd. An electrical field was created between a gold-palladium stub and the biological sample. The chamber was pumped with Argon gas, which was stripped of its electrons creating plasma, which aided in the coating of the sample

with the gold palladium. The sample was imaged using a Zeiss Auriga high resolution field-emission gun SEM, which was operated at electron beam energy of 5keV.

All images were taken using an in-lens secondary electron detector, which allowed for high resolution imaging. For all samples, a nominal working distance of 5mm was used.

2.9 Statistical analysis

Results were expressed as the mean \pm SEM. Medcalc (version 11.6.1) was used to statistically analyze the data. Significant differences between groups were determined by using the Mann-Whitney Rank-Sum test for independent (unpaired) samples, which were not normally distributed. A probability of $P < 0.05$ designated statistical significance.



Chapter 3: Results

3.1 Chemical analysis and determination of antioxidant capacity of fermented rooibos (*A.linearis*) herbal tea

The chemical analysis and characterization of an aqueous extract of fermented rooibos (R_f) were executed at the Cape Peninsula University of Technology (CPUT), Oxidant Research Laboratory, Bellville, Cape Town, South Africa under the supervision of Prof. J. Marnewick. Chemical analysis was carried out to determine the polyphenol, flavonol and flavanol content. Analysis revealed that the sample contained significant amounts of polyphenols which included aspalathin, an array of flavonols, as well as small amounts of flavanols. Antioxidant (AO) assays on the R_f sample included ferric reducing antioxidant power (FRAP) assay oxygen radical absorbance capacity assay (ORAC) assay, and the ABTS (2, 2'-azinobis (3-ethylbenzthialozine-6- sulphonic acid) (TEAC-Trolox equivalent antioxidant capacity) assay.

The chemical analysis showed a total polyphenolic content of 54.34mg/g (dry weight) and 1086.24mg/100ml (aqueous R_f), the presence of flavonols of 7.80mg/g (dry weight) and 156.05mg/100ml (aqueous R_f) and flavanols of 4.55mg/g (dry weight) and 90.96mg/100ml (aqueous R_f). Spectrophometric data also demonstrated 1.065mg/g aspalathin (dry weight) and 21.3mg/100ml (aqueous R_f).

AO assays demonstrated that the aqueous extract exhibited antioxidant potential.

Table 4. Polyphenolic composition of an aqueous extract of fermented *A.linearis*

	Equivalents	Quantity/100ml <i>(Expressed as aqueous R_f)</i>	Quantity/gram <i>(Expressed as dry weight R_f)</i>
Polyphenols			
Total Polyphenols	Gallic acid (GAE)	GAE 1086.24mg	GAE 54.34mg
Aspalathin	Aspalathin	21.3mg	1.065mg
Flavonols	Quercetin (QE)	QE 156.05mg	QE 7.80mg
Flavanols	Catechin (CE)	CE 90.96mg	CE 4.55mg
Antioxidant Assays			
FRAP	Ascorbic acid (AAE)	AAE 7395µmol	AAE 370µmol
ORAC	Trolox	TE 21149µmol	TE 1057µmol
ABTS	Trolox	TE 4906µmol	TE 245µmol
<p>*AAE= Ascorbic acid equivalents *CE = Catechin equivalents *GAE= Gallic acid equivalents *QE = Quercetin equivalents *TE = Trolox equivalents</p>			

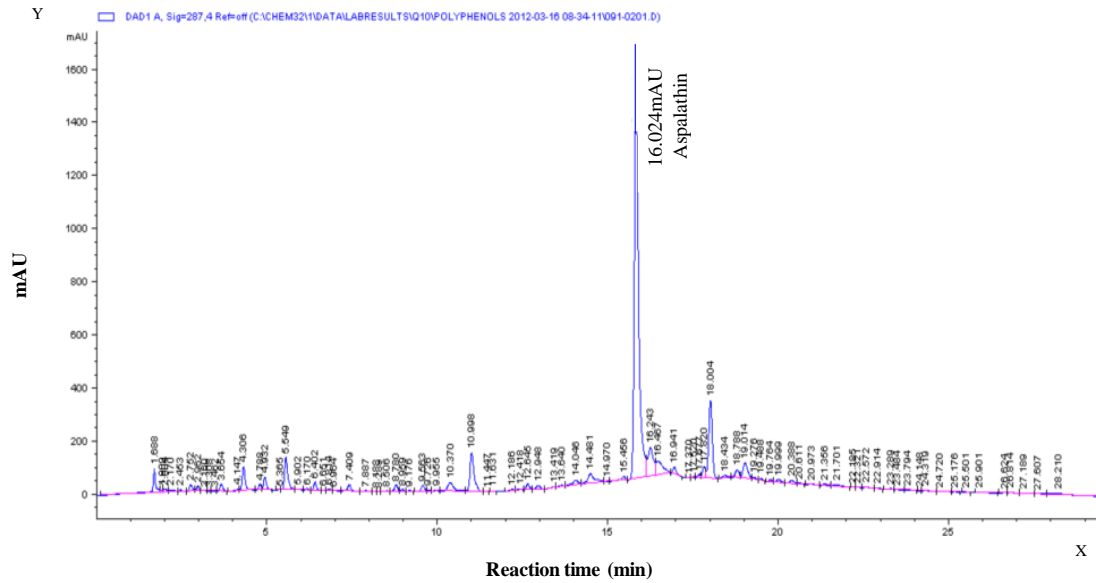


Figure 16. Illustration of HPLC results illustrating polyphenols present in an R_f sample.

Chromatographic analysis of the R_f sample generated a prevalent absorbance value of 16.024 mAU, confirming the presence of aspalathin.

Flowrate: 1ml/min

Column temperature: 23°C

Column: YMC-Pack Pro C18, 150 x 4.6mm I.D.

Runtime: 30 minutes

Detection wavelength: 287nm

Injection volume: 20ul

Mobile phase A: Water containing 300ul/L Trifluoroacetic acid

Mobile phase B: Methanol containing 300ul/L Trifluoroacetic acid

Gradient:

0 min: 35 % B

0-5 min: 35% B

5-25 min: 35% B to 80% B

25-28 min: 80% B to 35% B

28-30 min: 35% B

3.2 Trypan blue assay

3.2.1 Effect of acute ethanol exposure on live cell count

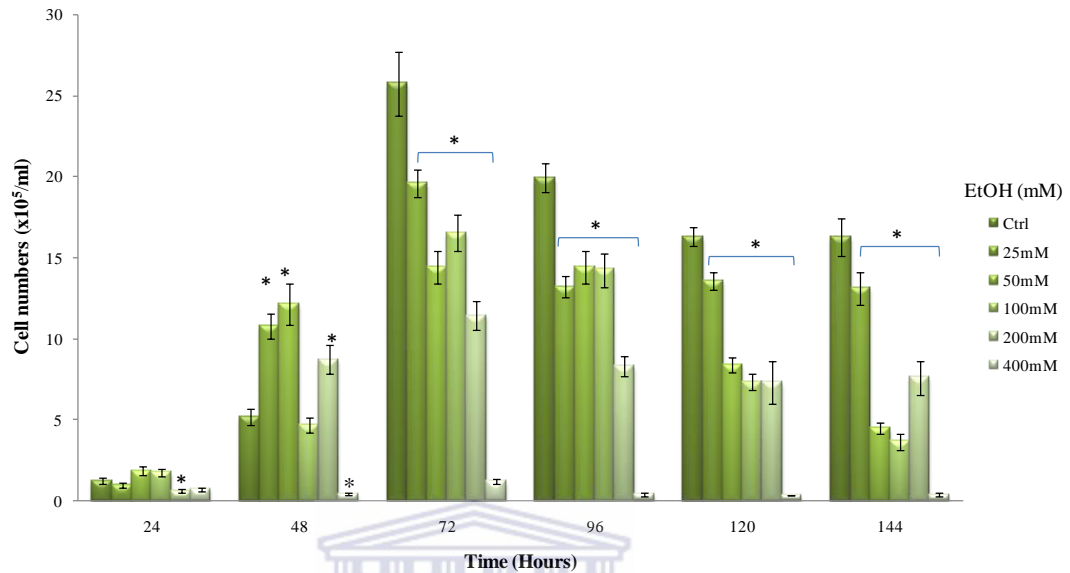


Figure 17. Effect of acute EtOH exposure on live cell count of bEnd5 cells compared to controls for selected time intervals. The *, denoted statistically significant differences in live cell numbers, between the experimental samples relative to controls. Data was represented as mean \pm SEM (n=5). Statistical significance was determined at a P-value <0.05 (See Methods); (See Appendix C, Table 1).

At 24 hrs, no significant differences in cell numbers was observed, relative to the controls with the exception of 200mM EtOH where a significant decrease in live cell numbers was observed, relative to the controls ($P < 0.027$). At 48 hrs, statistically significant differences in cellular proliferation was observed across all concentrations (25mM-400mM) of EtOH with the exception of 100mM EtOH, compared to the controls ($P < 0.009$). At 72 hrs statistically significant suppression in cell numbers were reflected across all EtOH concentrations in comparison to the controls ($P < 0.027$). After 72 hrs, a dose-dependent suppressive effect in cellular proliferation occurred for acute exposure to EtOH. At 96 hrs significant decreases in

live cell number was observed across all EtOH concentrations from 25mM to 400mM EtOH, relative to the control ($P<0.0001$). In addition, all time intervals demonstrated a significant decrease in cell numbers at the highest concentration of EtOH (400mM) which was unable to recover for the entire experimental timeframe ($P<0.0001$) (See Fig. 17).

3.2.2 The toxic effect of acute ethanol exposure on bEnd5 cells

The Trypan blue % viability was approximately within the 100th percentile across the experimental time interval from 24-144 hrs. The effect of the EtOH (mM) concentrations showed little to no toxicity (See Table 5. below).

Table 5. Effect of acute EtOH exposure on % toxicity using the Trypan blue assay.

EtOH (mM)	24hr	48hr	72hr	96hr	120hr	144hr
Ctrl	0.00	0.00	0.00	0.00	0.00	0.00
25	1.71	0.00	0.00	0.00	0.00	0.54
50	0.00	0.00	0.00	0.00	0.00	0.00
100	0.00	0.00	0.00	0.175	0.00	0.00
200	0.00	0.00	0.00	0.00	0.00	0.33
400	0.00	0.00	0.00	0.00	0.00	0.00

3.2.3 Effect of acute fermented rooibos exposure on live cell count

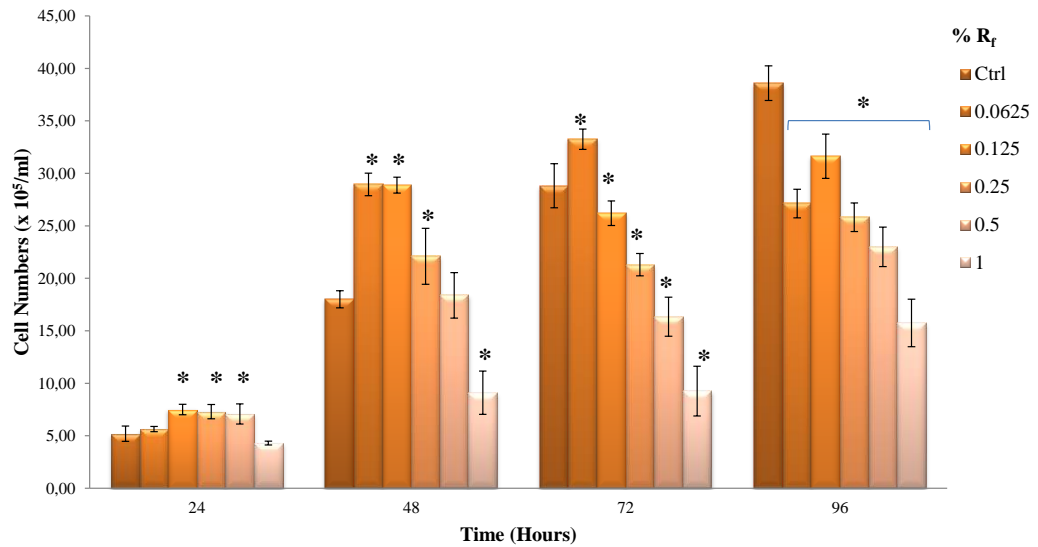


Figure 18. Effect of acute exposure to R_f on live cell count of bEnd5 cells compared to controls at selected time intervals. Our dose range was chosen based on its biphasic effects on the bEnd5 cell line, thus, this was the concentration required. The *, denoted statistically significant differences in cell numbers, between the experimental samples relative to controls. Data was represented as mean \pm SEM (n=5). Statistical significance was determined at a P-value <0.05 (See Methods); (See Appendix C, Table 4).

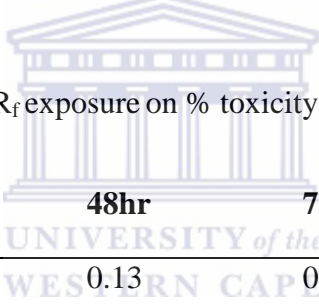
The initial effect at 24 hrs, resulted in all of the R_f concentrations reflecting an increase in cellular proliferation, with statistical significant increases at: 0.125%, 0.25% and 0.5 % R_f ($P < 0.049$), relative to the controls. At 48 hrs, 1% R_f remained significantly ($P < 0.002$) lower than the controls and 0.5% R_f appeared similar to the controls, with no statistically significant differences, however, the remaining R_f concentrations (0.0625%-0.25%) caused significant increases ($P < 0.001$) in cellular proliferation, relative to the controls. At 72 hrs, exposure to the lowest R_f concentration (0.0625%) expressed cell numbers significantly greater than the control ($P < 0.0002$), thereafter, a dose-related decrease was observed from 0.125% to 1% which resulted in cell numbers significantly lower than the control samples

($P < 0.0043$). At 96 hrs, all concentrations resulted in cell numbers significantly suppressed to values below those of the controls ($P < 0.007$). The control showed a linear increase in cell numbers over time, whereas 0.25% R_f becomes significantly suppressed over time and a negative effect takes longer to occur for the lower (0.0625% and (0.125%) concentrations of R_f (See Fig 18).

3.2.4 The toxic effect of acute fermented rooibos exposure on bEnd5 cells

The Trypan blue % viability was approximately within the 100th percentile across the experimental time interval from 24-96 hrs. The effect of the % R_f concentrations showed little to no toxicity (See Table 6. below).

Table 6. Effect of acute R_f exposure on % toxicity using the Trypan blue assay.



% R_f	24hr	48hr	72hr	96hr
Ctrl	1.53	0.13	0.00	0.58
0.05	4.17	0.51	0.00	1.96
0.0625	0.00	0.00	0.00	0.52
0.125	0.43	0.06	1.00	0.11
0.25	0.23	0.00	0.30	2.47
0.5	1.53	0.31	0.56	0.65
1	1.73	0.00	0.57	0.20

***Note:** The toxicity is reflective of the cidal and/or the anti-proliferatory effect of the EtOH and R_f on bEnd5 cell viability and proliferation as defined by the number

of dead cells, compared to the total number of cells (See Methods, Chapter 2, Section 2.4.2.2.).

3.3 Effect of selected compounds on mitochondrial activity using the reduced formazan (XTT) assay

Most experiments in the literature operate on a 96 hr time interval. For the purpose of this research study in some instances the timeframe needed to be extended beyond the 96 hrs, to 120 hrs or 144 hrs, if necessary. The mitochondrial activity (MA) reflected the amount of formazan formed within the assay which is reflective of a relative amount of MDH activity (See Chapter 2; 2.5.1: Materials and Methods).

3.3.1 Effect of acute ethanol exposure on bEnd5 mitochondrial activity

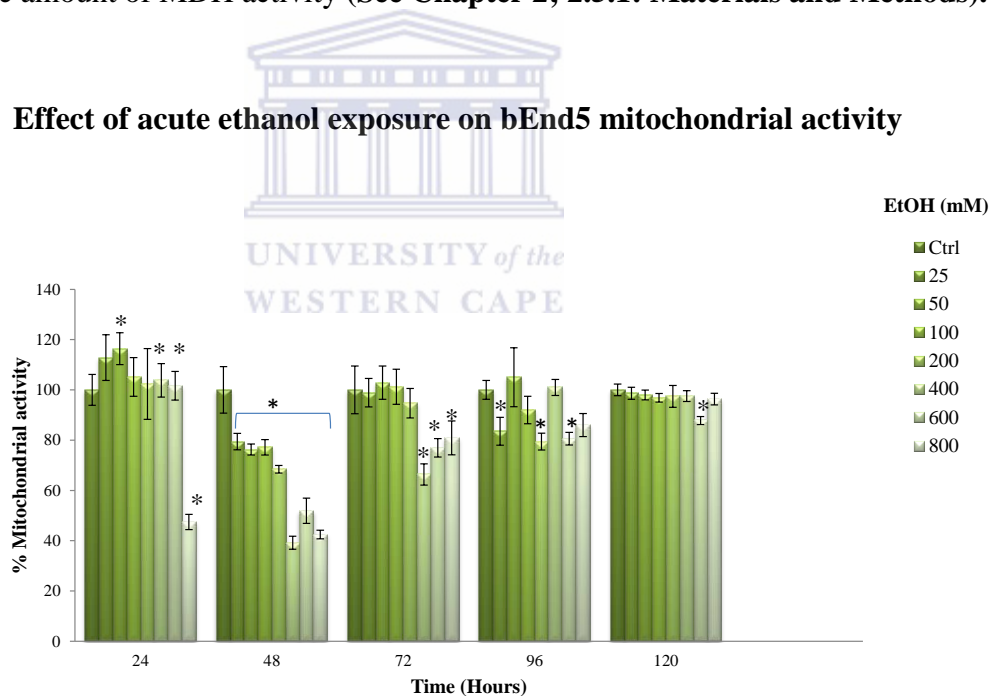


Figure 19. Effect of acute EtOH exposure on bEnd5 MA in comparison to controls at selected time intervals. The *, denotes statistically significant differences between experimental samples, compared to the controls. Data was represented as mean \pm SEM (n=5). Controls were normalized to 100% and data was expressed, relative to the control. Statistical significance was determined at a P-value <0.05 (See Methods); (See Appendix C, Table 2).

At 24 hrs, acute exposure to EtOH elevated the bEnd5 cell MA, relative to the controls. The lower concentrations of EtOH caused the bEnd5 cell MA to elevate, with only 50mM EtOH being significantly greater than controls ($P<0.006$), while the higher concentrations of 600mM and 800mM EtOH expressed significantly suppressed MA ($P<0.018$). At 48 hrs the MA was significantly suppressed across all EtOH concentrations, relative to the controls ($P<0.055$). By 72 hrs the effect of the concentrations 25mM-200mM showed no significant differences, whereas the highest concentrations of 400-800mM EtOH were still significantly suppressed compared to the controls ($P<0.009$). All cells expressed normal MA between 96-120 hrs so that at 120 hrs only one concentration displayed some difference, with significance only observed at 600mM EtOH exposure, relative to the controls ($P<0.0095$) (See Fig. 19).

3.3.2 Effect of chronic ethanol exposure on bEnd5 mitochondrial activity

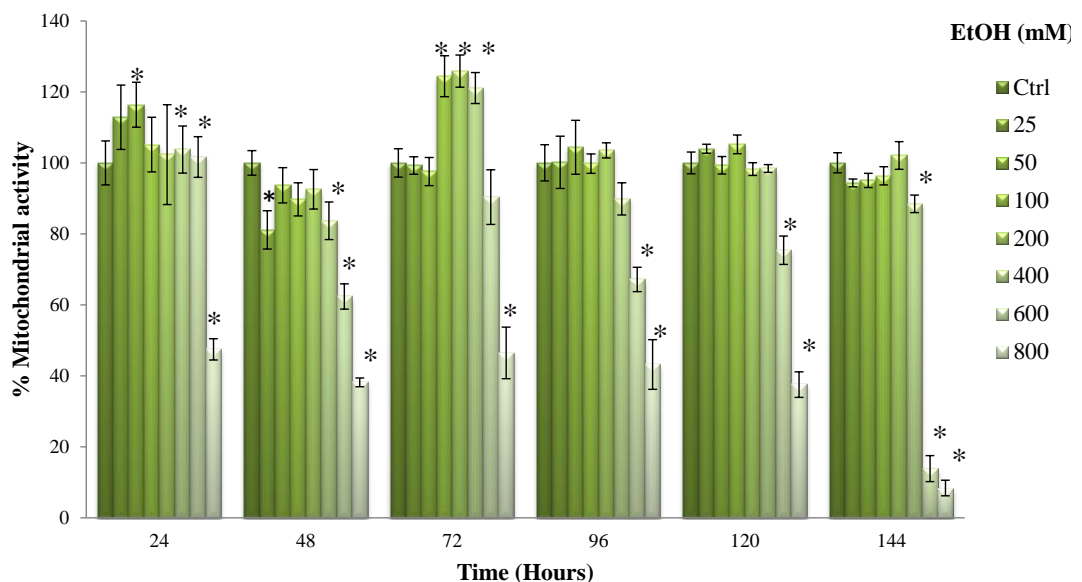


Figure 20. Effect of chronic EtOH exposure on bEnd5 MA in comparison to controls at selected time intervals. The *, denotes statistically significant differences between experimental samples and controls. Data was represented as mean \pm SEM (n=5). All controls were normalized to 100% and data

was expressed, relative to the control. Statistical significance was determined at a P-value <0.05 (See **Methods**); (See **Appendix C, Table 3**).

As opposed to the acute EtOH, which exposed cells for a 24 hr period, during chronic exposure cells were exposed to media daily, with the same EtOH concentrations. At 24 hrs, chronic EtOH exposure to the bEnd5 cells elevated its MA across all EtOH concentrations. This result was only significantly different for the higher concentrations of 600mM and 800mM EtOH treatments when compared to the controls ($P<0.018$). At 48 hrs, EtOH visibly suppressed MA across all EtOH concentrations compared to all the respective time intervals of exposure, with significant differences observed at the lowest concentration of 25mM EtOH and the higher concentrations of 400mM, 600mM and 800mM EtOH ($P<0.037$). Compared to the acute suppression, it is greater at 72 hrs at the lower concentrations, with no significant differences between the control and EtOH exposed cells. In the range of 100mM-400mM the bEnd5 MA was significantly elevated ($P<0.025$) and significantly suppressed at 800mM ($P<0.004$). By 96 hrs the concentrations displayed an elevation in MA, thereafter, expressing results similar to that of the control, however, the two highest concentrations were highly suppressed, compared to controls ($P<0.018$) and this phenomenon occurred for most of the experimental timeframe, from 24-144 hrs (See **Fig. 20**).

3.3.3 Effect of acute fermented rooibos exposure on bEnd5 mitochondrial activity

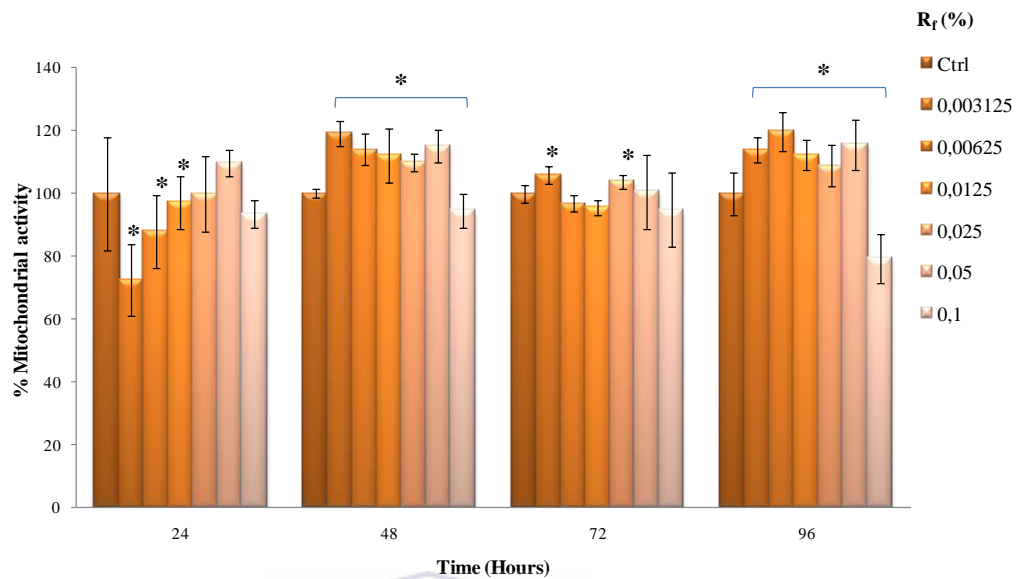


Figure 21. Effect of acute R_f exposure on bEnd5 cell MA in comparison to controls at selected time intervals. The *, denotes statistically significant differences between experimental samples and controls. Data was represented as mean \pm SEM (n=5). All controls were normalized to 100% and data was expressed, relative to the control. Statistical significance was determined at a P-value <0.05 (See Methods); (See Appendix C, Table 6).

There appears to be a biological effect that takes place where, at every 48 hrs a pattern of suppression and elevation in MA occurs. At 24 hrs the three lower concentrations of R_f expressed significant suppression ($P < 0.0010$) and no effect at the higher concentrations in comparison to the controls. On day 2, at 48 hrs, the MA appears to reflect statistical differences across all experimental samples, significantly greater than the controls ($P < 0.0105$), with the exception of 0.025% R_f which was showed slight suppression in MA. At 72 hrs, slight suppression is seen across all R_f concentrations with no significant differences observed, only at the lower concentration (0.003125%) and middle concentration (0.025%) of R_f compared to the control ($P < 0.007$). At 96 hrs, exposure all concentrations

maintained MA which was statistically different to the controls. Significant elevation in MA was observed between the R_f concentration range from 0.003125% - 0.05% ($P < 0.046$), with the exception of 0.1% which was unable to recover throughout the experimental timeframe, showing significant suppression in MA ($P < 0.0051$) (See Fig. 21).

3.3.4 Effect of chronic fermented rooibos exposure on bEnd5 mitochondrial activity

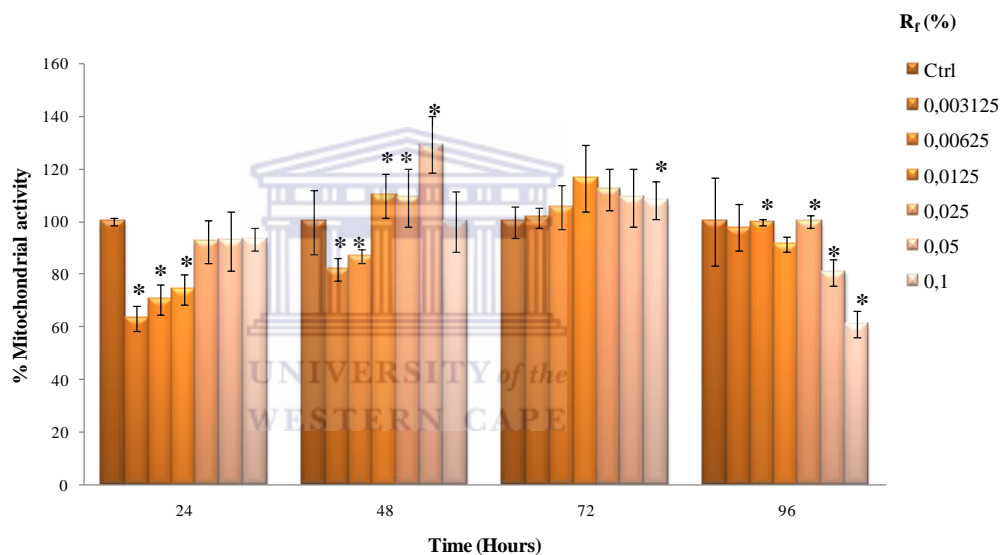


Figure 22. Effect of chronic R_f exposure on bEnd5 cell MA in comparison to controls at selected time intervals. The *, denotes statistically significant differences experimental samples and relative to controls. Data was represented as mean \pm SEM ($n=5$). All controls were normalized to 100% and data was expressed, relative to the control. Statistical significance was determined at a P-value < 0.05 (See Methods); (See Appendix C, Table 7).

Chronic exposure to R_f resulted in bEnd5 cells reaching MA between 60% and 80% at 24 hrs, showing clear suppression in MA. Chronic R_f exposure suppressed the MA across all R_f concentrations relative to the control samples, with the three lower concentrations showing statistical significance at 24 hrs ($P < 0.0010$). At 48 hrs

significant ($P < 0.0001$) suppression was observed at the lower concentrations (0.003125% and 0.00625%) of R_f and significant ($P < 0.008$) elevation at the higher concentrations (0.0125%-0.025%), relative to the controls. At 72 hrs MA was similar to the controls with statistical significance observed and at 0.1% R_f ($P < 0.047$). At 96 hrs two effects of MA was observed: the lower concentrations (0.003125-0.0125% R_f) reflected results similar to the controls, however, higher concentrations (0.025-0.1 % R_f) showed significant suppression in MA, to approximately 80%, relative to the controls ($P < 0.019$). The results suggest that daily/chronic exposure to R_f maintained, if not, normalized MA, with R_f concentrations expressing a similar effect as the control (See Fig. 22).

3.3.5 Effect of combination treatments of ethanol with fermented rooibos on bEnd5 mitochondrial activity

In view of the starting hypothesis, that R_f would alleviate the effects of EtOH, combinations of EtOH and R_f on the BBB ECs were investigated. The selected EtOH concentrations ranged from 25mM to slightly elevated physiological values of 50mM-100mM. The effect of EtOH on the MA of the bEnd5 cells, across the EtOH concentration range, did not statistically differ from each other, but differed from the controls and only within the first 48 hrs (See Fig. 19 and Fig. 20). Thus, combination experiments were limited to 48 hrs as that was the only experimental timeframe in which changes occurred in response to EtOH treatments. R_f treatments of 0.05% and 0.1% was utilized as it affected the MA in a predictable manner which was not statistically different from the controls (See Fig. 21 and 22).

3.3.5.1 Effect of acute combination treatments of ethanol with 0.05% fermented rooibos on bEnd5 mitochondrial activity

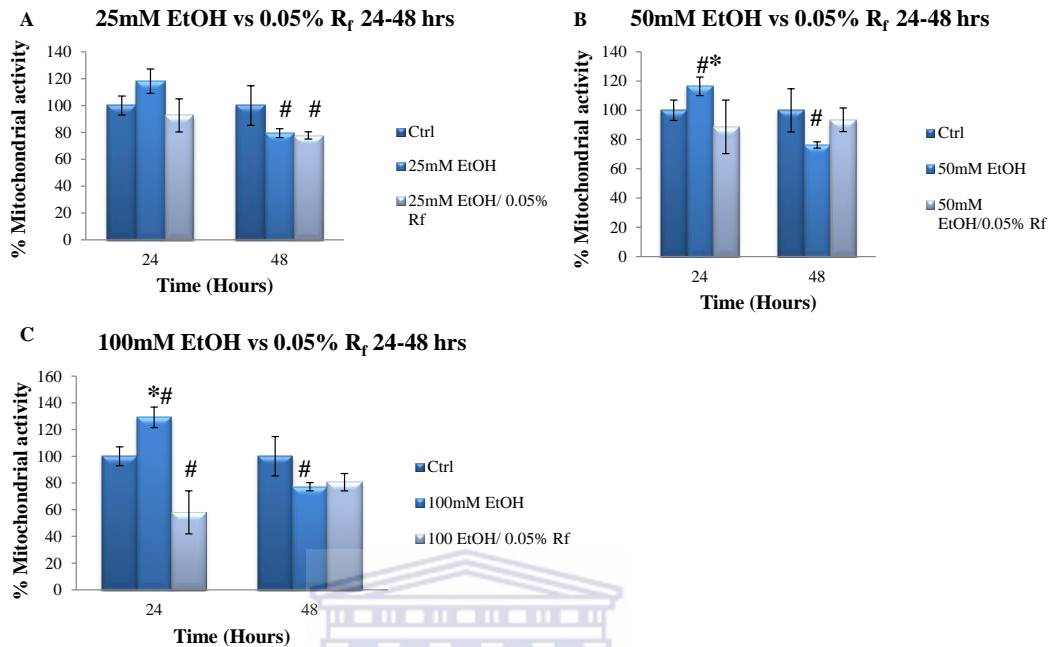


Figure 23. Comparison between acute treatments of EtOH and R_f compounds in combination. Fig. 23A, B and C represented the comparison between acute exposure to 25mM, 50mM and 100mM EtOH in combination with 0.05% R_f in relation to individual EtOH compounds treatments. The data was represented as mean±SEM (n=5) with the *, representing statistically significant differences between the EtOH concentration and the combination and the #, representing significant differences between the controls and the respective compound treatments. All controls were normalized to 100% and data was expressed, relative to the control. A P-value <0.05 designated statistical significance (See Methods); (See Appendix C, Table 8A).

Acute EtOH exposure to the bEnd5 cells elevated MA of the bEnd5 cells at 24 hrs, across all treatment conditions. This result was only significantly different for 50mM when compared to the controls (P<0.0102) (See Fig. 23B). In all cases the R_f combination treatments resulted in a reversal of this elevation, however, this reversal, was only statistically significant at the 50mM and 100mM EtOH group (P<0.029) (See Fig. 23B and 23C).

At 48 hrs, EtOH depressed MA, with significant differences across all treatments ($P < 0.005$) (See Fig. 23A, B and C) and the combination had no statistical effect on MA, with the exception of the 25mM EtOH group in combination with 0.05% R_f relative to the control at 48 hrs ($P < 0.005$).

3.3.5.2 Effect of chronic combination treatments of ethanol with 0.05% fermented rooibos on bEnd5 mitochondrial activity

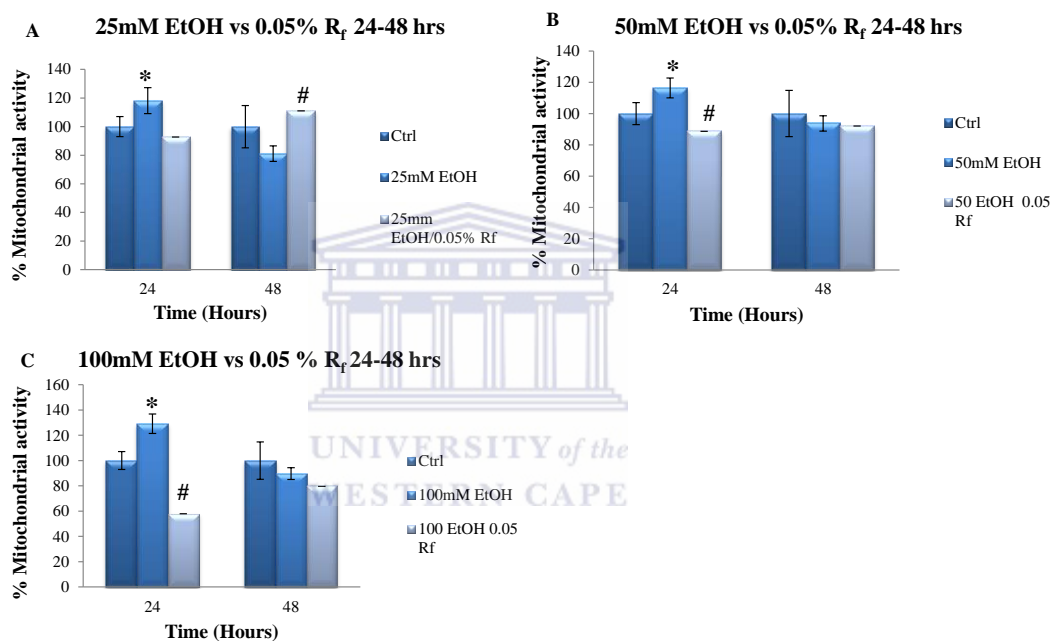


Figure 24. Comparison between chronic EtOH compound treatments and combination treatments of EtOH and % R_f . Fig. 24A, B and C represents the comparison between chronic exposure to 25mM, 50mM and 100mM EtOH in relation to combination treatments of the compounds. The data is represented as mean \pm SEM (n=5). The *, representing a significant difference between the EtOH and the combination treatment and the #, represented significant differences between the control and the respective compound treatments. All controls were normalized to 100% and data was expressed, relative to the controls. A P-value < 0.05 designates statistical significance (See Methods); (See Appendix C, Table 8B).

Chronic EtOH exposure to the bEnd5 cells elevated MA of the bEnd5 cells at 24 hrs, across all treatment conditions, with significant differences observed at 25mM and 100mM EtOH treatments, compared to the controls ($P < 0.027$) (See Fig. 24A and C). In all cases the R_f/EtOH combination treatments at 24 hrs resulted in a reversal of this elevation. The reversal, as a result of the combination treatments, only showed statistically significant suppression in MA in the 50mM ($P < 0.008$) and 100mM EtOH groups ($P < 0.007$) (See Fig. 24B and C).

At 48 hrs, EtOH displayed a trend indicating depression of MA, however, this was not found to be statistically different from the controls (See Fig. 24A, B and C). Only the combination of 25mM EtOH and 0.05% R_f, exhibited a statistically significant increase compared to the controls ($P < 0.007$) (See Fig. 24A).



3.3.5.3 Effect of acute combination treatments of ethanol with 0.1% fermented rooibos on bEnd5 mitochondrial activity

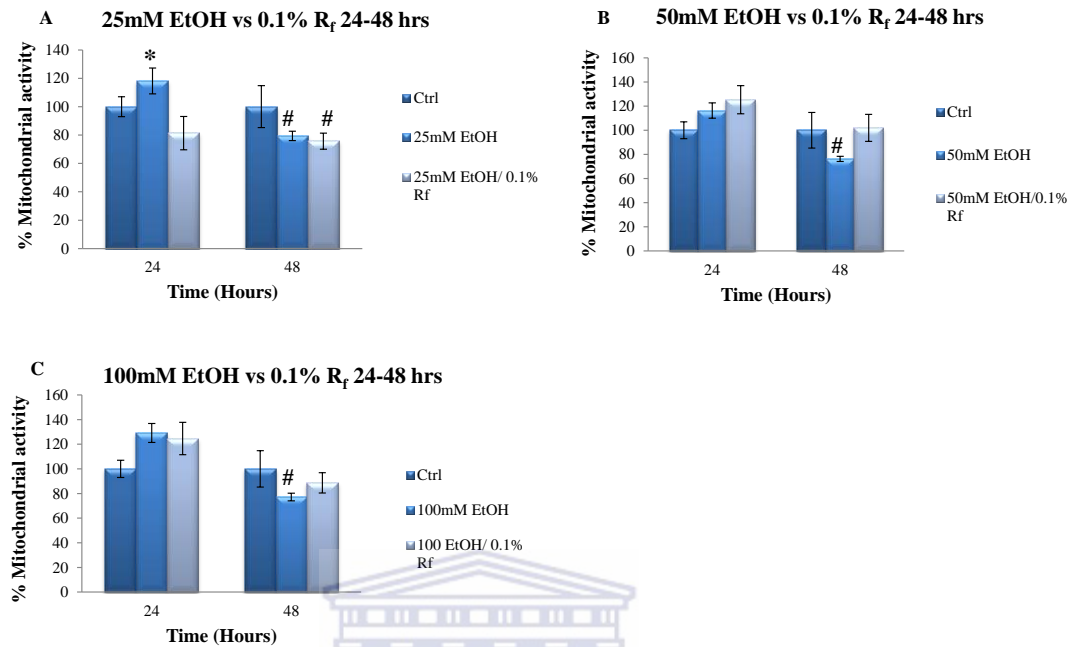


Figure 25. Comparison between acute EtOH and combination treatments. Fig. 25A, B and C represents the comparison between acute exposure to 25mM, 50mM and 100mM EtOH in relation to combination treatments of the EtOH and 0.1% R_f. The *, denotes statistical significance between the EtOH and the combination treatment and the #, represented the statistically significant difference between the selected compound treatments and the control. All controls were normalized to 100% and data was expressed, relative to the controls. A P-value <0.05 designated statistical significance. The data is represented as mean±SEM (n=5) (See Methods); (See Appendix C, Table 8C).

Acute EtOH exposure to the bEnd5 cells established a clear trend of elevation in the MA at 24 hrs, across the EtOH concentration range, although significant differences were not achievable, in comparison to the controls, given the small population group (See Fig. 25A, B and C). Only at physiological concentrations of 25mM EtOH, did we find a statistically significant ($P < 0.011$) reversal of the EtOH-induced effects, in comparison to the controls. (See Fig. 25A).

At 48 hrs, a trend was observed for the EtOH groups. EtOH depressed the MA, with significant differences across all treatments compared to the controls ($P < 0.005$) (See Fig. 25A, B and C). No significant differences were observed between the effect of the EtOH relative to the combination treatments across the respective treatment conditions, with the exception of the combination treatment of the 25mM EtOH group and 0.1% R_f, which was significantly decreased, compared to the controls ($P < 0.007$) (See Fig. 25A). With reference to the combination treatments, the 25mM EtOH group showed no significance at 25mM, however, at 50mM and 100mM, a trend was established, where the combination reversed the effects of the EtOH.

3.3.5.4 Effect of chronic combination treatments of ethanol with 0.1% fermented rooibos on bEnd5 on mitochondrial activity

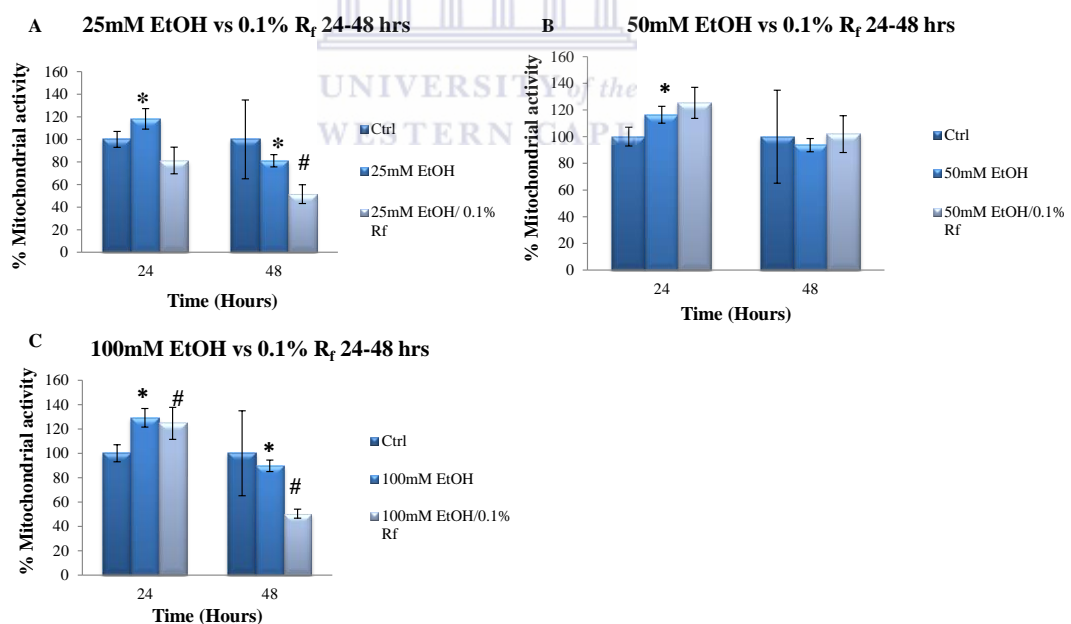


Figure 26. Comparison between chronic EtOH and combination treatments. Fig. 26A, B and C represents the comparison between chronic exposure to 25mM, 50mM and 100mM EtOH and a combination of EtOH and 0.1% R_f. The data is represented as mean \pm SEM (n=5) with the *, representing a significant difference between the EtOH concentration and the combination and the #, represented significant differences between the controls and the compound treatments. All controls

were normalized to 100% and data was expressed, relative to the controls. A P-value of <0.05 designates statistical significance (See Methods); (See Appendix C, Table 8D).

Chronic EtOH exposure to the bEnd5 cells elevated its MA at 24 hrs, across all EtOH treatments (25-100mM), with no significant differences observed across all treatments in comparison to the controls. Statistically significant differences were observed between the EtOH treatment (25-100mM) and the combinatory groups of: 25mM-100mM in combination with 0.1% R_f, ($P<0.045$) (See Fig. 26A, B and C). A reversal of the EtOH effect on MA by the R_f combination treatments was only observed in the 25mM EtOH group vs 0.1% R_f, with no statistical significant decrease (See Fig. 26A). There was, however, a trend at the use of the higher, 50mM-100mM EtOH in combination with 0.1% R_f groups, resulting in an elevation in MA, similar to, if not more viable than the EtOH treatment effects, with no statistical significant differences observed.

At 48 hrs, a trend was observed for the EtOH treatment groups. The EtOH groups depressed MA, with no significant differences across all treatments, compared to the controls (See Fig. 26A, B and C). Significant differences were, however, observed between the effect of the EtOH groups in comparison to the combination treatments in the 25mM and 100mM EtOH group vs 0.1% R_f, which showed a significant decrease from the EtOH treatments, in comparison to the combination treatments ($P<0.006$) (See Fig. 26A and C).

3.4 Transendothelial electrical resistance

3.4.1 Effect of chronic exposure to ethanol and fermented rooibos on transendothelial electrical resistance

3.4.1.1 Effect of chronic ethanol exposure on transendothelial electrical resistance

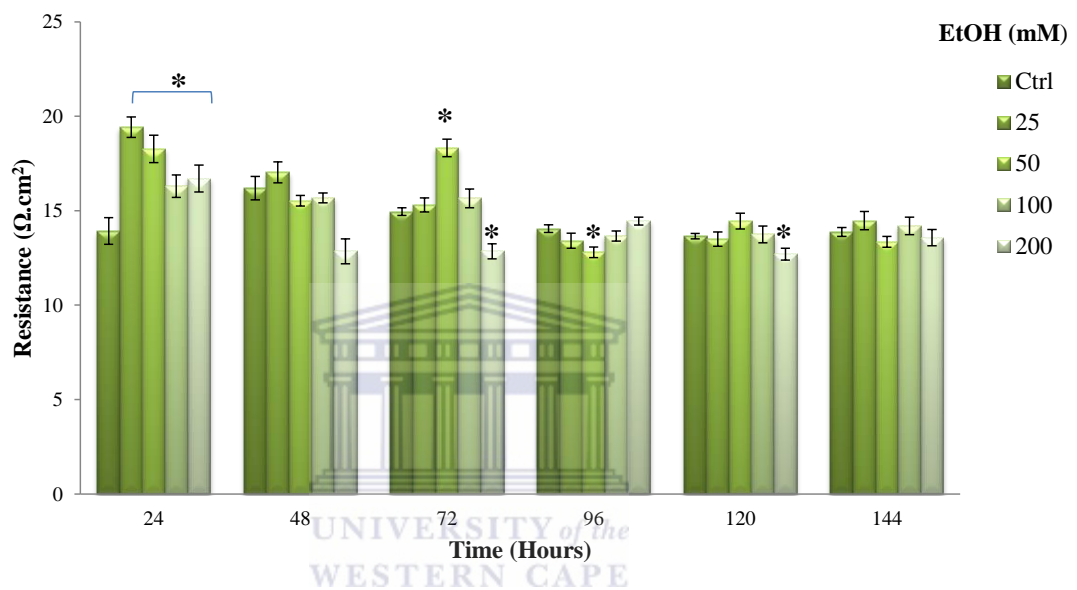


Figure 27. Effect of chronic exposure to EtOH-supplemented media in the presence of physiologically relevant levels of HC (500nM) on TEER measurements across the bEnd5 cell monolayer compared to controls (cells+SFM/HC-supplemented media) at selected time intervals. Data is represented as mean \pm SEM (n=4). The *, denoted statistically significant differences in the TEER over time between experimental samples, relative to the controls. Statistical significance was designated at a P-value <0.05 (See Methods); (See Appendix D, Table 1).

A dose-dependent effect was reflected at 24 hrs. All EtOH concentrations exhibited significantly elevated increases in TEER, relative to controls ($P < 0.026$). At 48 hrs resistance across the cell monolayer began to plateau with no significant differences observed across all concentrations. At 72 hrs, no differences were seen, with the exception of 50mM where a minute, but significant increase in TEER was observed,

relative to the controls ($P < 0.0001$). Between 96-120 hr time intervals, only small, yet significant changes occurred in resistance readings. At 96 hrs only 50mM EtOH exposure resulted in a significantly decreasing effect, in comparison to the controls ($P < 0.004$) and at 120 hrs, significant differences were only seen at the greatest concentrations of 200mM, relative to the control ($P < 0.003$). At 144 hrs no significant differences were observed when compared to the control. A time-dependent effect, across the entire experimental timeline (24-144 hrs), is negligible (See Fig. 27).

3.4.1.2 Effect of chronic fermented rooibos exposure on transendothelial electrical resistance

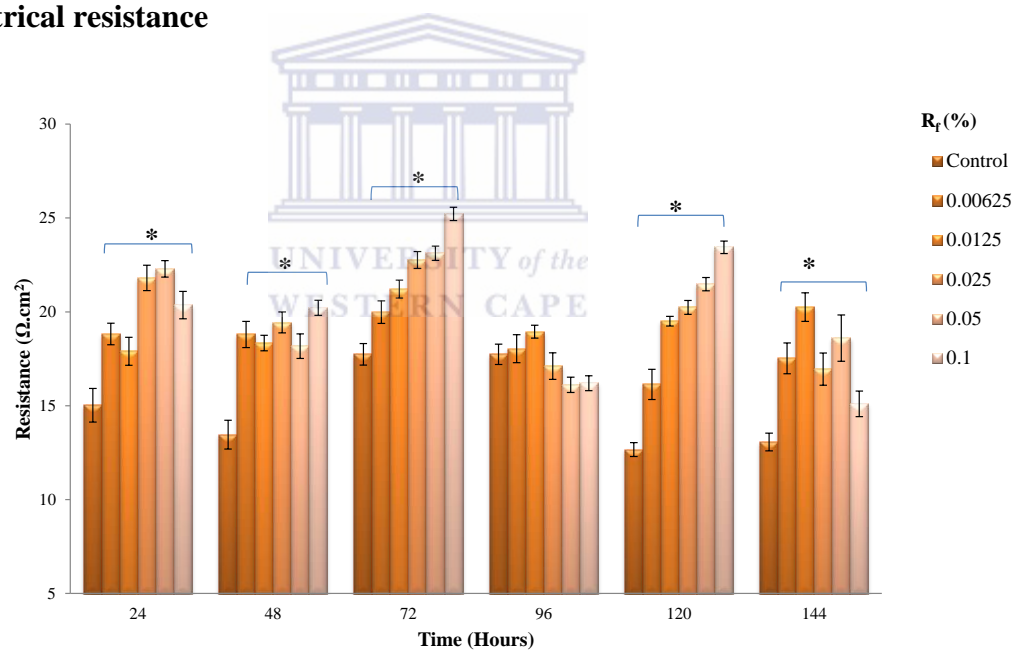


Figure 28. Effect of chronic R_f exposure on TEER compared to controls (cells+SFM/HC-supplemented media) at selected time intervals. The *, denotes statistically significant differences in the TEER of the experimental samples relative to the controls. Data was represented as mean \pm SEM (n=4). Statistical significance was designated at $P < 0.05$ (See Methods); (See Appendix D, Table 2).

A significant increase ($P < 0.05$) in resistance was observed at 24 hrs, 48 hrs and 72 hrs, reflecting a dose-dependent increases in TEER across all experimental samples, generating resistance reading significantly greater than the control samples ($P < 0.01$). At 96 hrs, no differences were observed between the experimental samples and the controls. At 120 hrs, significant, dose-dependent increases in TEER were observed across all R_f concentrations, relative to the control ($P < 0.0005$) and at 144 hrs significant increases in TEER was observed from 0.00625% - 0.05% R_f , relative to the control ($P < 0.007$) (See Fig. 28).

3.4.1.3 The effect of chronic exposure to ethanol in combination with 0.05% fermented rooibos on transendothelial electrical resistance

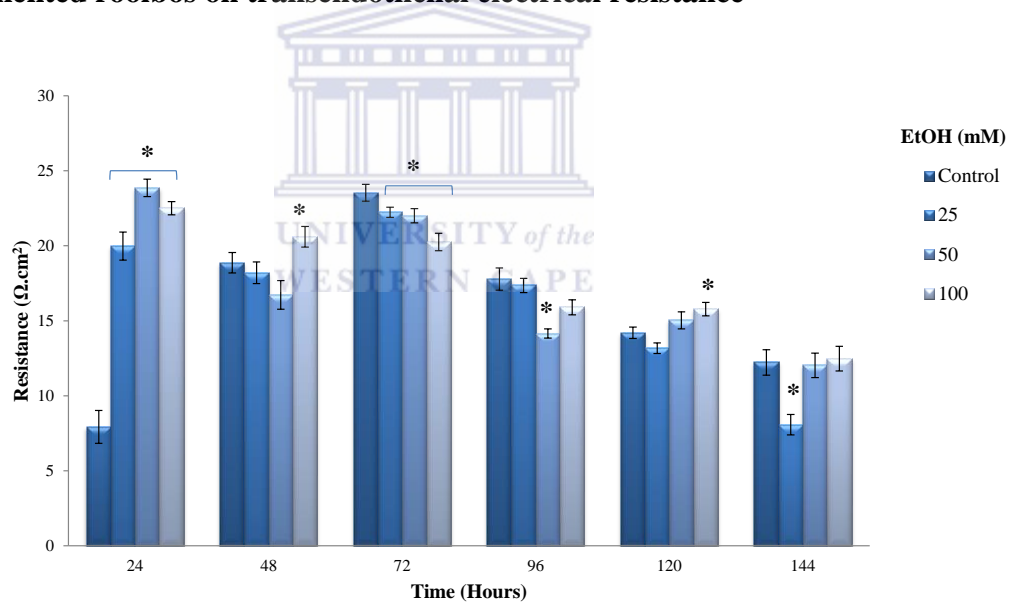


Figure 29. Effect of chronic R_f exposure (0.05%) in combination with EtOH: 25mM, 50mM and 100mM on TEER compared to controls (cells+SFM/HC-supplemented media) at selected time intervals. The *, denotes statistically significant differences in TEER, between the experimental samples and controls. Data was represented as mean \pm SEM ($n=4$). Statistical significance was determined at $P < 0.05$ (See Methods); (See Appendix D, Table 3).

A synergistic regression in TEER is exhibited in the combination treatments for R_f (0.05%) and EtOH (25mM-100mM), with a time and dose-dependent effect reflected from 24 hrs to 144 hrs exposure. At 24 hrs significant increases were observed across all combination treatments of R_f vs EtOH, relative to the controls (P<0.0001). At 48 hrs, a visible decrease in TEER, from 24 hrs was reflected. No significant differences were observed, relative to the control, with the exception of 100mM EtOH/0.05% R_f combination treatment, which showed statistically significant (P<0.047) elevation in TEER. Optimal TEER readings were reached at 72 hrs, with significant (P<0.047) decreases observed across all combination treatments, relative to the control. At 96 hrs, all treatments reflected TEER values lower than the control, with the 0.05% and 50mM EtOH combination treatment expressing significant decreases in TEER, relative to the control (P<0.0006). At 120 hrs a gradual decrease in TEER occurred with all treatments normalizing and exhibiting TEER values similar to the control, with the exception of the 0.05% R_f and 100mM EtOH combination which was significantly (P<0.023) greater than the control and at 144 hrs all TEER values normalized, however, the 0.05% R_f and 25mM combination reflected significant decreases in TEER relative to the control (P<0.0006) (See Fig. 29).

3.4.1.4 The effect of chronic exposure to ethanol in combination with 0.1% fermented rooibos on transendothelial electrical resistance

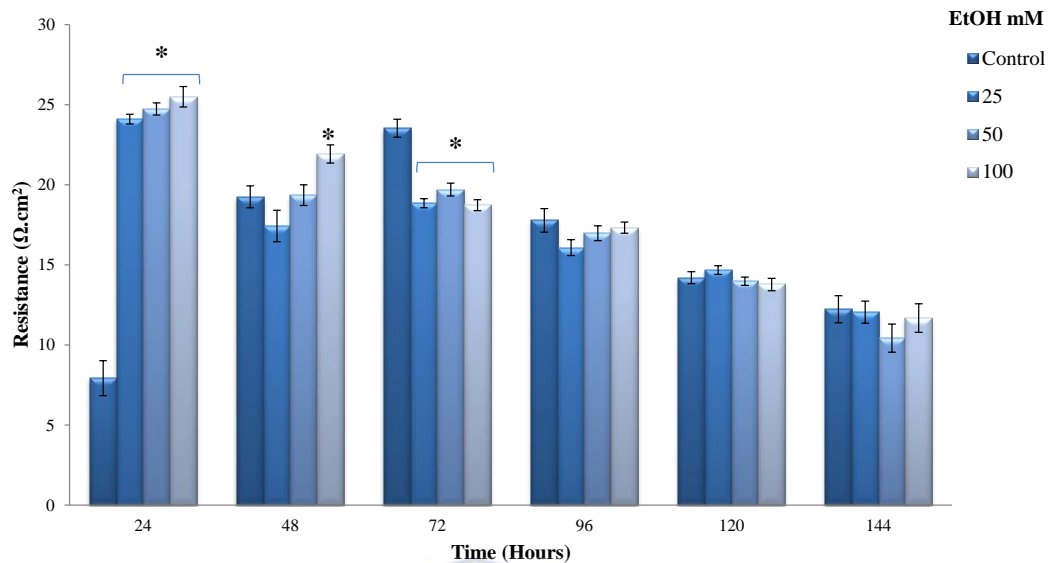


Figure 30. Effect of chronic R_f exposure (0.1%) in combination with EtOH: 25mM, 50mM and 100mM on TEER compared to controls (cells+SFM/HC-supplemented media) at selected time intervals. The *, denotes statistically significant differences in TEER, between the experimental samples and significant differences in TEER between combinations treatments relative to controls. Data was represented as mean \pm SEM (n=4). Statistical significance was determined at $P < 0.05$ (See Methods); (See Appendix D, Table 4).

A synergistic regression is produced in the combination treatments with 0.1% R_f and EtOH. A time and dose-dependent effect is observed from 24 hrs to 144 hrs exposure. At 24 hrs a significant increase in TEER was observed across all treatments of 0.1% R_f in combination with 25mM, 50mM and 100mM EtOH, relative to the controls ($P < 0.0001$), however, from 48 hrs, a visible decrease in TEER was observed, with a statistically significant ($P < 0.002$) increase in TEER seen at the 0.1% R_f and 100mM EtOH combination treatment, relative to the control. At 72 hrs, significant ($P < 0.0001$) decreases were observed across all combination treatments in comparison to the control and from 96 hrs-144hrs a gradual decrease in

TEER was observed over time, however, no significant differences were observed when compared to the controls (See Fig. 30).

3.5 High resolution scanning electron microscopy

3.5.1 Imaging cell confluence on a 12mm insert membrane

High definition SEM was employed to capture the ultrastructures of established confluent bEnd5 cell monolayers. In order to achieve optimal TEER readings, a closed circuit needed to be created, by the establishment of a 100% confluent bEnd5 cell monolayer. This was carried out by investigating the effect of cell density on the rate in which to achieve confluence using two cell densities of: 1×10^4 and 1×10^6 cells/well/insert. The bEnd5 cells, seeded at a density of 1×10^6 cells/well/insert effectively achieved 100% confluence within 24 hrs. The cells were treated with standard culture medium (supplemented DMEM-F12). This study was performed in order to validate the formation of a confluent bEnd5 cell monolayer, to investigate the bEnd5 cell surface topography of cells grown in close proximity and surface morphology of the bEnd5 cell after being subjected to a flow-based model.

In the context of this study, a confluent monolayer for investigating the bioelectrical and morphological characteristics of a bEnd5 cell monolayer was investigated. Two cell densities were employed in this study.

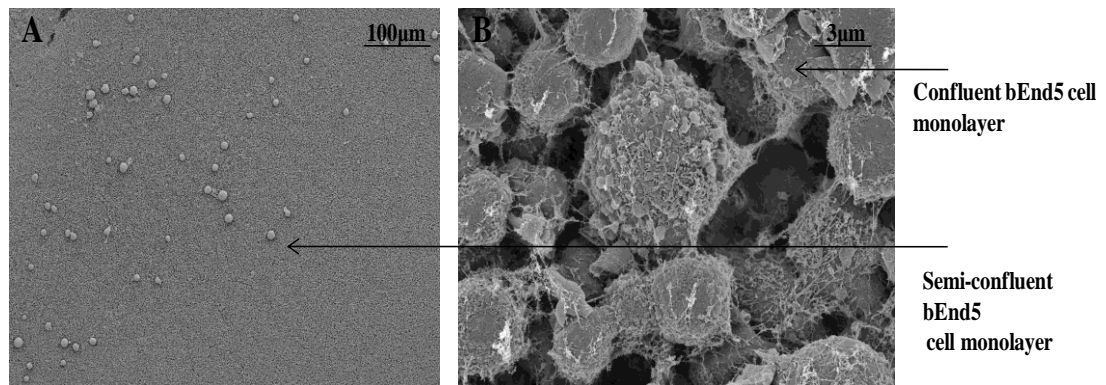


Figure 31. Comparison of bEnd5 cell confluence. (A) Semi-confluent (20%) bEnd5 cells distally located (1×10^4 cells/well/insert) and (B) represented a confluent (100%) bEnd5 monolayer with cells in close proximity (1×10^6 cells/insert/well) grown on a 12mm diameter mixed cellulose insert.

SEM micrographs revealed spherical and oval-like cell shapes. Semi-confluent and confluent monolayers were formed after 24 hrs exposure of bEnd5 cells to standard DMEM-F12. The ECs were seeded at a density of 1×10^4 cells/well/insert on a mixed cellulose ester filter insert, with a diameter of 12mm and a $0.45 \mu\text{m}$ pore size (MillicellTM) (A) and these cells achieved approximately 20% confluence by 24 hrs. cells appeared to be distally dispersed and, therefore, showed subsequent increased paracrine distance. Cells did not present with any vesicle formation or blebs on the surface topography. Sparse cells lacked in cell-to-cell communication, similar to work described by Dejana, (2004). Conversely the bEnd5 cells seeded at 1×10^6 cells/well/insert exhibited vesicle formation on its surface and visible cytoplasmic projections with numerous intercellular bridges formed between adjacent cells.

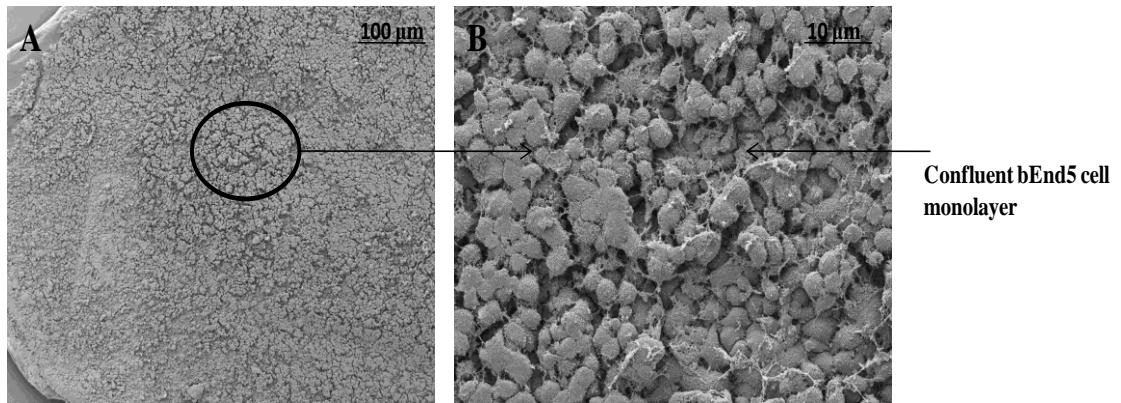


Figure 32. 100% Confluent bEnd5 cell monolayer seeded at a density of 1×10^6 cells/well/insert (insert=12mm diameter) after 24 hr exposure to DMEM-F12.

(A) Demonstrated bEnd5 cells grown to confluence on a mixed cellulose insert membrane surface. The bEnd5 cells were seeded at 1×10^6 cells/insert/well (Millicell™ insert). The insert was 12mm in diameter, $0.45 \mu\text{m}$ pore size and was placed in a 24-well microtiter plate. After 24 hrs the bEnd5 cells established a monolayer. (B) Demonstrated and enlarged image ($10 \mu\text{m}$) of a densely packed monolayer captured at $100 \mu\text{m}$ (A). The bEnd5 cells grew in close proximity, with very short paracrine distances between neighboring/adjacent cells.

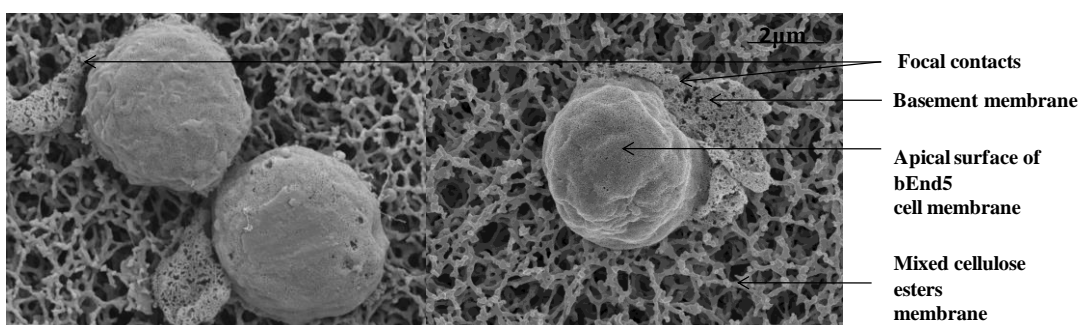


Figure 33. Establishment of the bEnd5 cell basement membrane after 24 hrs bEnd5 cells were grown in supplemented DMEM-F12 at a cell density of 1×10^4 cells on a 12mm mixed cellulose esters insert.

The basal surface of the EC seemed to produce a basement-membrane like matrix which attached itself to the surface of the insert. The laying down of a basement

membrane is crucial for the orientation of a cell as it allows the cell to distinguish between its apical and basolateral surfaces and, therefore, facilitates cell growth. The bEnd5 cell demonstrated the laying down of a fibrous network which embedded itself into the mixed cellulose ester membrane support structure on the basal surface of the cell. In addition it demonstrated two cells in close proximity showing focal contact with each other and the extracellular mixed cellulose ester membrane surface. The junctions found between cells are important as they are associated with the cell cytoskeletal arrangement and subsequent apical and basolateral orientation, which is essential for lumen determination (Dejana, 2004).



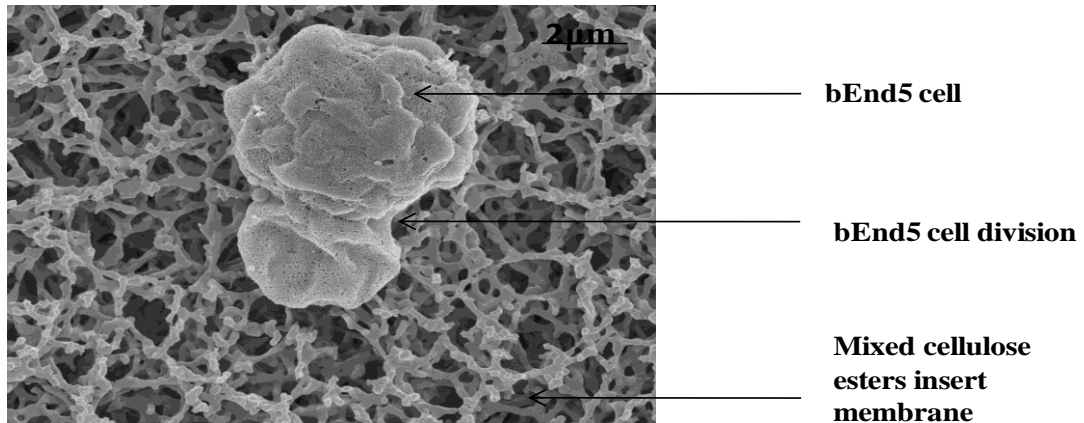


Figure 34. bEnd5 cell division in one cell grown on a mixed cellulose esters insert membrane

The bEnd5 cell demonstrated a bulging type of formation of its plasma membrane on its anterior lateral end. Based on literature this bulging is classified by a term called “blebbing”. A bleb is defined as a balloon-like, quasi-spherical protrusion of the plasma membrane. The blebs are evident within healthy cells during specific cell cycle stages (Barros et al., 2003). The bEnd5 cell, in this figure, demonstrated potential cell division which was either being initiated or has failed to occur. The cell membrane has been laid down in preparation for the extrusion of subcellular contents, but the completion of the actual process may have been inhibited, with the notion that blebs are filled from the cell body (Barros et al., 2003). With reference to work conducted by Barros et al. (2003), the specific cell could be undergoing apoptosis which is also characterized by blebbing, followed by a process known as apoptotic volume decrease (AVD) which results in a decrease in the intracellular pressure resulting in a collapsed appearance of the bleb, similar to work described by Barros et al. (2003) (See Fig. 34).

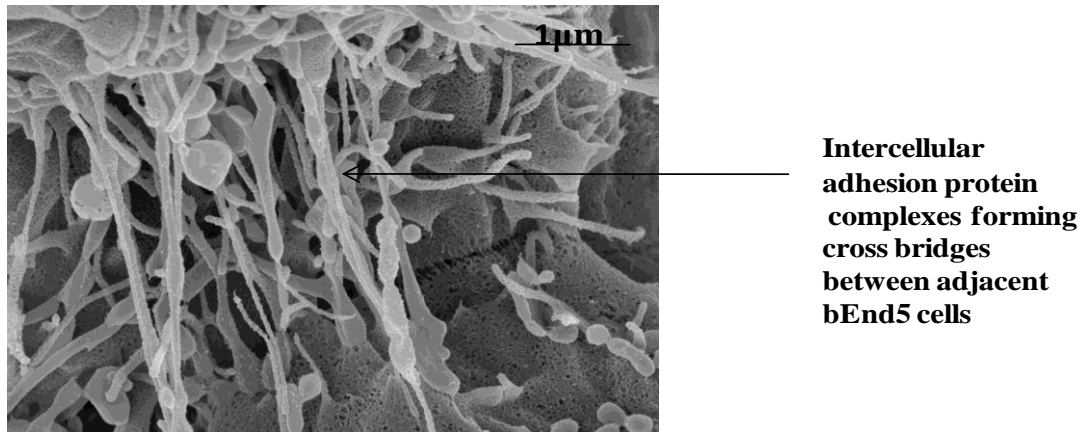


Figure 35. Cell-to-cell protein interactions between adjacently located bEnd5 cells grown on a mixed cellulose ester insert membrane.

Cell-to-cell protein junctions are expressed between adjacent bEnd5 cells grown in close proximity. These junctions demonstrated sites of attachment on the domains of neighboring cells and in so doing allowed for the adherens of adjacent bEnd5 cells, forming a continuous network of cross bridges in the EC monolayer. The intercellular cross bridges are potential transmembrane adhesive proteins at the endothelial junctions which aid in holding the cells together and in so doing, assists with TJ formation. After a 24 hr exposure to standard DMEM-F12 protein complexes were formed. Based on work done by Dejana, (2004), the AJs are formed in the initial stages of intercellular contact and it can, therefore, be presumed that these protein cross bridges may be part of the AJ family of proteins, such as VE-cadherin (Dejana, 2004) (See Fig. 35).

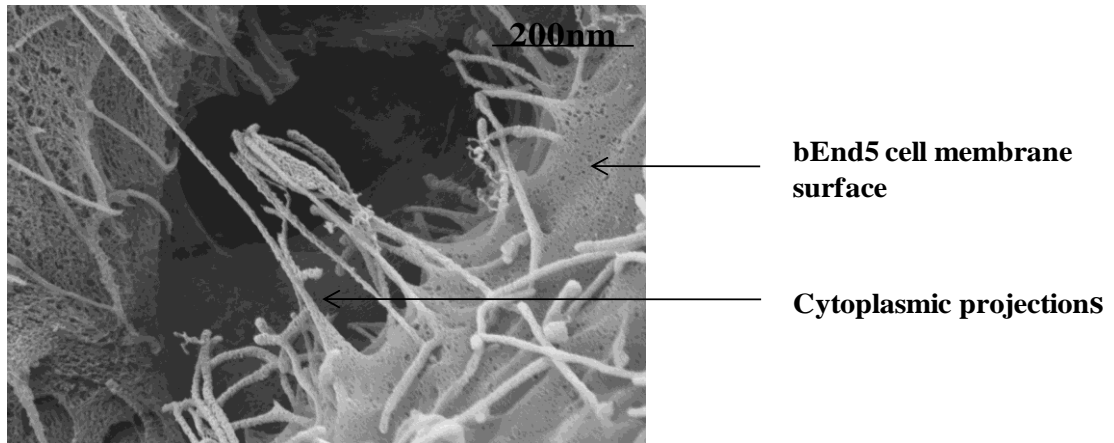


Figure 36. Cytoplasmic projections on the lateral border in the cleft between adjacent bEnd5 cells seeded at a density of 1×10^6 cells/well/insert.

The edges of the cell membrane surface appeared to express flap-like cytoplasmic extensions which was similar to research finding by Faso et al. (1994). The lateral border of the EC demonstrated visible extensions of the cell membrane toward the neighboring EC. The amorphous structure of the cell membrane demonstrated cytoplasmic projections along the entire lateral border of the cell, attaching to the neighboring cell which further supported its adherens-like protein nature, unlike TJs, which are prevalent on the apical surface of the EC, the AJs are more abundant along the cleft as described by Dejana, (2004).

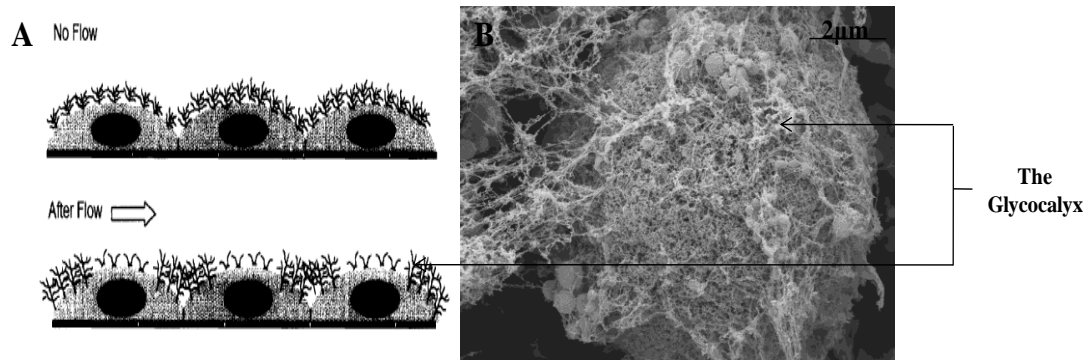


Figure 37. Formation of the schematic illustration of an EC glycocalyx (Yao et al., 2007) (A) and the glycocalyx of the bEnd5 cell membrane surface *in vitro* (B).

The bEnd5 cell surface expressed the formation of a bush-like structure of proteins on its apical surface. In theory, based on research findings reported, this protein coat is prevalent on the EC plasma membrane and is composed of glycosaminoglycans and glycoproteins and is usually formed upon exposure to shear stress as a result of fluid filled pathways (Martini, 2006; Adamson et al., 1992). The animated diagram of a typical EC glycocalyx is depicted in **Fig. 37A**, which showed the formation of protein-like structures on the apical surface of an EC. **Fig. 37B** demonstrated the appearance of the bush-like layer, which was inclined to cover the bEnd5 cell surface as a protective mechanism. The presumed “glycocalyx” appeared to be closely associated with the luminal (apical) region of the bEnd5 cell and in addition, it appeared more dense/clumped at the cell-to-cell junctions, compared to a more dispersed appearance, thinner looking, across the cell surface, similar to work described by Adamson et al. (1992).

Chapter 4: Discussion

4.1 Introduction: Importance of the blood-brain barrier integrity

The brain endothelium of the BBB is the major constituent vital to the functioning of the CNS (Navone et al., 2013). It is uniquely responsible for the regulation of the movement of substances between the blood and brain parenchyma, and is therefore, central to the brain as a regulator of the milieu in which the neurons function. The BBB is, thus, crucial for the regulation of a homeostatic brain microenvironment, within very strict parameters, which allow for the function of neurons (Haorah et al., 2005; Manzo-Avalos et al., 2010; White, 2003).

Should the BBB fail in regulating the passage of substances, the very function of the brain itself will be compromised. Any such compromising of the BBB will result in increased permeability which in turn results in the unregulated passive diffusion of substances into the brain tissue through the paracellular and transcellular pathways (Brown et al., 2007). Brain capillary ECs are distinctly different from all other ECs. They are characterized by a lack of fenestrations, low levels of transcellular endocytosis, expression of peptide transporters in a polarized manner and they form a low permeability barrier between the brain and blood (Kneisel and Wolburg, 2000), while the permeability of the paracellular pathways are regulated by TJs, which are not found in the systemic capillary system. Brain ECs are vulnerable to oxidative stress, which is generally caused by agents inducing ROS production. The literature has established that EtOH is a major contributor in the production of ROS, which causes oxidative damage within capillary endothelium and surrounding structures within the brain (Alikunju et al., 2011). It is surprising that EtOH affects

the BBB, due to it being classified as a small lipophilic molecule and its entry into the brain is unable to be regulated as it passively passes through the cellular components of the BBB (Banks, 2009; Rubin and Staddon, 1999). EtOH has the ability to disrupt the intracellular redox state, by dysregulating intracellular pathways and causes an imbalance in the redox status of the cell (Brocardo et al., 2011). This mechanism involves the brain's exposure to EtOH, which results in an elevation in the activity of the EtOH-metabolizing enzymes, subsequently causing an increased production of ROS. These metabolic processes are primarily produced within the mitochondria as a by-product of EtOH metabolism (Manzo-Avalos et al., 2010).

Since oxidative stress causes brain cells to become highly susceptible to oxidative injury (Lakhan et al., 2009; Won et al., 2002; Alikunju et al., 2011), the introduction of AOs' as a means to potentially combat the rise in ROS production brought about by EtOH is clinically, potentially significant. Commercial rooibos (fermented *A.linearis/ R_f*), is known for its AO capacity as a result of its high polyphenolic content (Marnewick et al., 2003; Lamosová et al., 1997; von Gadow et al., 1997). This study focused on R_f as a source of AO's, to counterbalance the EtOH-induced ROS production and in so doing, alleviate its subsequent pathophysiological impact. The working hypothesis is based on R_f's ability to protect against EtOH-induced changes to an *in vitro* BBB model system.

Four phases of investigation were carried out in order to ascertain how the AO capacity of R_f could attenuate the adverse effects of EtOH on an *in vitro* model of the BBB. The phases were conducted as follows: (1) The chemical analysis of an aqueous extract of *A.linearis*; (2) the study of cell morphology using electron micrographs of bEnd5 cell monolayers to assess and validate the establishment of

confluent bEnd5 cell monolayers, essential for bioelectrical experimentation, using a bicameral system; (3) *in vitro* analysis of the effects of both R_f and EtOH separately and (4) *in vitro* analysis of these effects in combination on selected physiological parameters of the bEnd5 cells.

4.2 Chemical analysis of fermented rooibos

Chemical analysis for R_f, showed high levels of a multitude of AOs' (See Results Table 4.), however, aspalathin is the dominant AO, as can be seen in the HPLC results which further endorsed its prevalence by illustrating large amounts of aspalathin (16.024 mAU) (See Fig. 16). As rooibos is administered largely within the South African population as a tea it is useful to relate the experimental concentrations relative to that of a cup of tea. Drinking a cup of rooibos tea results in approximately 0.17nM of aspalathin in the plasma (Breiter et al., 2011). Our study investigated an R_f concentration range of (0.003125-1%), which translates to 0.06nM-2nM, and approximates to 0.3-12 cups of tea.

The literature reports emphatically on R_f's therapeutic potential. The traditional uses of R_f within a South African context include: the alleviation of infantile colic, allergies, asthma and dermatological problems (Joubert et al., 2008). Over and above its medicinal value, R_f is also enjoyed in SA during the summer months as a cold lemon infused beverage and more recently has gained popularity in coffee and tea shops, served as “espresso, cappuccino, or latte” (Anon, 2006; Joubert et al., 2008). The latest concept was introduced in recent news (Cape Times, 21 October 2014), reporting on the implementation of R_f in the commercial making of wine

products as a means to alleviate the potential harmful effects of alcohol within the wine product (See Appendix F for article).

4.3 Effect of ethanol on cellular proliferation and mitochondrial activity

4.3.1 Effect of ethanol on cellular proliferation

The cellular proliferatory pattern in this study, demonstrated bEnd5 cellular proliferation to be greatly suppressed at 24 hrs with the higher concentrations of 200mM and 400mM showing marked cell suppression in comparison to the controls. Thereafter, a marked increase in proliferation at 48 hrs was observed. Studies conducted by Mikami et al. (1997), described the impact of EtOH on a fibroblastic cell line of mouse connective tissue, after exposure to a range of 12.5-200mM EtOH for a short-term (3 and 26 hrs), and reported on a marked reduction in cellular proliferation and an inhibition in cell growth, especially to the higher concentrations of EtOH (100 and 200mM) after 3-26 hrs. For the timeframe of 24-48 hrs, this study endorsed our research as it appears that at 48 hrs cells have recovered and have started to proliferate at a rate higher than the controls. A shortcoming of Mikami et al. (1997), is that the study ended at 24 hrs. Our study extended the investigation time up to 144 hrs and it was only at 72-144 hrs where a distinct pattern of suppression in cell proliferation of bEnd5 cells occurred, after acute exposure to EtOH (See Fig. 17). Significant suppression in cellular proliferation occurred in EtOH exposed cells which was observed from 72 hrs through to 144 hrs and was consistent. The suppression in this study is supported by reports in the literature which have clearly implicated EtOH effects on hepatocytes and astrocytes, reporting that EtOH at 20-217mM was able to suppress cellular proliferation (Higgins, 1987;

Mikami et al., 1997). In addition, EtOH has been reported to cause an increase in hepatocyte ROS production, resulting in a mild degree of cytotoxicity (Bailey and Cunningham, 1999).

The EtOH proliferation experiments show a decrease in cell proliferation, which could be due to two possibilities: (i) cells died, due to the toxic effects of EtOH and (ii) a decreased rate of cell division could be implicated. Our toxicological results confirmed, surprisingly, that cells did not die, across the entire selected EtOH concentration range (**See Results, Table 5**).

Energy is crucial for cell division and as EtOH is well known to be implicated in cellular metabolic pathways and thus, would affect the energy quotient of the cells. For this reason, the function of the mitochondria was investigated. In addition, malfunction of the mitochondria has been linked to an increase in ROS production, which is also reported to affect cell division.

***Energy quotient:** The amount of ATP available for the cells' metabolic processes.

4.3.2 bEnd5 Mitochondrial activity as an indicator of cell viability

4.3.2.1 Introduction: The role of the mitochondria

An array of neurodegenerative diseases have been directly linked to an over production of ROS, which is mostly produced within the mitochondria of a cell as a by-product of cellular metabolism/respiration. There is, therefore, a close relationship between ROS and the MA (Kirkinezos et al., 2001). The function of the mitochondria has been discussed at length in the literature review. It plays a pivotal role in the metabolism of EtOH which can be achieved via both oxidative and non-oxidative pathways which are involved in ROS generation. In the brain EC, EtOH is metabolized via catalase and CYP2E1 to acetaldehyde which occurs in the cytosol.

The acetaldehyde is the main by-product of the oxidative metabolism of EtOH which contributes to cell and tissue damage and is further metabolized to acetate via ALDH2, in the presence of nicotinamide adenine dinucleotide (NAD⁺) within the mitochondria (Zakhari, 2006). The by-products formed are: acetate, an increased NAD⁺:NADH ratio and increased ROS production. Thus, the ROS producing steps involves CYP450 and mitochondrial metabolism. EtOH metabolism, in extrahepatic tissue, such as the brain, does not, however, involve the enzyme ADH, only CYP P450 and catalase (Zakahri, 2006). Literature has reported that EtOH alters the mitochondrial function by decreasing respiratory rates and subsequent ATP levels (Manzo-Avalos et al, 2010). Literature has reported that mitochondrial levels of ROS may increase upon chronic consumption of EtOH (Manzo-Avalos et al., 2010). ROS are major role players in the modulation of cell function causing an array of pathological conditions when prevalent both chronically and transiently, at supraphysiological levels (Moldovan et al., 2006).

Furthermore, the mitochondrial dehydrogenase (MDH) activity is indicative of the cells' metabolic rate and by extension an indicator of cell viability (Seeley and Tate et al., 1995; Mikami et al., 1997). The XTT assay measures, quantitatively, MDH and thus, is a measure of the cells metabolic activity (**See Chapter 2; 2.5.1: Methods and Materials for the operating principle by which the XTT assay is performed**).

4.3.3 The correlation between the effects of ethanol on bEnd5 mitochondrial activity and cellular proliferation

Our data shows that after 24 hr exposure to EtOH there was an increase in mitochondrial activity (MA) which is reflective of an increase in the production of ATP and a subsequent increase in energy availability to the cell. With respect to cellular proliferation, however, 24 hr EtOH exposure shows no difference from the controls (**See Fig 17, Fig 19. and Fig 20.**).

In view of our hypothesis, it was surprising that, although the MA was not suppressed at 24 hrs, suppressive effects of EtOH only came into effect at 48 hrs, which speaks to the secondary causes of EtOH's ability to interfere with pathways of ATP production (Cunningham et al., 2004). The decrease in MA, observed at 48 hrs, after a 24 hr episode of EtOH exposure (acute experiments), was suppressed to approximately 20-60 % (**See Fig.19 and Fig. 20**). This depression of MA is indicative of a potential decrease in ATP production, and thus, a decrease in the availability of energy for crucial cellular activities. It is, therefore, not surprising that the decrease in energy availability, as depicted in a decrease in MA at 48 hrs, resulted in the suppression of cellular proliferation between 72-96 hrs (**Fig. 17**). The

implication of the energy suppression is crucial to cell division and therefore, at 72hrs a decrease in cellular proliferation occurred, which extended to 144 hrs.

Peculiarly, MA returned to normality by 72 hrs, but this was not able to reverse the long-term impact on cellular proliferation, extended to 144 hrs. These results report, for the first time, that a single exposure to EtOH causes long-term depression in bEnd5 cellular proliferation, and thus, potentially compromise the ability of the brain to regulate its homeostatic environment. Although the mitochondria responded by returning to normality, in both acute and chronic experiments, this has little effect on the suppressed proliferation profile of the cells thereafter. This may be due to secondary effects of increased ROS production, as the mitochondria responds to the adverse effects of alcohol exposure.

The decrease in MDH activity reflects a decrease in MA and ultimately a decrease in the production of energy. Literature has reported on the ability of alcohol metabolism to develop oxygen deficits (hypoxia), within liver tissue and this in turn inhibits the liver cells' ability to produce ATP (Cunningham et al., 2004). It is emphatically reported that the mitochondria, being a source of ROS, utilizes approximately 2% of O₂ in ROS production, under aerobic conditions, especially in the formation of superoxide (O₂⁻) and hydrogen peroxide (H₂O₂) (Vladimir et al., 2012). In the liver mitochondria of the rat the generation of ROS was estimated to range between 8.3x10⁻¹¹ mol/L and 4.8x10⁻⁹ mol/L, upon exposure to EtOH. (Bailey and Cunningham, 1999).

When comparing acute and chronic exposure to MA, suppression was maintained for chronic (daily) exposure. Only high concentrations, showed increased

suppression of MA, which differed from the acute exposure to EtOH, where MA showed recovery at all EtOH concentrations.

4.4 Effect of fermented rooibos on cellular proliferation, mitochondrial activity and toxicity

4.4.1 Effect of fermented rooibos on cellular proliferation

In our research study, exposure to R_f resulted in a dose-dependent suppression in cellular proliferation of the bEnd5 cells, with increasing amounts of AO exposure, which became more acute with time. These effects may have occurred due to an imbalance between ROS production and the introduction of AO. This imbalance is able to cause the same effect as ROS, as an excess in AO could promote a similar effect to excess ROS (Joubert et al., 2005). Our cells only responded to doses between (0.00625-1%) R_f , which translates on a “cup of tea” scale to approximately 0.5-12 cups. Thus, it is plausible that these effects will be observed *in vivo*, after drinking a cup volume of R_f . The initial effect of R_f resulted in a biphasic response from 24-72 hrs, but by 96 hrs all concentrations decrease relative to the control. Using aspalathin as a plasma marker, the literature indicates that drinking a cup of tea would result in similar values for aspalathin (See **discussion 4.2 Chemical analysis of fermented rooibos**). Exposure to high concentrations of R_f extract in a clinical context, could be achieved by means of administering R_f extract in a tablet form. Surprisingly, toxicity tests show almost 0% toxicity (See **Table 6**) of the bEnd5 cells, irrespective of a decline in the cell population, with respect to its cell numbers ($\times 10^5$ /ml), which show approximately 100% live cells (See **Appendix C, Table 5**). Thus, R_f is not killing cells, but potentially has an impact on the rate of

cell division. An increase in the concentration of R_f caused the same effect as EtOH, as AOs are harmful on its own and are only useful in the presence of oxidants, where its scavenging properties can be observed. The results endorse the harmful effects of ROS or oxidant species on cellular proliferation, thus, affecting the mitotic division of the cells. In addition, cellular proliferation is endorsed by the effects of R_f on MA, which is discussed in the following section.

4.4.2 Effect of rooibos - induced changes on bEnd5 mitochondrial activity

For both acute and chronic exposure to R_f , a directly proportional relationship was observed for R_f concentrations at 24 hrs. R_f resulted in suppression of the MA within 24 hrs, thereafter, all concentrations of R_f , but the highest concentrations, was elevated in a cyclic diurnal manner in both 48 hrs and 96 hrs (See Fig. 21 and Fig. 22).

R_f has been investigated as a potential antidote, because it results in an elevation in AOs and EtOH results in an increase in ROS, subsequently compromising the BBB. The antidotal effect is produced when ROS, produced as a result of EtOH exposure, is countered upon the introduction of AOs found in R_f . A biphasic response was seen at 24 hrs, and although we do not understand the exact mechanism by which this biphasic response occurs, plausible responses of biphasic data are well documented in the literature (Svedružić et al., 2012). One hypothesis which attempts to understand it, involves the effect of substances on protein conformation. Low concentrations of R_f may potentially have caused a change in the protein conformation, resulting in increased activity of the enzyme MDH and at higher R_f concentrations a conformational change in proteins may have resulted in a decrease

in MDH activity, thus, we observed a biphasic effect across a range of R_f concentrations. For this reason we conducted these studies with a low amount of moles as it generated a molecular and a subsequent physiological response within the bEnd5 cells.

4.4.3 Combinatory effect of ethanol and fermented rooibos on mitochondrial activity

The MA data, for the effect of EtOH on bEnd5 cells, revealed that at 48 hrs significant suppression of MA occurred (See Fig. 19 and 20), which resulted in the suppression of cellular proliferation from 72 hrs to 144 hrs (See Fig. 17). The working hypothesis of this study was based on evidence that EtOH produces its effects via ROS production and that the introduction of R_f , an extract high in AO, would reverse these effects.

Combination treatments could not reverse the suppressive effects, but in turn exacerbated it. This result may have occurred due to an imbalance in the redox status of the cell. Research conducted by Kirkinezos et al. (2001) further supported this conclusion with research findings reporting on incidences where the exogenous antioxidants exceeded the endogenous redox capacity of the cells mitochondria, causing cells to undergo stress, ultimately altering the normal functioning of its mitochondria (Kirkinezos et al., 2001).

During oxidative stress brain cells become highly susceptible to oxidative injury, due to the inadequate availability of both endogenous and exogenous AO levels in the brain (Lakhan et al., 2009; Won et al., 2002; Alikunju et al., 2011). *A.linearis*, known for its AO capacity as a result of its high polyphenolic content (Marnewick et al., 2003; Lamosöová et al., 1997; von Gadow et al., 1997) has been postulated to

protect against EtOH-induced changes to the rate of MA and subsequent cell viability.

The mitochondrial suppression may have resulted due to a synergistic effect caused by the oxidant nature of EtOH, and the potential pro-oxidant nature of the polyphenols found within R_f (Joubert et al., 2005), potentially causing an imbalance in the redox status of the cells mitochondria. Studies performed on raw polyphenolic elements of *A.linearis* found it to be comprised of antioxidants and/ pro-oxidants and, therefore, it is imperative to take into account the interaction of polyphenolic segments with free radicals in order to better elucidate the AO/pro-oxidant properties of *A.linearis* (Joubert et al., 2005).

Despite the fact that it has been suggested that flavonoid compounds may possibly contribute to a certain level of cytotoxicity due to their mutagenic properties; their ability to act as pro-oxidants and their ability to inhibit certain enzymes, research has shown exogenous AOs to have neuroprotective functions in various animal studies involving acute nervous system injury and neurodegenerative diseases (Calabrese et al., 2009).

Research reports have found AOs' seemed to target subcellular levels, specifically the mitochondria (Chaturvedi et al., 2008; Yang et al., 2009). AO such as ubiquinone, lipoic acid and Vitamin E and nitrous sojn traps have been targeted to the mitochondria (Murphy and Smith, 2007) and have shown neuroprotection in many models of neurodegenerative diseases and alcohol neurotoxicity (Silver-Marsiglio et al., 2005).

A range of neuroprotective mechanisms have been used based on mitochondrial protection from oxidative stress. Several classifications of mitochondrial defenses

have been developed. These include: inhibitors of ROS formation; exogenous AOs; agents that may increase reducing power necessary for ROS detoxification and simulation of genes which improve mitochondrial defenses (Ankarcrona, 1995; Perez-Pinzon et al., 2012). Based on results generated in this research study, R_f does not ameliorate or reverse EtOH effects, but rather exacerbates it in combination, in terms of the MA of the bEnd5 cells.

4.5 Endorsement of the BBB model

4.5.1 The high resolution morphological characteristics of an endothelial cell monolayer

The bicameral system was set up using bEnd5 cells, grown on a mixed cellulose insert membrane surface, within a 24-well microtiter plate. The insert was reported by the manufacturer to have a characteristic pore size of $0.45\mu\text{m}$. This implies that molecules of a maximum size of 450nm or less were able to pass through the porous membrane surface. The insert was essentially used for the orientation and facilitation of bEnd5 cell growth, thus, the presence of a specialized extracellular membrane surface is important for a cell to lay down its basement membrane.

The purpose of conducting high resolution SEM studies was to validate the *in vitro* bicameral model, from the perspective of how a monolayer is established three dimensionally and to evaluate how physiologically relevant EtOH concentrations (25mM) (Barnes and Singletary, 2000) impacted this monolayer from a morphological point of view.

Better elucidation of mechanisms regulating the BBB is aided by *in vitro* systems (Brown et al., 2007). The cell based models have greatly impacted brain research, in

that it provides knowledge on the morphology, physiology and pathophysiology of the BBB (Ceccheli et al., 1999; Nakagawa et al., 2009).

4.5.2 Effect of cell density on characteristic cell-to-cell interaction: Comparison between high and low cell densities

Cells seeded using two cell densities were investigated to inform us regarding the impact of cell density on cell monolayer confluence in a bicameral system. A low cell seeding density was studied in order to determine the effect of cell development in the absence of adjacent cells and their paracrine influences. In addition, we investigated the impact of a high cell seeding density on how cells develop in close proximity of each other. Under a low cell seeding density cells were observed, which were dispersed where paracrine influence was minimal. In our results the bEnd5 cells were benign of proteins, vesicle formation and blebs, in terms of the cells surface topography. These cells did not present with any vesicle formation on the surface topography, only a cell membrane surface was visible (**See Fig.34.**). These cells lacked in cell-to-cell communication, similar to work described by Dejana, (2004). Conversely the bEnd5 cells seeded at 1×10^6 cells/well/insert established a confluent monolayer. These cells were decisively different, exhibiting high, convoluted membrane structures, which included: vesicle formation on its surface and visible cytoplasmic projections with numerous intercellular junctional complexes formed between adjacent cells (**Fig. 31B, 35, 36**). The results endorses the fact that cells grown at higher cell densities express tremendous protein interaction. Thus, cells in close proximity exhibited shorter paracrine distances, and therefore, increased cell-to-cell paracrine communication which further endorses a confluent monolayer as a result of paracrine factors causing cells to engage with

each other. For this reason, a deduction can be made that a greater seeding density exhibited shorter paracrine distance and, therefore, increased cell-to-cell paracrine communication which was similar to findings described in research conducted by Kim and Dean et al. (2009). Thus, in ECs, cells tend to exhibit different morphological characteristics, which are highly influenced by the degree of confluence or sparsity of its cell monolayer (Dejana, 2004).

The relationship between cell density and cell-to-cell signaling are important parameters to consider when optimizing an experimental model and is essential for establishing a closed circuit, which is necessary for the commencement of studies on the bioelectrical effect of compounds/ substances on the structural integrity of the BBB *in vitro*.

4.5.3 The basement membrane

Intrinsic to the development of all epithelia, is the development of a basement membrane, this is true for the endothelium of the BBB as well. The basement membrane is important for the cell to morphologically evolve apical and basolateral surfaces. This SEM study demonstrated, for the first time, the process of laying down a bEnd5 EC basement membrane (See Fig.33), which seamlessly integrated itself into the extracellular mixed cellulose ester membrane of the insert. Thus, the *in vitro* model mimicked the *in situ* morphology by the establishment of a basement membrane. Although a basement membrane has been observed using transmission electron microscopy (TEM), this is the first time that the establishment of a basement membrane was visualized under high resolution SEM, emanating from a single cell, which is the forerunner of the monolayer. This fibrous network which formed the

basal lamina is known to consist of a myriad of proteins which include glycoprotein families, such as: laminin, collagen IV, nidogens and heparan sulfate (HS) proteoglycans. In addition, it contains the proteoglycan, agrin HS, found within the basement membrane of brain microvessels (Barber et al., 1997). This is an essential protein in that it is closely associated with the expression of claudins (Rascher et al., 2002; Luissint et al., 2012). Additionally the protein, B1-integrin, aids in the attachment of the brain ECs to the basement membrane which highly influences the expression of claudin-5 localization at the TJs (Osada et al., 2011) and brain EC polarity. Thus, the establishment of the basement membrane in the monolayer allowed for the cell to be expressed morphologically and functionally in alignment with the *in situ* morphology of the Brain ECs, thereby, endorsing the BBB model.

4.5.4 Shear stress and the glycocalyx

In vivo, the heterogenous nature of blood in combination with the hemodynamic forces generated by the flow of blood contributes to shear stress in BMVECs (Luissint et al., 2012). The application of high resolution SEM in this study made it possible to observe the surface topography of a monolayer of bEnd5 cells grown on an insert for the first time. The apical surface gave rise to the formation of a thin fibrous network. The literature reports that the bEnd5 cells developed a surface extracellular network, comprised of proteoglycans, glycoproteins and glycolipids, commonly referred to as a glycocalyx. (Damiano et al., 2002). The glycosaminoglycans (GAGs) are linear type polydisperse heteropolysaccharides which are formed by variations of repeat disaccharide units. Some GAG forms found, include: chondroitin/dermatan sulfate (CS), HS and Hyaluronic acid (HA). The most prominent GAG on the EC, being the HS, constitutes greater than 50% of

the GAG profile (Tarbell et al., 2010; Martini, 2006). The *in vivo* function of the glycocalyx is to aid in the reduction of shear stress as a result of blood flow (Damiano et al., 2002). The observation of the development of this glycocalyx structure on the apical surface of our monolayer also endorses our BBB model of the *in vivo* scenario, as the literature hypothetically relates the development of the glycocalyx as a response to shear stress. It was postulated that in our model, shear stress was introduced with flow forces caused by the daily changing of media in the insert of our bicameral model, subjecting the bEnd5 cell monolayer to a degree of flow, further concretizing this model, making it analogous to the *in vivo* situation. Irrespective of its negligible role as a resistance barrier, the glycocalyx serves to lubricate and protect as the glycoproteins and glycolipids form a viscous layer on the outside of a cell and its components are sticky in nature which aids in anchoring the cells (Martini, 2006). It is for this reason that molecular protective barriers, such as the glycocalyx, must be acknowledged for their role in acting as a three-dimensional molecular sieve (Curry and Michel, 1980).

The resistance across a bEnd5 cell monolayer could be attributed to an array of factors. The influence of both shear stresses as a result of ECs' subjected to flow, cell density and subsequent changes in cell morphology influences the way the EC grows in a cultured environment. Standard light microscopy is limited to estimate the thickness of an EC monolayer of a biological specimen. In light microscopy, bEnd5 cells appear to be polygonal in terms of its cell body structure, exhibiting indistinguishable borders (data not shown), similar to work described by Jaffe et al. (1973). With reference to electron micrographical information retrieved using SEM; three-dimensional (3D) ultrastructures of a confluent bEnd5 cell monolayer were able to be investigated. The bEnd5 cells remained attached to the surface of the

extracellular baseline, expressed distinct cell borders and were inclined to grow towards each other, reflective of its adherent nature (See Fig.31 and Fig.32). Light microscopy, however, is a limiting factor in that only two-dimensional (2D) cell images could be viewed.

4.5.5 Elucidating the paracellular space in the light of SEM: Tight junctions and adherens junctions

TJs are found on the apical surface, of the brain ECs. These are intercellularly located and functions in inhibiting the paracellular transport of substances into the CNS (Schreibelt et al., 2007). In terms of what is known in theory, ECs of the BBB contain claudins with two extracellular loops and 4 transmembrane domains which interact, heterophilically and homophilically, with claudins on adjacent cells (Furuse et al., 1998; Furuse et al., 1999; Schreibelt et al., 2007).

SEM analysis cannot differentiate between the specific protein molecules' making up the TJs. For this reason, one has to utilize other criteria in making a plausible identification of structures. SEM is unable to show substructures and, therefore, we only see what protrudes from the cell membrane surface. In theory, it is emphatically stated that TJ loops are formed. Thus looking at the paracellular space between the monolayer we were able to see intercellular looped structures which can be identified as claudins and occludins on the apical surface of the Brain EC. These apically located proteins form loop-like structures, which appear tight against each other.

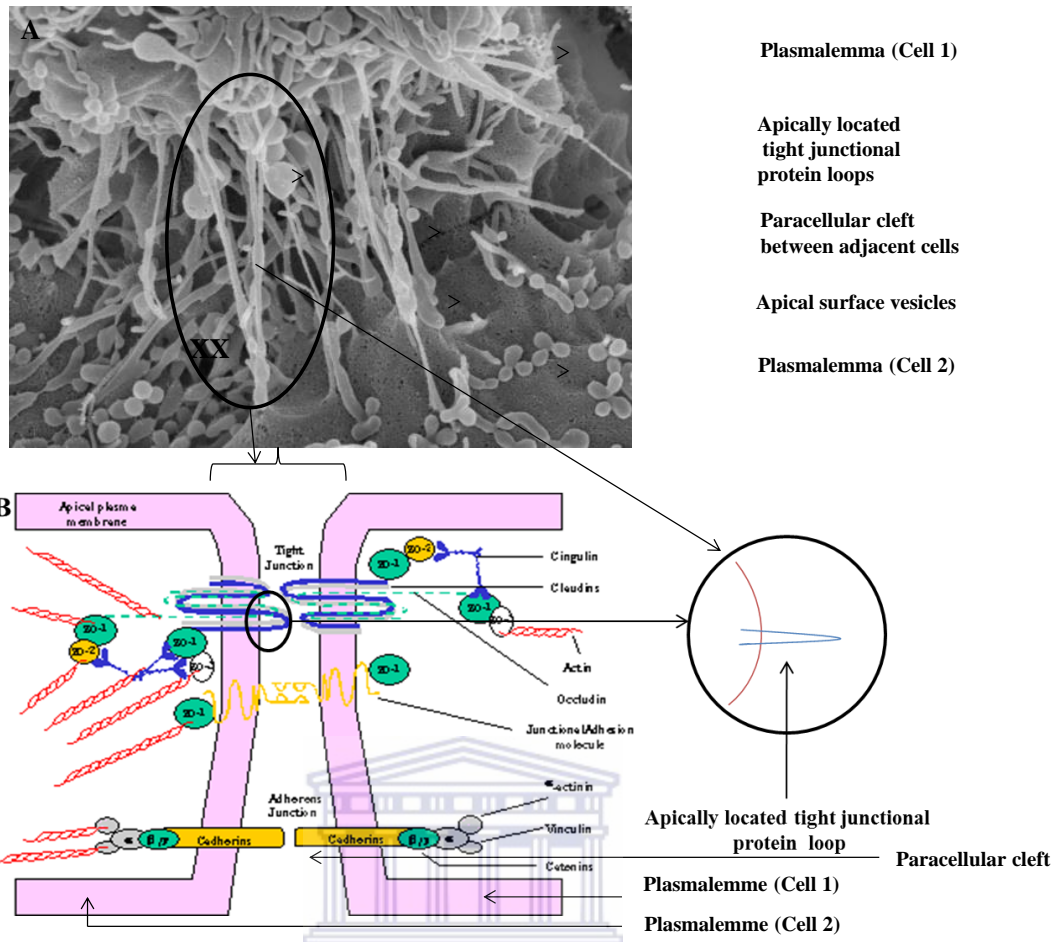


Figure 38. The micrograph in A. is a paracellular area between 2 cells and depicts the molecular interaction between two adjacent cells, SEM looks at the cell from a surface perspective (see XX on diagram A); B. is a schematic diagram of the tight junctional protein complexes between two adjacent cells (<http://www.pharmacology.arizona.edu/images/faculty/davisfig2.gif>).

Based on the above comparison (See Fig.38), what we see is not loop-like TJ structures, but rather for the first time we saw tightly woven rod-like loops on the apical surface of the cells which are analogous to the loops represented in the schematic diagram above. We, thus, contend that these loops are in fact the TJ proteins within the paracellular space.

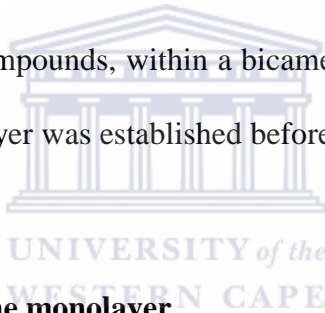
Additionally, the experiments in this study seemed to also reveal AJs which were seen on the lateral borders, deeper down in the cleft of adjacent cells. AJs which

function in binding lateral cell surfaces together are supported by our micrographic data (Dejana, 2004). SEM data strongly endorses the BBB model used in this study.

4.6 Bioelectrical studies: Transendothelial electrical resistance

4.6.1 Introduction: Effect of ethanol and fermented rooibos on transendothelial electrical resistance optimization of a monolayer

Transendothelial electrical resistance (TEER) studies can be defined as a construct of the degree of transcellular and paracellular permeability across a brain EC monolayer. This bioelectrical study was performed on a TEER system in order to determine the integrity of the barrier after its exposure to EtOH, R_f and a combination of these compounds, within a bicameral system. The bicameral system with a confluent monolayer was established before commencing the measurement of TEER.



4.6.2 Optimization of the monolayer

500nM of hydrocortisone (HC) was utilized to optimize TEER, by enhancing the barrier properties of the bEnd5 cell monolayer (Weidenfellar et al., 2005). The optimization of a TEER system was investigated using two regimes of exposure: (i) acute exposure (24 hr/ once-off) and (ii) chronic exposure (daily for 24-144 hrs) over a period of 6 days. The acute exposure showed a marked increase in TEER, relative to the controls. Conversely, chronic exposure to HC in combination with serum free media (SFM) resulted in marked increases in TEER compared to the controls across the entire experimental timeline (See Appendix E, 1.1 and 1.2). Based on literature reported in cancer research, the use of HC is known to slow rapid cellular proliferation, and was therefore administered as a means to slow tumour

progression (Jacobs and Woods, 1995). In addition, it is also a modulator of TJ protein organization in a way that enhances barrier integrity (Weidenfellar, 2005). HC (500nM) in combination with SFM generated higher TEER readings in comparison with HC and 10% FBS supplemented DMEM-F12 (See **Appendix E, 1.1 and 1.2**). As a result, chronic HC and SFM were employed to optimize the TEER system for a period of 6 days (24-144 hrs). The TEER results generated after the use of both SFM and HC endorsed work conducted by Nitz et al. (2003) who reported on the use of HC as a hormonal regulator of BBB permeability (Hoheisel 1998; Nitz et al., 2003). In addition, it was reported that serum, when in contact with the basolateral compartment of the brain microvascular ECs, caused a breakdown in the TJs of microvascular ECs in culture and, thus, the presence of serum in normally employed concentrations such as 10% (v/v) weakened the barrier properties of porcine brain capillary ECs (PBCEC) (Nitz et al., 2003). Based on previous research, HC at 500nM was able to result in the reorganization of the actin cytoskeleton in porcine and murine brain ECs, resulting in the longitudinal reorganization of the ZO-1 and occludin and in so doing re-enforcing barrier properties, subsequently resulting in increased TEER (Weidenfellar et al., 2005).

4.6.3 The effect of ethanol on TEER

The literature has reported that EtOH disrupted EC integrity, subsequently decreasing TEER (Haorah et al., 2005; Xu et al., 2012) by way of rearranging its stress sensitive actin fibers and subsequently changing cytoskeleton dynamics of the cell (Xu et al., 2012). On the contrary, the current study showed an increase in TEER readings across the bEnd5 cell monolayer, after exposure to EtOH for 24 hrs, compared to controls, which reached lower TEER values of approximately 25% (See Fig. 27) for the remainder of the experimental timeframe (72-144 hrs). The lowest EtOH concentrations had the highest effect on TEER, causing a 24 hr dose-dependent effect. At 48 hrs, only the supraphysiological levels/concentrations showed a drop in TEER, thus, one only sees a physiological effect within a physiological range at 24 hrs and this appears to be causing an increase in resistivity. For the remainder of the timeframe, cells appear to have adapted to the change in its growing environment by decreasing in TEER and reaching values similar to the controls. The decrease in TEER may have resulted as it is known that EtOH, by definition, causes a decrease in permeability due to ROS production. EtOH is a non-conducting substance, which when added to media, increases the resistivity of that media. It is definitely not due to placing alcohol within the insert, as the experimental blank, containing both standard media (supplemented DMEM-F12) and EtOH was subtracted to normalize TEER readings. In so doing, it controlled for the effect of EtOH on the resistivity of the TEER system, therefore, there must be a physiological effect on the monolayer, as it becomes less permeable at 24 hrs, which is about a 25% increase in TEER relative to the controls. From 24-144 hrs; however, a time-dependent effect across the experimental timeline is negligible (See Fig. 27).

4.6.4 Equivalent electrical circuit for TEER experiments

The electrical equivalent circuit helps in understanding the rationale for TEER. The circuit describes the theoretical basis of TEER by expanding the various components that reflect a TEER measurement. An equivalent circuit may reflect changes in resistivity of the fluid bathing the cells. The resistivity of the media/solution is a separate parameter, unrelated to the permeability of the cell monolayer. The effect of the apical compartment (R_{fa}) and the basolateral compartment (R_{fb}) being in series within the equivalent circuit would produce an additive effect on TEER. Thus, a change in the ionic content of the media will have a quantitative effect on the resistivity. The equivalent circuit of the blank refers to the resistivity of the media, insert membrane and the resistance of the fluid in R_{fb} of the bicameral model, which is situated in series. Measuring these quantities will give us an equivalent circuit measuring TEER. These effects are subtracted so that we fundamentally eliminate the effect of R_{fa} , R_1 and R_{fb} in order to achieve an effective resistance across the cell monolayer. The summation of the various populations of channels in different open-close states on each membrane reflects the permeability of that particular membrane. This particular system of permeability refers to the resistance across a cell membrane, therefore, the effect of transcellular resistance across the apical surface (R_a) and the basolateral surface (R_b) of the cell membrane needs to be considered. The transcellular resistance, which is reflective of transcellular permeability, is regulated by the ratio of ionic channels open, and therefore, the cell membrane is a selective regulator of ionic flow. The paracellular permeability is caused by TJ expression, thus, an under or over expression of a specific TJ protein will directly influence the permeability across the cell monolayer. The resistance caused by the TJs (R_{TJ}) is a non-selective regulator of ion flow and is, therefore, an important

consideration when investigating the bioelectrical barrier properties of the bEnd5 cell monolayer.

4.6.4.1 True resistance of a monolayer = $R_{\text{experiment}} - R_{\text{blank}}$

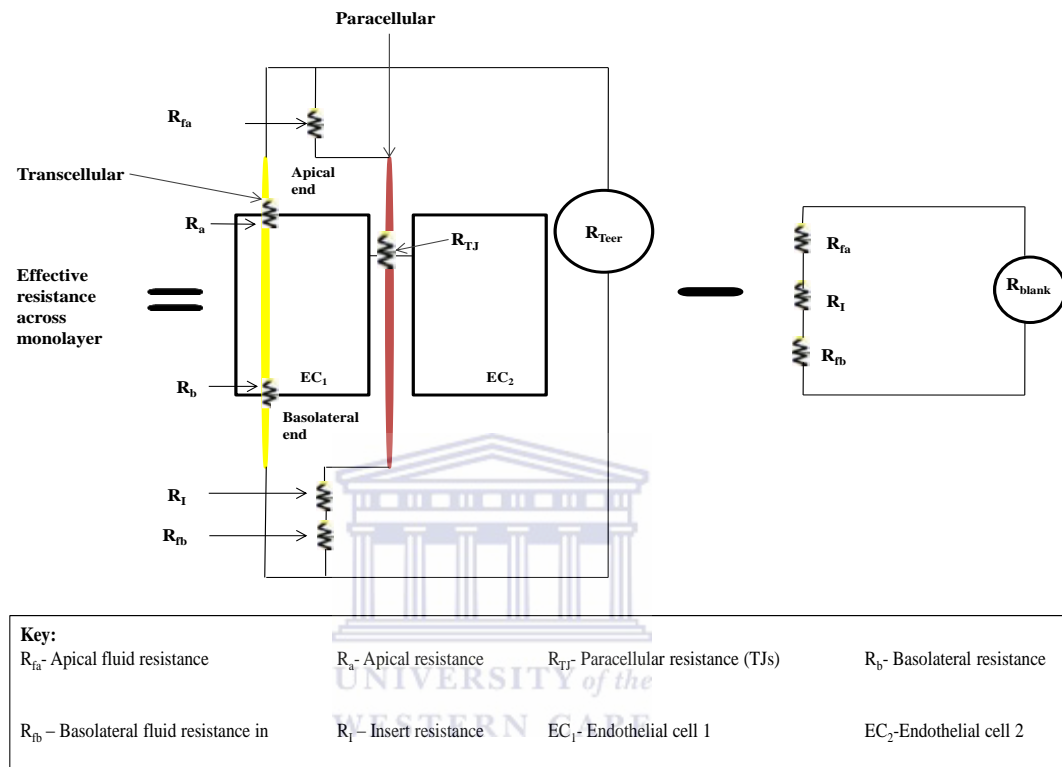


Figure 39. Effective/true resistance of a monolayer using an equivalent circuit.

R_{fb} and R_{fa} reflected the resistance of fluids, which may change the ionic composition of the media and influence the resistivity. **Fig. 39** represents the various components of an electrical circuit which reflects the resistance across the bEnd5 EC monolayer. The red solid line represents the paracellular pathway and the solid yellow line represents the transcellular pathway. We hereby describe the equivalent electrical circuit for the blank resistance measured across a blank insert, containing media+compounds which are subtracted in order to establish the true resistance across the cell monolayer.

4.6.5 Effect of fermented rooibos on TEER

The bEnd5 cell monolayers were treated with R_f on a daily basis, thus, ensuring that cells were exposed to a constant concentration of R_f . A dose-dependent increase was observed, followed by a plateau effect (See Fig. 28). After 24 hrs, a cyclic effect on the monolayer repeated itself every 48 hrs. Control measures were put in place to ensure that the addition of R_f media did not change the resistivity. This was unlikely, due to the amount of R_f added. Within 24 hrs of observing the dose-related effect, no effect was observed (plateau effect). Thus, the dose-response has to be a physiological response whereby the lower concentrations of R_f were able to neutralize smaller quantities of ROS species and the greater concentrations of R_f , reduced/neutralized greater amounts of ROS production. By reducing the ion/oxidant content of the media, it resulted in an increase in resistivity and subsequent increase in TEER (See Equivalent electrical circuit, Fig. 39: R_{fa} and R_{fb}). Thus, it is clear that it is not a resistivity effect, due to the addition of R_f to the media. Based on this 48 hr cyclic effect we may deduce that the cell responded by a negative-feedback mechanism after its exposure to the antioxidant by producing endogenous oxidants, in just sufficient quantities to reduce the dose-response.

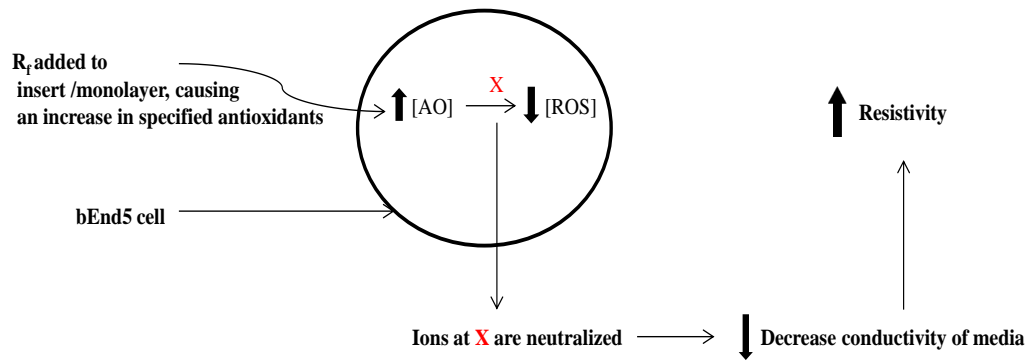


Figure 40. Directly proportional relationship between antioxidant (AO) concentration's and ROS production. The more ROS neutralized, the greater the ionic depletion of the media, and therefore, the greater the resistivity. This providing an explanation for the dose-dependent effect observed, during the course of the experiment.

The cellular components in this environment responded to this suppression in ROS, which produced an increase in TEER. ROS production is intimately involved in the ionic concentration of the cellular environment. The addition of R_f results in a decrease in ROS, causing an increase in TEER, due to the indirectly proportional relationship which exists between resistivity and R_f as an antioxidant. The exact feed-back mechanism is unknown at this stage in the research, but we can assume that the mitochondria are involved and, thus, the response may well be a physiological effect. This suggested that the high antioxidant capacity of R_f on the bioelectrical properties of the bEnd5 cell has a transient effect by increasing the resistivity of the media bathing the bEnd5 cell monolayer. The plateau effect seen at 96 hrs (See Fig. 28) could be attributed to the compensation of the mitochondrial gradient as a result of depletion in the ionic content of the cellular environment. It is unlikely that this is an effect at the level of either transcellular/ paracellular permeability, as the effect of the various R_f concentrations resulted in a dose-related

effect and was too small to be attributed to an effect on permeability across the transcellular pathways.

4.6.6 Effect of ethanol and fermented rooibos in combination on TEER

It is well established that the EtOH-induced oxidation caused ROS production, resulting in an increase in oxidants and subsequently decreased resistivity, which could be attributed to ROS production and the compromising of paracellular TJs (Haorah et al., 2005). Our hypothetical position was that concurrent treatment of cells with R_f would neutralize the oxidative producing effect of EtOH metabolism on the bEnd5 cell environment. However, the effect of EtOH and R_f in combination resulted in a dose-dependent decrease in TEER. The impact of EtOH induced an increase in ROS production, even with small amounts; thus, R_f concentrations in small amounts with EtOH resulted in a decrease in TEER, as EtOH could have potentially overpowered the AO effect of the R_f concentrations used. Although, R_f may neutralize a substantial amount of oxidants, only a minute amount of oxidants are required to produce a permeability effect.

The results for the effect of EtOH on permeability endorsed findings by Phillips et al. (1997) who reported that there was no consistent evidence of any alcohol-induced effects that could indicate a disruption of the vessels and the endothelial TJs. Unpublished results on SEM data clearly showed that the cell monolayer remained intact, irrespective of the exposure of EtOH to the monolayer over a period of 144 hrs. Adjacent bEnd5 cells were able to tightly adhere to each other throughout the experimental timeframe. Thus, this tightly packed cell monolayer may have further endorsed the bicameral system.

Chapter 5

5.1 Conclusion

Our study has shown that alcohol produces profound damage to the BBB and subsequently has a long-term ability to compromise the homeostatic environment of the neuron. The main findings in this study were that: (a) alcohol has a long-term effect on the proliferation of the bEnd5 cells, (b) the decrease in cellular proliferation was not caused by the toxic effects of alcohol and (c) the decrease in proliferation was linked to a decrease in MA, which was linked to the decreasing ability of the cell to produce the metabolic energy necessary for cell division.

The study showed that rooibos (across a physiologically relevant range) did not significantly reverse the ROS-induced effects of alcohol, but rather exacerbated the effects. Furthermore, rooibos, on its own, caused a redox imbalance within the cell, which seemed to cause a long-term, biphasic suppression in cell proliferation.

Our working hypothesis was based on the understanding that the combination treatments would reverse the negative effects of EtOH exposure. However, this study points to a synergistically negative effect on the bEnd5 cells. Theoretically, the introduction of equivalent circuits as a means to better elucidate membrane permeability was novel to this model and our endorsement of the model in terms of the SEM study has made significant progress.

Our study, thus, highlights, for the first time the negative effects of both EtOH and R_f on the physiological function of the BBB, which may be pertinent for human physiology. The ability of bEnd5 cells to remain viable after exposure to supra high concentrations of EtOH, shows the extreme physiological robustness of these cells.

5.2 Future Perspectives

In order to deepen our understanding of how EtOH and R_f affect bEnd5 cellular proliferation, it is suggested that flow cytometry analysis be conducted, to clarify the stage of mitosis in which cell division is inhibited. Furthermore, the exciting results found in the SEM component of the study could be expanded through investigating the effects of various experimental substances on the pathology of the BBB and how introducing a tincture of R_f could better ameliorate potential pathology.

CHAPTER 6

6.1 References

- Abdul Muneer, P.M., Alikunju, S., Szlachetka, A.M. and Haorah, J. (2011) Inhibitory effects of alcohol on glucose transport across the blood-brain barrier leads to neurodegeneration: preventive role of acetyl-L: -carnitine. *Psychopharmacol. (Berl)*. **214**, 707-18.
- Abel, E.L. and Sokol, R.J. (1987) Incidence of fetal alcohol syndrome and economic impact of FAS-related anomalies. *Drug Alcohol Depend.* **19**, 51-70.
- Abel, E.L. (1995) An update on the incidence of FAS: FAS is not an equal opportunity birth defect. *Neurotoxicol Teratol.* **17**, 437-443.
- Abel, E.L. (1998) Fetal alcohol abuse syndrome, New York: Plenum Press.
- Adamson, R.H. and Clough, G. (1992) Plasma proteins modify the endothelial cell glycocalyx of frog mesenteric microvessels. *J Physiol.* **445**, 473-86.
- Agarwal, D.P. (2001) Genetic polymorphisms of alcohol metabolizing enzymes. *Pathol Biol (Paris)*. **49**, 703-9.
- Alikunju, S., Abdul Muneer, P.M., Zhang, Y., Szlachetka, A.M. and Haorah, J. (2011) The inflammatory footprints of alcohol-induced oxidative damage in neurovascular components. *Brain Behav Immun.* **25 Suppl 1**, S129-36.
- Ankarcrona, M., Dybukl, J.M., Bonfoco, E., Zhivotovsky, B., Orrenius, S., Lipton,

S.A., and Nicolera, P. (1995) Glutamate-induced neuronal death: a succession of necrosis or apoptosis depending on mitochondrial function, *Neuron* **15**, 961-973.

Anon., (2006). Is that rooibos in my cappuccino? *South African Food Rev.* **33**, 24.

Armulik, A., Genove, G., Mae, M., Nisancioglu, M.H., Wallgard, E., Niaudet, C., He, L., Norlin, J., Lindblom, P., Strittmatter, K., Johansson, B.R. and Betsholtz, C. (2010) Pericytes regulate the blood-brain barrier. *Nat.* **468**, 557-61.

Ayache, J., Beaunier, L., Boumendil, J., Ehret, G. and Laub, D. (2010) Sample preparation handbook for transmission electron microscopy techniques. Preliminary preparation techniques. New York, USA: Springer Science+Business media, pp 72-74.

Bailey, S. M. and Cunningham, C. C. (1999) Effect of dietary fat on chronic ethanol-induced oxidative stress in hepatocytes. *Alcohol Clin Exp Res.* **23**, 1210-1218.

Ballabh, P., Braun, A. and Nedergaard, M. (2004) The blood-brain barrier: an overview: structure, regulation, and clinical implications. *Neurobiol Dis.* **16**, 1-13.

Bajčan, D., Harangozo, L., Hrabovska, D. and Boncikova, D. (2013) Optimizing conditions for spectrophotometric determination of total polyphenols in wines using Folin-Ciocalteu reagent. *J. Microbiol, Biotechnol and Food Sci.*

2(1), 1699-1708.

Banks, W.A. (2009) Characteristics of compounds that cross the blood-brain barrier.

BMC Neurol. **9 Suppl 1**, S3.

Barber, A.J., Leith, E. (1997) Agrin accumulates in the brain microvascular basal

lamina during development of the blood-brain barrier. *Dev Dyn.* **208**, 62-74.

Barnes, S. L.; Singletary, K. W., and Frey, R. (2000) Ethanol and acetaldehyde

enhance benzo[a]pyrene-DNA adduct formation in human mammary epithelial cells. *Carcinogenesis* **21(11)**, 2123-8.

Barros, L.F., Kanaseki, T., Sabirov, R., Morishima, S., Castro, J., Bittner, C.X.,

Maeno, E., Ando-Akatsuka, Y. and Okada, Y. (2003) Apoptotic and necrotic blebs in epithelial cells display similar neck diameters but different kinase dependency. *Cell Death Differ.* **10**, 687-97.

Begley, D.J. (2004) ABC transporters and the blood-brain barrier. *Curr Pharm Des.*

10, 1295-312.

Benzie, I. F. and Strain, J. J. (1996) The ferric reducing ability of plasma (FRAP) as

a measure of "antioxidant power": the FRAP assay. *Anal Biochem.* **239(1)**, 70-6.

Benzie, I. F. and Szeto, Y. T. (1999) Total antioxidant capacity of teas by the ferric

reducing/antioxidant power assay. *J Agric Food Chem.* **47(2)**, 633-6.

- Borlak, J., Walles, M., Levsen, K., Thum, T. (2003) Verapamil: metabolism in cultures of primary human coronary arterial endothelial cells. *Drug Metab Dispos.* **31**, 888-891.
- Bozzola, J.J., and Russel, L.D. (1999) Electron microscopy. In: Chapter 3, Specimen preparation for scanning electron microscopy. 2nd edition,. Mississauga, Canada: Jones and Barlett publishers Inc. pp 54.
- Bramati, L., Minoggio, M., Gardana, C., Simonetti, P., Mauri, P. and Pietta, P. (2002) Quantitative characterization of flavonoid compounds in rooibos tea (*Aspalathus linearis*) by LC-UV/DAD. *J Agric Food Chem.* **50**, 5513-9.
- Breiter, T., Laue, C., Kressel, G., Gröll, S., Engelhardt, U.H., and Hahn, A. (2011) Bioavailability and antioxidant potential of rooibos flavonoids in humans following the consumption of different rooibos formulations, *Food Chem.* **128**, 338-347.
- Brick, J., PHD. (2005) Intoxikon International. Alcohol and drug studies: research and educational consulting.
- Brocardo, P.S., Gil-Mohapel, J. and Christie, B.R. (2011) The role of oxidative stress in fetal alcohol spectrum disorders. *Brain Res Rev.* **67**, 209-25.
- Brown, R.C., Morris, A.P., and O'Neil, G. (2007) Tight junction protein expression and barrier properties of immortalized mouse brain microvessel endothelial cells. *Brain Res.* **1130**, 17-30.
- Burd, L.; Roberts, D.; Olson, M., and Odendaal, H. (2007) Ethanol and the placenta:

a review. *J Matern Fetal Neonatal Med.* **20(5)**, 361-75.

Buske, C. (2013) Zebrafish shoaling behavior: its development, quantification, neuro-chemical correlates, and application in a disease model. Published (PhD), University of Toronto.

Calabrese, V., Cornelius, C., Mancuso, C., Barone, E., Calafalo, S., Bates, T., Rizzarelli, E., and Koslova, A.T. (2009) Vitagenes, dietary antioxidants and neuroprotection in neurodegenerative diseases. *Front Biosci.* **14**, 376-397.

Cardoso, F.L., Brites, D. and Brito, M.A. (2010) Looking at the blood-brain barrier: molecular anatomy and possible investigation approaches. *Brain Res Rev.* **64**, 328-63.

Cecchelli, R., Dehouck, B., Descamps, L., Fenart, L., Buee-Scherrer, V. V., Duhem, C., Lundquist, S., Rentfel, M., Torpier, G. and Dehouck, M.P. (1999) *In vitro* model for evaluating drug transport across the blood-brain barrier. *Adv Drug Deliv Rev.* **36**, 165-178.

Chaturvedi, R.K. and Beal, M.F. (2008) Mitochondrial approaches for neuroprotection. *Ann N Y Acad Sci.* **1147**, 395-412.

Chen, Y., Zhu, Q.J., Pan, J., Yang, Y. and Wu, X.P. (2009) A prediction model for blood-brain barrier permeation and analysis on its parameter biologically. *Comput Methods Programs Biomed.* **95**, 280-7.

Cofan, M., Nicolas, J.M., Fernandez-Sola, J., Robert, J., Tobias, E., Sacanella, E., Estruch, R. and Urbano-Marquez, A. (2000) Acute ethanol treatment

decreases intracellular calcium-ion transients in mouse single skeletal muscle fibres *in vitro*. *Alcohol Alcohol*. **35**, 134-8.

Coisne, C., Dehouck, L., Faveeuw, C., Delplace, Y., Miller, F., Landry, C., Morissette, C., Fenart, L., Cecchelli, R., Tremblay, P. and Dehouck, B. (2005) Mouse syngenic *in vitro* blood-brain barrier model: a new tool to examine inflammatory events in cerebral endothelium. *Lab Invest*. **85**, 734-46.

Colgan, O.C., Collins, N.T., Ferguson, G., Murphy, R.P., Birney, Y.A., Cahill, P.A. and Cummins, P.M. (2008) Influence of basolateral condition on the regulation of brain microvascular endothelial tight junction properties and barrier function. *Brain Res*. **1193**, 84-92.

Cummings, F.R. (2006) "Hot-wire chemical vapour deposition of carbon nanotubes, MSc thesis, University of the Western Cape.

Cunningham, C.C. and Van Horn, C.G. (2004) Energy availability and alcohol-related liver pathology. *Alcohol and Hlth*. **27(4)**, 291-299.

Curry, F.E., Michel, C.C. (1980) A fibre matrix model of capillary permeability. *Microvascular Res*. **20**, 96-99.

Damiano, E.R. and Stace, T.M. (2002) A mechano-electrochemical model of radial deformation of the capillary glycocalyx. *J. Biophys*. **82**, 1153-75.

Deitrich, R., Zimatkin, S. and Pronko, S. (2006) Oxidation of ethanol in the brain and its consequences. *Alcohol Res Hlth*. **29**, 266-73.

Dietrich, R.A., and Harris, R.A. (1996) How much alcohol should I use in my experiments? *Alcohol. Clin. Exp. Res.* **20**, 1-2.

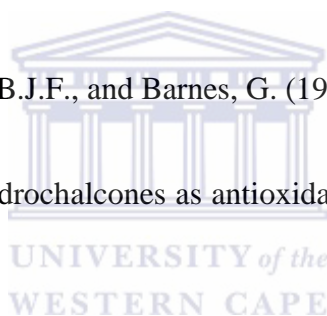
Dejana, E. (2004) Endothelial cell-cell junctions: happy together. *Nat Rev Mol Cell Biol.* **5**, 261-70.

Dong, J., Sulik, K.K. and Chen, S.Y. (2010) The role of NOX enzymes in ethanol-induced oxidative stress and apoptosis in mouse embryos. *Toxicol Lett.* **193**, 94-100.

Dore-Duffy, P. (2008) Pericytes: pluripotent cells of the blood brain barrier. *Curr Pharm Des.* **14**, 1581-93.

Dziedzic, S.Z., Hudson, B.J.F., and Barnes, G. (1985)

Polyhydroxydihydrochalcones as antioxidants for lard. *J. Agric, Food Chem.* **33**, 244-246.



Erickson, L. (2003) Rooibos tea: research in antioxidant and antimutagenic properties. *HerbalGram. American botanical council* **59**, 34-45.

Farin, F.M., Pohlman, T.H. and Omiecinski, C.J. (1994) Expression of cytochrome P450s and microsomal epoxide hydrolase in primary cultures of human umbilical vein and endothelial cells. *Toxicol Appl Pharmacol.* **124**, 1-9.

Farshori, P. and Kachar, B. (1999) Redistribution and phosphorylation of occludin during opening and resealing of tight junctions in cultured epithelial cells. *J Membr Biol.* **170**, 147-56.

Faso, L., Trowbridge, R.S., Quan, W., Yao, X.L., Jenkins, E.C., Maciulis, A., Bunch, T.D. and Wisniewski, H.M. (1994) Characterization of a strain of cerebral endothelial cells derived from goat brain which retain their differentiated traits after long-term passage. *In vitro Cell Dev Biol Anim.* **30A**, 226-35.

Fernandes, Y. and Gerlai, R. (2009) Long-term behavioral changes in response to early developmental exposure to ethanol in zebrafish. *Alcoholism, Clin and Exp Res.* **33(4)**, 601-609.

Floyd, R. L., Sobell, M., Velasquez, M. M., Ingersoll, K., Nettleman, M., Sobell, L., Mullen, P. D., Ceperich, S., von Sternberg, K., Bolton, B., Johnson, K., Skarpness, B., and Nagaraja, J. (2007) Preventing alcohol-exposed pregnancies: a randomized controlled trial. *Am J Prev Med.* **32(1)**, 1-10.

Förster, C., Silwedel, C., Golenhofen, N., Burek, M., Kietz, S., Mankertz, J. and Drenckhahn, D. (2005) Occludin as direct target for glucocorticoid-induced improvement of blood-brain barrier properties in a murine *in vitro* system. *J Physiol.* **565**, 475-86.

Förster, C., Burek, M., Romero, I.A., Weksler, B., Couraud, P.O. and Drenckhahn, D. (2008) Differential effects of hydrocortisone and TNFalpha on tight junction proteins in an *in vitro* model of the human blood-brain barrier. *J Physiol.* **586**, 1937-49.

Fraga, C.G., Galleano, M., Verstraeten, S.V. and Oteiza, P.I. (2010) Basic biochemical mechanisms behind the health benefits of polyphenols. *Mol*

Aspects of Med, **31(6)**, 435-445.

Freshney, R.I. and Freshney, M.G. (2002) Culture of epithelial cells. In: Maas-Szabowski, N., Stark, H., and Fusenig, N.E. (eds.) Cell interaction and epithelial differentiation. 2nd edition. Glasgow, Scotland: John Wiley & Sons, Inc. pp 33.

Freshney, R.I. and Vunjak-Novakovic, G. (2006) Culture of cells for tissue engineering. In: R.I. Freshney (eds.) Basic principles of cell culture. New York, USA: John Wiley & Sons, Inc. pp 11.

Furuse, M., Fujita, K., Hiragi, T., Fujimoto, K., and Tsukita, S. (1998) Claudin-1 and -2: novel integral membrane proteins localizing at tight junctions with no sequence similarity to occluding. *J. Cell Biol.* **141**, 1539-1550.

Furuse, M., Sasaki, H., and Tsukita, S. (1999) Manner of interaction of heterogenous claudin species within and between tight junction strands. *J. Cell Biol.* **147**, 891-903.

Gardel, M.L. (2004) Elasticity of f-actin networks. Published thesis (PhD), Harvard University.

Gemma, S. Vichi, S., Testai, E. (2006) Individual susceptibility and alcohol effects: biochemical and genetic aspects. *Ann. It. Super. Sanita.* **42**, 8-16.

Gil-Mohapel, J., Boehme, F., Kainer, L. and Christie, B.R. (2010) Hippocampal cell loss and neurogenesis after fetal alcohol exposure: insights from different rodent models. *Brain Res Rev.* **64**, 283-303.

- Glogauer, M., Arora, P., Chou, D., Janmey, P.A., Downey, G.P. and McCulloch, C.A. (1998) The role of actin-binding protein 280 in integrin-dependent mechanoprotection. *J Biol Chem.* **273**, 1689-98.
- Gumbleton, M. and Audus, K.L. (2001) Progress and limitations in the use of *in vitro* cell cultures to serve as a permeability screen for the blood-brain barrier. *J Pharm Sci.* **90**, 1681-98.
- Hagerman, A. E., Rice, M. E., Ritchard, N. T. (1998) Mechanisms of protein precipitation for two tannins, pentagalloyl glucose and epicatechin16- (4-8)-catechin (procyanidin) *J of Agric and Food Chem.* **46**, 2590-2595.
- Hannigan, J.H. (1996) What research with animals is telling us about alcohol-related neurodevelopmental disorder. *Pharmacol Biochem Behav.* **55**, 489-99.
- Haorah, J., Heilman, D., Knipe, B., Chrastil, J., Leibhart, J., Ghorpade, A., Miller, D.W. and Persidsky, Y. (2005) Ethanol-induced activation of myosin light-chain kinase leads to dysfunction of tight junctions and blood-brain barrier compromise. *Alcohol Clin Exp Res.* **29**, 999-1009.
- Haorah, J., Knipe, B., Leibhart, J., Ghorpade, A. and Persidsky, Y. (2005) Alcohol-induced oxidative stress in brain endothelial cells causes blood-brain barrier dysfunction. *J Leukoc Biol.* **78**, 1223-32.
- Harper, C. (1998) The neuropathology of alcohol-specific brain damage, or does alcohol damage the brain? *J. Neuropathol Exp Neurol.* **57**, 101-110.
- Hawkins, B.T. and Davis, T.P. (2005) The blood-brain barrier/neurovascular unit in

health and disease. *Pharmacol Rev.* **57**, 173-85.

Higgins, P.J. (1987) Cell cycle phase-specific perturbation of hepatic tumour cell growth kinetics during short-term *in vitro* exposure to ethanol. *Alcoholism: Clin Exp Res.* **11**, 550-555.

Hoebel, B.G., Steyrer, E. and Graier, W.F. (1998) Origin and function of epoxyeicosatrienoic acids in vascular endothelial cells: more than just endothelium-derived hyperpolarizing factor? *Clin Exp Pharmacol Physiol.* **25**, 826-830.

Hoheisel, D., Nitz, T., Franke, H., Wegener, J., Hakvoort, A., Tilling, T. and Galla, H.J. (1998) Hydrocortisone reinforces the blood-brain properties in a serum free cell culture system. *Biochem Biophys Res Commun.* **247**, 312-5.

Huang, H.L., Hsing, H.W., Lai, T.C., Chen, Y.W., Lee, T.R., Chan, H.T., Lyu, P.C., Wu, C.L., Lu, Y.C., Lin, S.T., Lin, C.W., Lai, C.H., Chang, H.T., Chou, H.C. and Chan, H.L. (2010) Trypsin-induced proteome alteration during cell subculture in mammalian cells. *J Biomed Sci.* **17**, 36.

Hummer, W. and Schreier, P. (2008) Analysis of proanthocyanidins. *Mol Nutr Food Res.* **52(12)**, 1381-98.

Ito, A., Shinohara, K. and Kator, K. (1991) Protective action of rooibos tea (*Aspalathus linearis*) extract against inactivation of L5178Y cells by H₂O₂. In: proceedings of the international symposium on tea science. The organizing committee of ISTS, Shizuoko, Japan, pp, 381-384.

- Jacobs, P. and Woods, L. (1995) General and oncologic haematology for nursing and paramedical professions, 1st edn. Cape Town, South Africa.
- Jaffe, E.A., Nachman, R.L., Becker, C.G. and Minick, C.R. (1973) Culture of human endothelial cells derived from umbilical veins. Identification by morphologic and immunologic criteria. *J Clin Invest.* **52**, 2745-56.
- James, P.B. (1992) Pathogenesis of multiple sclerosis: a blood-brain barrier disease. *J R Soc Med.* **85**, 713-4.
- Janzer, R.C. (1993) The blood-brain barrier: cellular basis. *J Inherit Metab Dis.* **16**, 639-47.
- Joubert, E. (1994) Processing of rooibos tea under controlled conditions (*Aspalathus linearis*). Ph.D. (Food Science) Dissertation. Stellenbosch University, Stellenbosch, South Africa.
- Joubert, E. (1996) HPLC quantification of the dihydrochalcones, aspalathin and nothofagin in rooibos tea (*Aspalathus linearis*) as affected by processing. *Food Chem.* **55**, 403-411.
- Joubert, E. and Ferreira D. (1996), Antioxidants of Rooibos tea – a possible explanation for its health promoting properties. *The SA J. Food Sci and Nutrition*, **8(3)**, 79-83.
- Joubert, E., De Villiers, O.T. (1997) Effect of fermentation and drying conditions on the quality of rooibos tea, *Int. J. Food Sci and Technol.* **32**, 127-134.

- Joubert, E., Winterton, P., Britz, T.J., Ferreira, D. (2004) Superoxide anion radical and α,α -dipheyl- β -picrylhydrazyl radical scavenging capacity of rooibos (*Aspalathus linearis*) aqueous extract, crude phenolic fractions, tannin and flavonoids, *Food Res Int.* **37**, 133-138.
- Joubert, E., Winterton, P., Britz, T.J. and Gelderblom, W.C. (2005) Antioxidant and pro-oxidant activities of aqueous extracts and crude polyphenolic fractions of rooibos (*Aspalathus linearis*). *J Agric Food Chem.* **53**, 10260-7.
- Joubert, E., Gelderblom, W.C.A., Louw, A., and de Beer, D. (2008) South African herbal teas: *Aspalathus linearis*, *Cyclopia spp.* And *Athrixia*. *J Ethnopharmacol.* **119**, 376-412.
- Kalaria, R.N. (1992) The blood-brain barrier and cerebral microcirculation in Alzheimer disease. *Cerebrovasc Brain Metab Rev.* **4**, 226-60.
- Kanda, T., Yamawaki, M., Iwasaki, T. and Mizusawa, H. (2000) Glycosphingolipid antibodies and blood-nerve barrier in autoimmune demyelinating neuropathy. *Neurology* **54**, 1459-64.
- Kanda, T., Numata, Y. and Mizusawa, H. (2004) Chronic inflammatory demyelinating polyneuropathy: decreased claudin-5 and relocated ZO-1. *J Neurol Neurosurg Psychiatry* **75**, 765-9.
- Kapucuoglu, N., Coban, T., Raunio, H., Pelkonen, O., Edwards, R.J., Boobis, A.R. and Iscan, M. (2003) Immunohistochemical demonstration of the expression of CYP2E1 in human breast tumour and non-tumour tissues. *Cancer Lett.*

196, 153-159.

Karnovsky, M.J. (1967) The ultrastructural basis of capillary permeability studied with peroxidase as a tracer. *J Cell Biol.* **35**, 213-36.

Kashiwamura, Y., Sano, Y., Abe, M., Shimizu, F., Haruki, H., Maeda, T., Kawai, M. and Kanda, T. (2011) Hydrocortisone enhances the function of the blood-nerve barrier through the up-regulation of claudin-5. *Neurochem Res.* **36**, 849-55.

Kelm, M.A., Hammerstone, J.F., and Schmitz, H.H. (2005) Identification and quantification of flavanols and proanthocyanidins. *Clin and Develop Immunol.* **12**(1), 35-41.

Khong, T.Y. (2004) Placental vascular development and neonatal outcome. *Semin Neonatol.* **9**, 255-63.

Kim, K., Dean, D., Mikos, A.G. and Fisher, J.P. (2009) Effect of initial cell seeding density on early osteogenic signal expression of rat bone marrow stromal cells cultured on cross-linked poly (propylene fumarate) disks. *Biomacromol.* **10**, 1810-7.

Kirkinetzos, I.G. and Moraes, C.T. (2001) Reactive oxygen species and mitochondrial diseases. *Semin Cell Dev Biol.* **12**, 449-57.

Kneisel, U. and Wolburg, H. (2000) Tight junctions of the blood-brain barrier. *Cell. Mol. Neurobiol.* **20**, 57-76.

- Koeppen, B.H. and Roux, D.G. (1966) C-glycosylflavonoids. The chemistry of aspalathin. *J Biochem.* **99**, 604-609.
- Kucharska, J., Ulicna, O., Gvozdjakova, A., Sumbalova, Z., Vancova, O., Bozek, P., Nakano, M., Greksak, M. (2004) Regeneration of coenzyme Q₁₀ redox state and inhibition of oxidative stress by rooibos tea (*Aspalathus linearis*) administration in carbon tetrachloride liver damage. *Physiol Res.* **53**, 515-521.
- Lach, B., Rippstein, P., Atack, D., Afar, D.E. and Gregor, A. (1993) Immunoelectron microscopic localization of monoclonal IgM antibodies in gammopathy associated with peripheral demyelinating neuropathy. *Acta Neuropathol.* **85**, 298-307.
- Lakhan, S.E., Kirchgessner, A., and Hoffer, M. (2009) Inflammatory mechanisms in ischemic stroke: therapeutic approaches. *J Transl Med.* **7**, 97.
- Lamosövä, D., Juráni, M., Greksák, M., Nakano, M., and Vaneková, M. (1997) Effect of rooibos tea (*Aspalathus linearis*) on chick skeletal muscle cell growth in culture. *Comp Biochem Physiol.* **116(1)**, 39-4.
- Leopoldini, M., Russo, N. and Toscano, M. (2011) The molecular basis of working mechanism of natural polyphenolic antioxidants. *Food Chem.* **25(2)**, 288-306.
- Li, D., Zhen, H., Xingcai, L., Wu-gao, Z. and Jian-guang, Y. (2005) Physico-chemical properties of ethanol-diesel blend fuel and its effect on

performance and emissions of diesel engines. *Renewable Energy* **30**,967-976.

Luissint, A., Artus, C., Glacial, F., and Ganeshamoorthy, K. (2012) Tight junctions at the blood-brain barrier: physiological architecture and disease-associated dysregulation. *Fluids and Barriers of the CNS* **9**,23.

Lundquist, S., Renftel, M., Brillault, J., Fenart, L., Cecchelli, R. and Dehouck, M.P. (2002) Prediction of drug transport through the blood-brain barrier *in vivo*: a comparison between two *in vitro* cell models. *Pharm Res.* **19**, 976-81.

Manning, M. A. and Eugene Hoyme, H. (2007) Fetal alcohol spectrum disorders: a practical clinical approach to diagnosis. *Neurosci Biobehav Rev.* **31(2)**, 230-8.

Manzo-Avalos, S., and Saavedra-Molina, A. (2010) Cellular and mitochondrial effects of alcohol consumption. *Int J Environ Res Public Hlth.* **7**, 4281-4304.

Marais, C. (1996) Struktuur en sintese van metaboliete uit rooibostee (*Aspalathus linearis*). Fisiologiese aktiwiteit en biomimetiese model vir die fermentasieproses. PhD Dissertation, University of Free State. South Africa.

Marnewick, J.L., Joubert, E., Swart, P., Van Der Westhuizen, F. and Gelderblom, W.C. (2003) Modulation of hepatic drug metabolizing enzymes and oxidative status by rooibos (*Aspalathus linearis*) and Honeybush (*Cyclopia intermedia*), green and black (*Camellia sinensis*) teas in rats. *J Agric Food Chem.* **51**, 8113-9.

Marnewick, J.L., Rautenbach, F., Venter, I., Neethling, H., Blackhurst, D.M.,

- Wolmarans, P., Macharia, M. (2011) Effect of rooibos (*Aspalathus linearis*) on oxidative stress and biochemical parameters in adults at risk for cardiovascular disease. *J. Ethnopharmacol.* **133**, 46-52.
- Martini, F. (2006) Fundamentals of anatomy and physiology. In: The cellular level of organization. 6th edition. San Francisco, CA: Pearson Education, Inc. pp 67.
- Mascotti, K., McCullough, J. and Burger, S.R. (2000) HPC viability measurement: trypan blue versus acridine orange and propidium iodide. *Transfusion*, **40**, 693-6.
- May, P.A., and Gossage, J.P. (2001) Estimating the prevalence of fetal alcohol syndrome: a summary. *Alcohol Res. Hlth.* **25**, 159-167.
- McMurrough, I. and McDowell, J. (1978) Chromatographic separation and automated analysis of flavanols. *Anal Biochem.* **91(1)**, 92-100.
- Mikami, K., Haseba, T. and Ohno, Y. (1997) Ethanol induces transient arrest of cell division (G2 + M block) followed by G0/G1 block: dose effects of short- and longer-term ethanol exposure on cell cycle and cell functions. *Alcohol Alcohol* **32**, 145-152.
- Moldovan, L., Mythreye, K., Goldschmidt-Clermont, P.J. and Satterwhite, L.L. (2006) Reactive oxygen species in vascular endothelial cell motility. Roles of NAD(P)H oxidase and Rac1. *Cardiovasc Res.* **71**, 236-46.
- Munin, A. and Edwards-Lévy, F. (2011) Encapsulation of natural polyphenolic

compounds; a review. *Pharmaceutics* **3**, 793-829.

Murphy, M.P. and Smith, R.A. (2007) Targeting antioxidants to mitochondria by conjugation to lipophilic cations. *Annu Rev Pharmacol Toxicol.* **47**, 629-56.

Nakagawa, S., Deli, M.A., Kawaguchi, H., Shimizudani, T., Shimano, T., Kittel, Á., Tanaka, K., Niwa, M. (2009) A new blood-brain barrier model using primary rat brain endothelial cells, pericytes and astrocytes. *Neurochem Int.* **54**, 253-263.

Navone, S.E., Marfia, G., Nava, S., Invernici, G., Cristini, S., Balbi, S., Sangiorgi, S., Ciusani, E., Bosutti, A., Alessandri, G., Slevin, M. and Parati, E.A. (2013) Human and mouse brain-derived endothelial cells require high levels of growth factors medium for their isolation, *in vitro* maintenance and survival. *Vasc Cell.* **5**, 10.

Nitta, T., Hata, M., Gotoh, S., Seo, Y., Sasaki, H., Hashimoto, N., Furuse, M. and Tsukita, S. (2003) Size-selective loosening of the blood-brain barrier in claudin-5-deficient mice. *J Cell Biol.* **161**, 653-60.

Nitz, T., Eisenblätter, T., Psathaki, K., and Galla, H. (2003) Serum-derived factors weaken the barrier properties of cultured porcine brain capillary endothelial cells *in vitro*. *Brain Res.* **981**, 30-40.

Niwa, Y. and Miyachi, Y. (1986) Antioxidant action of natural health products and Chinese herbs. *Inflam.* **10**, 79-91.

Ohtsuk, S., Yamaguchi, H., Katsukura, Y. (2008) mRNA expression levels of tight

junction protein genes in mouse brain capillary endothelial cells highly purified by magnetic cell sorting. *J Neurochem.* **104**, 147-154.

Ohtsuki, S., and Terasaki, T. (2007) Contribution of carrier-mediated transport systems to the blood-brain barrier as a supporting and protecting interface for the brain; importance for CNS drug discovery and development, *Expert Rev.* **24 (9)**, 1745-1758.

Omidi, Y., Campbell, L., Barar, J., Connell, D., Akhtar, S. and Gumbleton, M. (2003) Evaluation of the immortalised mouse brain capillary endothelial cell line, b.End3, as an *in vitro* blood-brain barrier model for drug uptake and transport studies. *Brain Res.* **990**, 95-112.

Osada, T., Gu, Y.H., Kanazawa, M. Tsubota, Y., Hawkins, B.T., Spatz, M., Milner, R., del Zoppo, G.J. (2011) Interendothelial claudin-5 expression depends on cerebral endothelial cell –matrix adhesion by beta (1)-integrins. *J Cereb Blood Flow Metab.* **31**, 1972-1985.

Parsons, O.A. (1998) Neurocognitive deficits in alcohol and alcoholics and social drinkers: a continuum. *Alcohol Clin Exp Res.* **22**, 954-961.

Passeleu-Le Bourdonnec, C., Carrupt, P.A., Scherrmann, J.M. and Martel, S. (2013) Methodologies to assess drug permeation through the blood-brain barrier for pharmaceutical research. *Pharm Res.* **30**, 2729-56.

Pekny, M., Stanness, K.A., Eliasson, C., Betsholtz, C. and Janigro, D. (1998) Impaired induction of blood-brain barrier properties in aortic endothelial

cells by astrocytes from GFAP-deficient mice. *Glia* **22**, 390-400.

Perez-Pinzon, M.A., Stetler, R.A. and Fiskum, G. (2012) Novel mitochondrial targets for neuroprotection. *J Cereb Blood Flow Metab.* **32**, 1362-76.

Perrière, N., Yousif, S., Cazaubon, S., Chaverot, N., Bourasset, F., Cisternino, S., Decleves, X., Hori, S., Terasaki, T., Deli, M., Scherrmann, J.M., Temsamani, J., Roux, F. and Couraud, P.O. (2007) A functional *in vitro* model of rat blood-brain barrier for molecular analysis of efflux transporters. *Brain Res.* **1150**, 1-13.

Perron, N.R. and Brumaghim, J.L. (2009) A review of the antioxidant mechanisms of polyphenol compounds related to iron binding. *Cell Biochem and Biophys.* **53(2)**, 75-100.

Petri, B. and Bixel, M.G. (2006) Molecular events during leukocyte diapedesis, *J. FEBS*, **273**, 4399-4407.

Phillips, D.E., Krueger, S.K., Wall, K.A., Smoyer-Dearing, L.H. and Sikora, A.K. (1997) The development of the blood-brain barrier in alcohol-exposed rats. *Alcohol* **14(4)**, 333-343.

Postek, M.T., Howard, K.S., Johnson, A.H. and McMichael, K.L. (1980) *Scanning Electron Microscopy: A Student's Handbook*, edn. Ladd Research Industries: Postek, M.T. Jr.

Prior, R. L., Hoang, H., Gu, L., Wu, X., Bacchiocca, M., Howard, L., Hampsch-Woodill, M., Huang, D., Ou, B., and Jacob, R. (2003) Assays for

hydrophilic and lipophilic antioxidant capacity (oxygen radical absorbance capacity (ORAC) (FL)) of plasma and other biological and food samples. *J Agric Food Chem.* **51(11)**, 3273-9.

Rabe, C., Steenkamp, J.A., Joubert, E., Burger, J.F.W., Ferreira, D., (1994) Phenolic metabolites from rooibos tea (*Aspalathus linearis*) *Phytochem.* **35**, 1559-1565.

Rahman, K. (2007) Studies on free radical, antioxidants and co-factors. *Clinical Intervention in Aging* **2(20)**, 219-236.

Ramirez, S.H., Potula, R., Fan, S., Eidem, T., Papugani, A., Reichenbach, N., Dykstra, H., Weksler, B.B., Romero, I. A., Couraud, P.O. and Persidsky, Y. (2009) Methamphetamine disrupts blood-brain barrier function by induction of oxidative stress in brain endothelial cells. *J Cereb Blood Flow Metab.* **29(12)**, 1933-1945.

Rascher, G., Fischmann, A., Krogger, S., Duffner, F., Grote, E.H., Wolburg, H. (2002) Extracellular matrix and blood-brain barrier in glioblastoma multiforme: spatial segregation of tenascin and agrin. *Act Neuropathol.* **104**, 85-91.

RE, R., Pellegrini, N., Proteggente, A., Pannala, A., Yang, M., and Rice-Evans, C. (1999) Antioxidant activity applying an improved ABTS radical cation decolorization assay. *Free Radic Biol Med.* **26(9-10)**, 1231-7.

Re, F., Moresco, R., and Masserini, M. (2012) Nanoparticles for neuroimaging. *J*

Physics **45**, 1-12.

Rebrin, I., Zicker, S., Wedekind, K.J., Paetau-Robinson, I., Packer, L., Sohal, R.S.

(2005) Effect of antioxidant enriched diets on glutathione redox status in tissue homogenates and mitochondria of the senescence-accelerated mouse, *Free Radic Biol and Med.* **39**, 549-557.

Reese, T.S. and Karnovsky, M.J. (1967) Fine structural localization of a blood-brain barrier to exogenous peroxidase. *J Cell Biol.* **34**, 207-17.

Reiss, Y., Hoch, G., Deutsch, U. and Engelhardt, B. (1998) T cell interaction with ICAM-1-deficient endothelium *in vitro*: essential role for ICAM-1 and ICAM-2 in transendothelial migration of T cells. *Eur J Immunol.* **28**, 3086-99.

Ribatti, D., Nico, B., Crivellato, E. and Artico, M. (2006) Development of the blood-brain barrier: a historical point of view. *Anat Rec B New Anat.* **289**, 3-8.

Riley, E. P. and McGee, C. L. (2005) Fetal alcohol spectrum disorders: an overview with emphasis on changes in brain and behavior. *Exp Biol Med* (Maywood). **230(6)**, 357-65.

Roche. 2005. Colorimetric assay (XTT based) for the non-radioactive quantification of cell proliferation and viability kit-information sheet.

Rohnelt, R.K., Hoch, G., Reiss, Y. and Engelhardt, B. (1997) Immunosurveillance modelled *in vitro*: naive and memory T-cells spontaneously migrate across

unstimulated microvascular endothelium. *Int Immunol.* **9**, 435-50.

Rubin, L.L. and Staddon, J.M. (1999) The cell biology of the blood-brain barrier. *Annu Rev Neurosci.* **22**, 11-28.

Salihu, H.M., Kornosky, J.L., Lynch, O., Alio, A.P., August, E.M. and Marty, P.J. (2011) Impact of prenatal alcohol consumption on placenta-associated syndromes. *Alcohol* **45**, 73-9.

Schreibelt, G., Kooij, G., Reijkerker, A., van Doorn, R., Gringhuis, S.I., van der Pol, S., Weksler, B.B., Romero, I.A., Couraud, P.O., Piontek, J., Blasig, I.E., Dijkstra, C.D., Ronken, E. and de Vries, H.E. (2007) Reactive oxygen species alter brain endothelial tight junction dynamics via RhoA, PI3 kinase, and PKB signaling. *J. FASEB* **21**, 3666-76.

Seeley, R.R., Stephens, T.D., and Tate, P. (1995) Nutrition, metabolism and temperature regulation, anatomy and physiology. 3rd edition. St, Louis, Missouri: Mosby-Year Book, Inc. pp 72.

Siddiqui, R., Pleass, R., Mortazavi, P. and Khan, N. A. (2011) Non-vertebrate models to study parasite invasion of the central nervous system. *Trending Parasitol.* **27(1)**,5-10.

Silver-Marsiglio, K.I., Pan, Q., Paiva, M., Madorsky, I., Khurana, N.C., and Heaton, M.B. (2005) Mitochondria targeted vitamin E and vitamin E mitigate ethanol-mediated effects on cerebellar granule cell antioxidation defense systems. *Brain Res.* **1052**, 202-211.

- Smith, K. and Hunter, I.S. (2008) Efficacy of common hospital biocides with biofilms of multi-drug resistant clinical isolates. *J Med Microbiol.* **57**, 966-73.
- Snijman, P. W., Joubert, E., Ferreira, D., Li, X-C., Ding, Y., Green, I. R. (2009) Antioxidant activity of the dihydrochalcones aspalathin and nothofagin and their corresponding flavones in relation to other rooibos (*Aspalathus linearis*) flavonoids, epigallocatechin gallate, and Trolox. *J Agric and Food Chem.* **57**, 6678-6684.
- Sprung, R., Bonte, W., Rudell, E., Domke, M., Frauenrath, C. (1981) On the problem of endogenous alcohol. Endogenous ethanol: further investigations. *Alcohol Drugs Behav.* **18**(2), 65-70.
- Stanley, L., Winterton, P., Marnewick, J.L., Gelderblom, W. C. A., Joubert., and Britz, T. J. (2001) Influence of processing stages on antimutagenic and antioxidant potentials of rooibos tea. *J Agric and Food Chem.* **49**, 114-117.
- Steiner, O., Coisne, C., Engelhardt, B. and Lyck, R. (2011) Comparison of immortalized bEnd5 and primary mouse brain microvascular endothelial cells as *in vitro* blood-brain barrier models for the study of T cell extravasation. *J Cereb Blood Flow Metab.* **31**, 315-27.
- Svedružić, Ž. M., Popovič, K. and Šendula-Jengiđ, V.(2013) Modulator of γ -secretase activity can facilitate the toxic side effects and pathogenesis of Alzheimer's Disease. *PLoS One.* **8**(1), e50759, 1-13.
- <http://www.ncbi.nlm.nih.gov/pmc/articles/PMC3538728/>

[Accessed 13 October 2014].

Tanobe, K., Nishikawa, K., Hinohara, H., Okamoto, T., Saito, S., Goto, F. (2003)

Blood-brain barrier and general anesthetics. *Masui*. **52**, 840-845.

Taraschi, T.F. and Rubin, E. (1985) Biology of disease: effects of ethanol on the

chemical and structural properties of biologic membranes. *Laboratory Invest.*

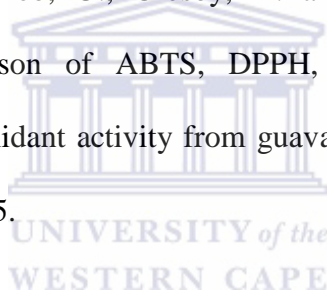
52, 120-131.

Tarbell, J.M. (2010) Shear stress and the endothelial transport barrier. *Cardiovasc*

Res. **87**, 320-30.

Thaipong, K., Boonprakob, U., Crosby, K. and Cisneros-Zevallos, L.a.B.D.H.

(2006) Comparison of ABTS, DPPH, FRAP and ORAC assays for estimating antioxidant activity from guava fruit extracts. *J Food Comp and Anal.* **19**, 669-675.



Thomas, J. D. and Riley, E. P. (1998) Fetal alcohol syndrome: does alcohol

withdrawal play a role? *Alcohol Hlth Res World* **22(1)**, 47-53.

Tsai, J., Floyd, R.L., Green, P.P. and Boyle, C.A. (2007) Patterns and average

volume of alcohol use among women of childbearing age. *J Matern Child*

Hlth. **11**, 437-45.

Tuma, P. and Hubbard, A.L. (2003) Transcytosis: crossing cellular barriers. *Physiol*

Rev. **83**, 871-932.

Vauzour, D., Rodriquez-Mateos, A., Corona, G., Oruna-Concha, M.J., and Spencer,

- J.P.E. (2010) Mechanisms of Human Health: Prevention of Disease and Mechanisms of Action. *Nutr.* **2**, 1106-1131.
- Viljoen, D. L.; Gossage, J. P.; Brooke, L.; Adnams, C. M.; Jones, K. L.; Robinson, L. K.; Hoyme, H. E.; Snell, C.; Khaole, N. C.; Kodituwakku, P.; Asante, K. O.; Findlay, R.; Quinton, B.; Marais, A. S.; Kalberg, W. O., and May, P. A. (2005) Fetal alcohol syndrome epidemiology in a South African community: a second study of a very high prevalence area. *J Stud Alcohol* **66(5)**, 593-604.
- von Gadow, A., Joubert, E. and Hansmann, C.F. (1997) Comparison of the antioxidant activity of rooibos tea (*Aspalathus linearis*) with green, oolong and black tea. *Food Chem.* **60 (1)**, 73-77.
- Wallace, T. C. and Giusti, M. M. (2010) Evaluation of parameters that affect the 4-dimethylaminocinnamaldehyde assay for flavanols and proanthocyanidins. *J Food Sci.* **75(7)**, C619-25.
- Weidenfeller, C., Schrot, S., Zozulya, A. and Galla, H.J. (2005) Murine brain capillary endothelial cells exhibit improved barrier properties under the influence of hydrocortisone. *Brain Res.* **1053**, 162-74.
- Weinbaum, S., Tarbell, J.M. and Damiano, E.R. (2007) The structure and function of the endothelial glycocalyx layer. *Annu Rev Biomed Eng.* **9**, 121-67.
- Weiner, H. (1987) Subcellular localization of acetaldehyde oxidation on liver, *Ann. NY Acad Sci.* **492**, 25-34.

- Weiss, N., Miller, F., Cazaubon, S. and Couraud, P. (2008) The blood-brain barrier in brain homeostasis and neurological disease. *Biochimica et Biophysica Acta*. **1788** (2009), 842-857.
- White, A.M. (2003) What happened? Alcohol, memory blackouts, and brain. *Alcohol. Res. Hlth*. **27**, 186-196.
- Wilhelm, I., Fazakas, C. and Krizbai, I.A. (2011) *In vitro* models of the blood-brain barrier. *Acta Neurobiol Exp (Wars)*. **71**, 113-28.
- Wisman, K. N., Perkins, A. A., Jeffers, M. D., and Hagerman, A. E. (2008) Accurate assessment of the bioactivities of redox-active polyphenolics in cell culture. *J Agric Food Chem*. **56**, 7831-7837.
- Won, S.J., Kim, D.Y., and Gwag, B.J. (2002) Cellular and molecular pathways of ischemic neuronal death, *J Biochem Mol Biol*. **35**, 67-86.
- Xu, M., Chen, G., Fu, W., Liao, M., Frank, J.A., Bower, K.A., Fang, S., Zhang, Z., Shi, X. and Luo, J. (2012) Ethanol disrupts vascular endothelial barrier: implication in cancer metastasis. *Toxicol Sci*. **127**, 42-53.
- Yao, N. and Wang, Z.L. (2005) Handbook of microscopy for nano technology. 1st edition. NY, USA: Kluwer Academic Publishers.
- Yao, Y., Rabodzey, A., and Dewey Jr, F. (2007) Glycocalyx modulates the motility and proliferative response of vascular endothelium to fluid shear stress, *Am. J Physiol Heart Circ Physiol*. **293**, H1023-H1030.

- Yang, T., Roder, K.E. and Abbruscato, T.J. (2007) Evaluation of bEnd5 cell line as an *in vitro* model for the blood-brain barrier under normal and hypoxic/aglycemic conditions. *J Pharm Sci.* **96**, 3196-213.
- Yang, L., Calingasan, N.Y., Wille, E.J., Cormier, K., Ferrante, R.J., Beal, M.F. (2009) Combination therapy with coenzyme Q10 and creatine produces additive neuroprotective effects in models of Parkinson's and Huntington's diseases, *J Neurochem.* **109**, 1427-1439.
- Yoshikawa, T., Oyamada, Y., Ueda, S., Tanigawa, T., Takemura, T., Sugino, S., Kondo, M. (1990) Scavenging effects of *Aspalathus linearis* (Rooibos tea) on active oxygen species. *Exp Med Biol.* **264**, 171-174.
- Zakhari, S. (2006) Overview: how is alcohol metabolized by the body? *Alcohol Res Hlth.* **29**, 245-54.
- Zhao, Y., Cui, J.G. and Lukiw, W.J. (2006) Natural secretory products of human neural and microvessel endothelial cells: Implications in pathogenic "spreading" and Alzheimer's disease. *Mol Neurobiol.* **34**, 181-92.
- Zulueta, A., Esteve, M.J. and Frigola, A. (2009) ORAC and TEAC assays comparison to measure the antioxidant capacity of food products. *Food Chem.* **114**, 310-316.

6.2 Web-based References

Biotium, Inc. 2011. Glowing Products for Science

http://search.cosmobio.co.jp/cosmo_search_p/search_gate2/docs/BTI_/30007.20110602.pdf [Accessed 25 April 2014].

International drinking guidelines (2010)

<http://www.icap.org/Table/InternationalDrinkingGuidelines> [Accessed 9 November 2014].

Killoran, A., Canning, U., Doyle, N., and Sheppard, L. (Centre for Public Health Excellence NICE). (2010) Review of effectiveness of law limiting blood alcohol concentration levels to reduce alcohol-related road injuries and deaths.

<http://www.nice.org.uk/media/3FE/1A/BloodAlcoholContentEffectivenessReview.pdf> [Accessed 20 May 2013].

Modernisation Programme, Blue Print (2010), Workstream on the prevention and treatment of harmful alcohol and drug use, Provincial Government, Western Cape, South Africa.

http://www.westerncape.gov.za/other/2010/7/provincial_government_of_western_cape_-_substance_abuse_blueprint.pdf [Accessed 21 April 2012].

OECD SIDS. (2004) Initial assessment report for SIAM: Ethanol, cas.no: 64-17-5. Berlin, Germany. 19-22 October. UNEP publications, viewed 23 May 2012. <http://www.inchem.org/documents/sids/sids/64175.pdf> [Accessed 20 June 2012].

2012].

Policy Brief 2008, Fetal Alcohol Spectrum Disorders in Cape Town, South Africa:
A huge challenge requiring multi-faced prevention strategies, viewed 10
April 2014. <http://www.mrc.ac.za/policybriefs/FetalAlcoholSpectrum.pdf>

[Accessed 17 March 2012].

Rendall-Mkosi, K., London, L., Adnams, C., Morojele, N., McLoughlin, J.,
Goldstone, C. 2008, Fetal Alcohol Spectrum Disorder in South Africa:
Situational and Gap Analysis,
http://www.unicef.org/southafrica/SAF_resources_fetalalcohol.pdf

[Accessed 29 April 2014].

Schneider, M., Norman, R., Parry, C., Bradshaw, D. and Plüddeman, A. (2007),
Estimating the burden of alcohol abuse in South Africa 2000, Burden of
Disease Unit and Alcohol and Drug Abuse Research Unit, Retrieved from
<http://www.mrc.ac.za/bod/Alcoholburdentechnical.pdf> [Accessed 30
October 2014].

Vladimir-Knežević, S., Blažeković, B., Štefan, M.B. and Babac, M. (2012), Plant
polyphenols as antioxidants influencing the human health, phytochemicals as
nutraceuticals – global approaches to their role in nutrition and health, Dr
Veketeshwer Rao (Ed.), ISBN: 978-953-51-0203-8, In Tech, Available from:
<http://www.intechopen.com/books/phytochemicals-as-nutraceuticals-global-approaches-to-their-role-in-nutrition-and-health/plant-polyphenols-as-antioxidants-influencing-the-human-health>. [Accessed 18 October 2014].

Figure 2. Chapter: 1

(http://medical-dictionary.thefreedictionary.com/_/viewer.aspx?path=dorland&name=formula_structural.jpg) [Accessed 24 June 2014].

Figure 9. Chapter: 1

http://www.frenchglory.com/polyphenols_classification.pdf

[Accessed 3 April 2012].

Figure 10. Chapter: 1

(<http://www.chemspider.com/Chemical-Structure.26286888.html>) [Accessed 3 July 2014].



Figure 11. Chapter: 1

(<http://www.esc.rutgers.edu/publications/general/fs1065.htm>) [20 October 2014].

Chapter 2: 2.6.1 Transendothelial electrical resistance across a bEnd5 cell monolayer, operating principle

<http://www.gbo.com/bioscience>; www.millipore.com/millicell [Accessed 15 April 2012].

Figure 12. Chapter: 2 2.6.2 Experimental model of the blood-brain barrier

http://www.pharmadirections.com/_blog/Formulation_Development_Blog/post/Biop_harmaceutics_Classification_System_and_In-vitro_membrane_models/
[Accessed 26 April 2014].

Figure 38. Chapter: 4

<http://www.pharmacology.arizona.edu/images/faculty/davisfig2.gif> [Accessed 23 May 2014].



APPENDIX A

Table 1. Breakdown of provincial drug related crime trends for the past 5 years

(Provincial Government, Western Cape, South Africa-Modernisation programme, 2010)

Reported Cases						
Province	2003/2004	2004/2005	2005/2006	2006/2007	2007/2008	2008/2009
Eastern Cape	7,893	9,061	7,511	7,231	8,003	8,437
Free State	3,550	4,063	5,074	5,462	4,525	4,561
Gauteng Province	9,195	10,471	13,753	12,256	12,348	13,338
KwaZulu-Natal	13,599	19,290	23,206	26,228	24,100	23,819
Limpopo	1,706	1,786	1,977	2,178	3,198	3,316
Mpumalanga	1,314	1,714	1,794	2,068	1,770	1,642
North West Province	3,350	4,634	5,502	6,085	7,004	7,345
Northern Cape	2,142	2,550	2,085	2,114	2,201	1,933
Western Cape	19,940	30,432	34,788	41,067	45,985	52,781
RSA	62,689	84,001	95,690	104,689	109,134	117,172

Crime Ratio per 100 000 of the population						
Province	2003/2004	2004/2005	2005/2006	2006/2007	2007/2008	2008/2009
Eastern Cape	114.2	131.4	109.0	104.9	115.9	128.2
Free State	119.6	138.4	171.8	184.6	152.9	158.5
Gauteng Province	101.1	114.1	147.4	128.7	127.5	127.7
KwaZulu-Natal	139.6	197.2	235.7	264.3	240.7	235.7
Limpopo	32.0	33.6	37.0	40.6	59.2	62.9
Mpumalanga	37.8	49.7	51.7	59.0	50.1	45.7
North West Province	100.3	138.2	165.3	180.3	206.4	214.5
Northern Cape	200.8	238.0	193.3	193.1	199.7	171.7
Western Cape	443.2	666.6	749.4	864.8	950.1	1,003.1
RSA	135.1	180.3	204.1	220.9	228.1	240.7

Table 2. Summary of FAS prevalence in various U.S. and selected foreign studies by methodology (May et al., 2001)

Type and Location of Study	Years Covered	Rate of FAS per 1,000 births	Population	Source
Passive Method				
United States	1979-1992	0.20	General	CDC 1993
	1992	0.37	General	CDC 1995
	1993	0.67	General	CDC 1995
	1981-1986	0.60	African-American	Chavez et al. 1988
		0.08	Hispanic	Chavez et al. 1988
		2.90	American Indian	Chavez et al. 1988
		0.03	Asian	Chavez et al. 1988
		0.09	White	Chavez et al. 1988
Atlanta	1981-1989	0.10	General	CDC 1997
Alaska	1977-1992	0.20 - 0.30	Alaska, non-native	Egeland et al. 1998
		3.00 - 5.20	Alaska Native	Egeland et al. 1998
North Dakota	1991-1994	1.10 - 2.00	General	Burd et al. 1996
Clinic-Based Studies				
United States	Various studies (avg.)	1.90	Western World	Abel and Sokol 1987
	Various studies (avg.)	2.20	United States and Canada	Abel and Sokol 1987
	Various studies (avg.)	0.33	United States	Abel and Sokol 1991
United States and other countries	Various studies (avg.)	0.97	Western World	Abel 1995
	Various studies (avg.)	1.95	United States	Abel 1995
	Various studies (avg.)	2.29	African-American	Abel 1995
	Various studies (avg.)	0.26	White American	Abel 1995
Active Case Ascertainment				
United States	Various studies (avg.)	9.00	Plains Indian	May et al. in press

	1969 - 1982	1.40	Navajo	May et al. 1983
	1969-1982	2.00	Pueblo	May et al. 1983
	1969-1982	9.80	Southwestern Plains Indian	May et al. 1983
	1969-1982 (avg.)	1.80	Southwestern Indian	May et al. 1983
Washington State	1995-1997	3.10	1st grade students (one county)	Clarren et al. 2001
NOTE: avg. = average; CDC = Centers for Disease Control and Prevention; FAS = fetal alcohol syndrome.				



APPENDIX B

Table 1. Standard series of gallic acid was prepared for the measurement of polyphenols by marking 6 Eppendorf tubes A-F. The stock solution was diluted as follows to make a series of standards as described in the table below:

Tube	Gallic acid stock solution (μl)	10% EtOH (μl)	Concentration (mg/L)	Well number
A	0	1000	0	A1-A3
B	25	975	20	A4-A6
C	62.5	937.5	50	A7-A9
D	125	875	100	A10-A12
E	312	688	250	B1-3
F	625	375	500	B4-6

Table 2. Standard series of ascorbic acid was prepared for the FRAP assay by marking 6 Eppendorf tubes labelled A-F. The amount of standard stock solution and diluents were added to each tube, and the stock solution was diluted to make a series of standards as follows:

Tube	Ascorbic acid stock solution (μl)	dH₂O (μl)	Standard concentration (μM)	Well number
A	0	1000	0	A1-A3
B	50	950	50	A4-A6
C	100	900	100	A7-A9
D	200	800	200	A10-A12
E	500	500	500	B1-3
F	1000	0	1000	B4-6

Table 3. Standard series of Trolox was prepared for the ORAC assay by marking 6 Eppendorf tubes labelled A-F. The stock solution was diluted as follows to make a series of standards as described in the table below:

Tube	Standard concentration (μM)	Trolox stock solution (μl)	Phosphate Buffer (μl)	Well number
A	0	0	750	A1-A3
B	83	125	625	A4-A6
C	167	250	500	A7-A9
D	250	375	375	A10-A12
E	333	500	250	B1-3
F	417	625	125	B4-6

Table 4. Standard series of Trolox was prepared for the ABTS (TEAC) radical cation scavenging assay by marking 6 Eppendorf tubes A-F. The amount of standard stock solution and diluents was added to each tube as described in the table below. The stock solution was diluted as follows to make a series of standards as described in the table below:

Tube	Trolox standard (μl)	EtOH (μl)	Trolox conc. (μM)	Well number
A	0	1000	0	A1-A3
B	50	950	50	A4-A6
C	100	900	100	A7-A9
D	150	850	150	A10-A12
E	250	750	250	B1-3
F	500	500	500	B4-6

Table 5. Standard series of quercetin was prepared for the measurement of flavonols by marking 6 Eppendorf tubes labeled A-F. The amount of standard stock solution and diluents were added to each tube, and the stock solution was diluted to make a series of standards as follows:

Tube	Quercetin stock (μl)	95 % EtOH (μl)	Quercetin (mg/L)	Well Number
A	0	1000	0	A1-A3
B	75	925	5	A4-A6
C	125	875	10	A7-A9
D	250	750	20	A10-A12
E	500	500	40	B1-B3
F	1000	0	80	B4-B6

Table 6. Standard series of the catechin was prepared for the measurement of flavanols by marking 6 Eppendorf tubes labeled A-F. The amount of standard stock solution and diluents were added to each tube, and the stock solution was diluted to make a series of standards as follows:

Tube	Catechin stock (μl)	MeOH (μl)	Catechin (μM)	Catechin (mg/L)	Well Number
A	0	1000	0	0	A1-A3
B	5	995	5	1.36	A4-A6
C	10	990	10	2.72	A7-A9
D	25	975	25	6.8	A10-A12
E	50	950	50	13.6	B1-B3
F	100	900	100	27.2	B4-B6

Table 7. Plate layout for antioxidant assays (96-well plate)

	1	2	3	4	5	6	7	8	9	10	11	12
A	Blank_Ass Assay	Blank_Ass Assay	Blank_Ass Assay	Cal_0001 Assay 50 mg/L	Cal_0001 Assay 50 mg/L	Cal_0001 Assay 50 mg/L	Cal_0002 Assay 100 mg/L	Cal_0002 Assay 100 mg/L	Cal_0002 Assay 100 mg/L	Cal_0003 Assay 200 mg/L	Cal_0003 Assay 200 mg/L	Cal_0003 Assay 200 mg/L
B	Cal_0004 Assay 400 mg/L	Cal_0004 Assay 400 mg/L	Cal_0004 Assay 400 mg/L	Cal_0005 Assay 800 mg/L	Cal_0005 Assay 800 mg/L	Cal_0005 Assay 800 mg/L	Ctrl_0001 Assay	Ctrl_0001 Assay	Ctrl_0001 Assay	Ctrl_0002 Assay	Ctrl_0002 Assay	Ctrl_0002 Assay
C	Un_0001 Assay 1:1	Un_0001 Assay 1:1	Un_0001 Assay 1:1	Un_0002 Assay 1:1	Un_0002 Assay 1:1	Un_0002 Assay 1:1	Un_0003 Assay 1:1	Un_0003 Assay 1:1	Un_0003 Assay 1:1	Un_0004 Assay 1:1	Un_0004 Assay 1:1	Un_0004 Assay 1:1
D	Un_0005 Assay 1:1	Un_0005 Assay 1:1	Un_0005 Assay 1:1	Un_0006 Assay 1:1	Un_0006 Assay 1:1	Un_0006 Assay 1:1	Un_0007 Assay 1:1	Un_0007 Assay 1:1	Un_0007 Assay 1:1	Un_0008 Assay 1:1	Un_0008 Assay 1:1	Un_0008 Assay 1:1
E	Un_0009 Assay 1:1	Un_0009 Assay 1:1	Un_0009 Assay 1:1	Un_0010 Assay 1:1	Un_0010 Assay 1:1	Un_0010 Assay 1:1	Un_0011 Assay 1:1	Un_0011 Assay 1:1	Un_0011 Assay 1:1	Un_0012 Assay 1:1	Un_0012 Assay 1:1	Un_0012 Assay 1:1
F	Un_0013 Assay 1:1	Un_0013 Assay 1:1	Un_0013 Assay 1:1	Un_0014 Assay 1:1	Un_0014 Assay 1:1	Un_0014 Assay 1:1	Un_0015 Assay 1:1	Un_0015 Assay 1:1	Un_0015 Assay 1:1	Un_0016 Assay 1:1	Un_0016 Assay 1:1	Un_0016 Assay 1:1
G	Un_0017 Assay 1:1	Un_0017 Assay 1:1	Un_0017 Assay 1:1	Un_0018 Assay 1:1	Un_0018 Assay 1:1	Un_0018 Assay 1:1	Un_0019 Assay 1:1	Un_0019 Assay 1:1	Un_0019 Assay 1:1	Un_0020 Assay 1:1	Un_0020 Assay 1:1	Un_0020 Assay 1:1
H	Un_0021 Assay 1:1	Un_0021 Assay 1:1	Un_0021 Assay 1:1	Un_0022 Assay 1:1	Un_0022 Assay 1:1	Un_0022 Assay 1:1	Un_0023 Assay 1:1	Un_0023 Assay 1:1	Un_0023 Assay 1:1	Un_0024 Assay 1:1	Un_0024 Assay 1:1	Un_0024 Assay 1:1



APPENDIX C

Table 1. Effect of acute exposure to selected concentrations of EtOH on bEnd5 live cell numbers, using the Trypan blue assay at selected time intervals (mean±SEM; n=5).

		EtOH					
Time (hrs)/							
Compound							
(in mM)	24 hrs	48 hrs	72 hrs	96 hrs	120 hrs	144 hrs	
Ctrl	1.23±0.19	5.18±0.49	25.78±1.97	19.95±0.91	8.43±0.58	21.15±1.17	
25	0.97±0.16	10.83±0.76	19.65±0.85	13.24±0.66	4.82±0.55	13.13±1.03	
50	1.85±0.28	12.16±1.24	14.43±1.03	14.43±0.99	8.41±0.49	4.48±0.35	
100	1.78±0.22	4.68±0.45	16.56±1.14	14.25±1.05	7.36±0.48	3.67±0.48	
200	0.61±0.12	8.75±0.91	11.44±0.89	8.36±0.61	14.58±1.31	7.60±1.02	
400	0.73±0.11	0.45±0.09	1.23±0.17	0.43±0.094	0.00±0.00	0.40±0.09	

Table 2. Effect of acute exposure to selected concentrations of EtOH on bEnd5 mitochondrial activity, using the XTT assay at selected time intervals (mean±SEM; n=5).

EtOH						
Time (hrs)/ Compound (in mM)	24 hrs	48 hrs	72 hrs	96 hrs	120 hrs	144 hrs
Ctrl	100.00±0.00	100.00±0.00	100.00±0.00	100.00±0.00	100.00±0.00	100.00±0.00
25	111.00±6.57	79.43±3.31	98.86±5.65	84.64± 5.55	98.62±2.39	77.60±6.45
50	101.8 ±6.04	76.28±2.20	102.87±6.62	95.62±11.74	97.98±1.94	62.98±3.43
100	99.67±2.56	77.14±3.08	101.22±6.99	82.39± 5.46	96.85±1.72	76.66±7.48
200	96.48±7.36	70.76±1.52	94.71±5.86	83.48± 3.36	93.78±2.91	98.08±0.72
400	86.18±6.23	39.17±2.59	66.36±6.06	97.04± 3.20	97.56±2.15	96.85±3.79
600	74.14±8.94	48.30±4.08	76.94±3.68	80.59± 2.49	87.80±1.59	97.68±2.12
800	48.07±1.62	42.46±1.74	45.95±8.29	85.99± 4.57	94.23±1.01	94.18±4.25

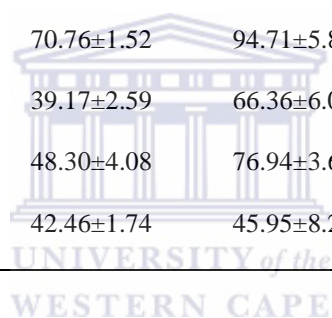


Table 3. Effect of chronic exposure to selected concentrations of EtOH on bEnd5 mitochondrial activity, using the XTT assay at selected time intervals (mean±SEM; n=5).

EtOH						
Time (hrs)/ Compound (in mM)	24 hrs	48 hrs	72 hrs	96 hrs	120 hrs	144 hrs
Ctrl	100.00±0.00	100.00±0.00	100.00±0.00	100.00±0.00	100.00±0.00	100.00±0.00
25	111.00±6.57	81.12±5.40	99.27±2.45	100.76±2.68	103.99±1.24	94.36±1.12
50	101.8 ±6.04	93.69±4.96	97.58±3.97	104.40±2.58	99.34±2.47	96.66±1.48
100	99.67±2.56	89.72±4.68	124.42±5.74	99.79±2.72	105.23±2.66	96.33±2.57
200	96.48±7.36	92.55±5.59	125.86±4.55	103.52±2.14	98.27±1.78	98.49±1.79
400	86.18±6.23	83.71±5.29	121.09±4.39	89.87±4.54	98.43±1.09	88.46±2.45
600	74.14±8.94	62.36±3.56	90.38±7.69	67.16±3.43	75.41±3.98	13.88±3.66
800	48.07±1.62	38.16±1.25	46.46±7.28	43.21±6.98	37.56±3.59	8.40±2.22

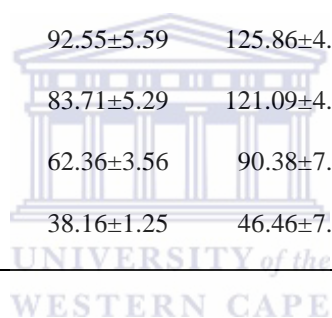


Table 4. Effect of acute exposure to selected concentrations of R_f on bEnd5 live cell numbers, using the Trypan blue assay at selected time intervals (mean \pm SEM; n=5).

Fermented				
Rooibos				
Time (hrs)/				
Compound	24 hrs	48 hrs	72 hrs	96 hrs
(%)				
Ctrl	5.20 \pm 0.73	18.00 \pm 0.81	28.83 \pm 2.10	38.59 \pm 1.65
0.0625	5.64 \pm 0.25	28.95 \pm 1.07	33.25 \pm 0.97	27.13 \pm 1.37
0.125	7.50 \pm 0.49	28.88 \pm 0.76	26.20 \pm 1.17	31.63 \pm 2.11
0.25	7.30 \pm 0.68	22.10 \pm 2.66	21.30 \pm 1.07	25.83 \pm 1.36
0.5	7.08 \pm 0.96	18.83 \pm 2.16	16.35 \pm 1.86	23.00 \pm 1.88
1	4.30 \pm 0.18	9.10 \pm 2.06	9.25 \pm 2.37	15.75 \pm 2.27

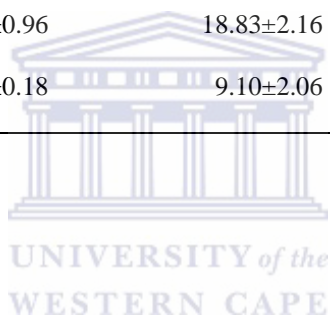


Table 5. Effect of acute exposure to selected concentrations of R_f on bEnd5 % live cell number, using the Trypan blue assay at selected time intervals (mean \pm SEM; n=5).

Fermented				
Rooibos				
Time (hrs)/				
Compound (%)	24 hrs	48 hrs	72 hrs	96 hrs
Ctrl	100.00 \pm 0.00	100.00 \pm 0.00	100.00 \pm 0.00	99.93 \pm 0.07
0.05	98.06 \pm 1.25	100.00 \pm 0.00	100.00 \pm 0.00	99.21 \pm 0.45
0.0625	100.00 \pm 0.00	100.00 \pm 0.00	100.00 \pm 0.00	99.70 \pm 0.22
0.125	100.00 \pm 0.00	100.00 \pm 0.00	99.41 \pm 0.41	100.00 \pm 0.00
0.25	100.00 \pm 0.00	100.00 \pm 0.00	100.00 \pm 0.00	97.53 \pm 1.13
0.5	99.41 \pm 0.40	100.00 \pm 0.00	100.00 \pm 0.00	99.81 \pm 0.13
1	98.27 \pm 0.88	100.00 \pm 0.00	100.00 \pm 0.00	100.00 \pm 0.00

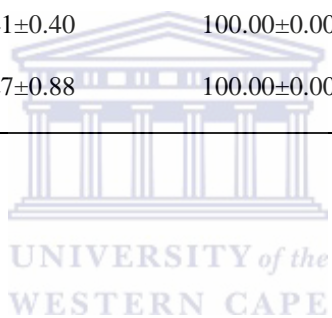


Table 6. Effect of acute exposure to selected R_f concentrations on bEnd5 mitochondrial activity, using the XTT assay at selected time intervals (mean \pm SEM; n=5).

Fermented				
Rooibos				
Time (hrs)/				
Compound (%)	24 hrs	48 hrs	72 hrs	96 hrs
Ctrl	100.00 \pm 0.00	100.00 \pm 0.00	100.00 \pm 0.00	100.00 \pm 0.00
0.003125	63.51 \pm 3.15	119.19 \pm 1.69	105.96 \pm 1.63	113.81 \pm 1.79
0.0625	70.58 \pm 6.87	114.13 \pm 3.85	96.89 \pm 2.63	119.88 \pm 3.99
0.0125	74.36 \pm 8.04	112.19 \pm 4.97	95.51 \pm 2.73	112.32 \pm 6.26
0.025	92.60 \pm 6.47	109.95 \pm 8.72	103.81 \pm 2.49	108.90 \pm 4.74
0.05	96.88 \pm 9.63	115.21 \pm 2.77	100.69 \pm 2.18	115.47 \pm 6.48
0.1	93.53 \pm 4.36	94.55 \pm 9.11	94.83 \pm 11.86	83.15 \pm 7.99

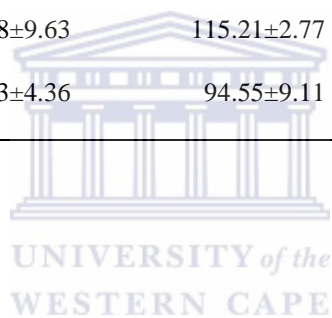


Table 7. Effect of chronic exposure to selected R_f concentrations on bEnd5

mitochondrial activity, using the XTT assay at selected time intervals (mean±SEM; n=5).

Fermented				
Rooibos				
Time (hrs)/				
Compound (%)	24 hrs	48 hrs	72 hrs	96 hrs
Ctrl	100.00±0.00	100.00± 0.00	100.00± 0.00	100.00±0.00
0.003125	63.51±3.51	81.97± 4.52	101.51± 3.86	97.95±8.66
0.0625	70.58±6.87	86.94± 2.56	105.61± 8.46	95.34±1.22
0.0125	74.36±8.04	110.02± 8.24	116.63±12.78	91.73±2.87
0.025	92.60±6.47	109.02±10.95	112.36±7.81	100.10±2.30
0.05	96.88±9.63	129.43±10.88	109.13±11.04	80.95±5.08
0.1	93.53±4.36	86.73± 5.28	94.83±11.86	79.33±7.91

Table 8A. Effect of acute combination treatments of selected EtOH concentrations with 0.05% R_f concentrations on bEnd5 mitochondrial activity, using the XTT assay at selected time intervals (mean±SEM; n=5).

Acute		
EtOH/0.05%R _f		
Time (hrs)/		
Compound(in mM)	24 hrs	48 hrs
Ctrl	100.00± 0.00	100.00±0.00
25	92.67±12.33	77.73±2.75
50	88.66±18.27	93.52±8.06
100	58.00±16.11	80.57±6.56



Table 8B. Effect of chronic combination treatments of selected EtOH concentrations with 0.05% R_f concentrations on bEnd5 mitochondrial activity, using the XTT assay at selected time intervals (mean±SEM; n=5).

Chronic		
EtOH/0.05% R_f		
Time (hrs)/		
Compound(in mM)	24 hrs	48 hrs
Ctrl	100.00± 0.00	100.00±0.00
25	92.66±12.32	110.98±5.54
50	88.67±18.27	92.05±8.83
100	58.00±16.11	79.54±5.73



Table 8C. Effect of acute combination treatments of selected EtOH concentrations with 0.1% R_f concentrations on bEnd5 mitochondrial activity, using the XTT assay at selected time intervals (mean±SEM; n=5).

Acute EtOH/0.1%		
R _f		
Time (hrs)/		
Compound(in mM)	24 hrs	48 hrs
Ctrl	100.00± 0.00	100.00± 0.00
25	81.33±11.77	75.71± 5.70
50	125.33±11.67	102.02±11.25
100	124.67±13.14	88.66± 8.26



Table 8D. Effect of chronic combination treatments of selected EtOH concentrations with 0.1% R_f concentrations on bEnd5 mitochondrial activity, using the XTT assay at selected time intervals (mean±SEM; n=5).

Chronic		
EtOH/0.1% R_f		
Time (hrs)/		
Compound(in mM)	24 hrs	48 hrs
Ctrl	100.00± 0.00	100.00± 0.00
25	81.33±11.75	51.52± 8.33
50	125.33±11.67	101.89±13.81
100	124.67±13.14	50.38± 3.69



APPENDIX D

Table 1. Effect of chronic exposure to selected concentrations of EtOH on bEnd5 cell monolayer permeability, using TEER measurements at selected time intervals (mean±SEM; n=4).

Time (hrs)/ Compound(in mM)	EtOH					
	24 hrs	48 hrs	72 hrs	96 hrs	120 hrs	144 hrs
Ctrl	13.93±0.70	16.20±0.62	14.95±0.21	14.05±0.21	13.90±0.15	13.88±0.24
25	19.43±0.54	17.03±0.55	15.30±0.37	13.41±0.40	13.50±0.38	14.48±0.49
50	18.28±0.73	15.53±0.28	18.33±0.46	12.79±0.28	14.45±0.41	13.35±0.29
100	16.30±0.59	14.93±0.26	15.65±0.49	13.66±0.27	13.74±0.44	14.20±0.47
200	16.70±0.71	15.68±0.66	12.85±0.40	14.35±0.21	12.70±0.31	13.58±0.43

Table 2. Effect of chronic exposure to selected concentrations of R_f on bEnd5 cell monolayer permeability, using TEER measurements at selected time intervals (mean±SEM; n=4).

		Fermented				
		Rooibos				
Time (hrs)/						
Compound (%)	24 hrs	48 hrs	72 hrs	96 hrs	120 hrs	144 hrs
Ctrl	15.03±0.90	13.46±0.77	17.74±0.57	17.73±0.54	12.67±0.37	13.07±0.47
0.0625 %	18.83±0.57	18.81±0.70	19.99±0.60	18.04±0.71	16.14±0.71	17.53±0.82
0.0125 %	17.90±0.75	18.34±0.41	21.21±0.48	18.85±0.34	19.50±0.26	20.25±0.76
0.025 %	21.81±0.67	19.44±0.56	22.76±0.45	17.11±0.71	20.24±0.37	16.95±0.86
0.05 %	22.29±0.44	18.18±0.66	23.13±0.38	16.12±0.41	21.48±0.35	18.60±1.23
0.1 %	20.36±0.73	20.22±0.40	25.22±0.36	16.20±0.40	23.44±0.33	15.10±0.68

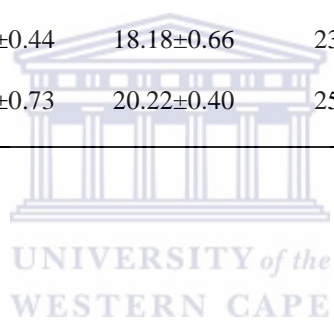


Table 3. Effect of chronic exposure to selected concentrations of EtOH in combination with 0.05% R_f on bEnd5 cell monolayer permeability, using TEER measurements at selected time intervals (mean±SEM; n=4).

		EtOH/0.05%					
		R _f					
Time (hrs)/		24 hrs	48 hrs	72 hrs	96 hrs	120 hrs	144 hrs
Compound	(in mM)						
Ctrl		7.93±1.09	19.25±0.76	23.25±0.56	17.78±0.74	14.20±0.38	12.23±0.85
25		19.98±0.93	18.20±0.73	22.23±0.34	17.35±0.47	13.16±0.35	8.06±0.68
50		23.48±0.68	18.90±2.36	22.00±0.48	14.15±0.31	15.03±0.57	12.03±0.81
100		22.73±0.48	20.60±0.69	20.25±0.58	15.90±0.50	15.76±0.45	12.48±0.82



Table 4. Effect of chronic exposure to selected concentrations of EtOH in combination with 0.1% R_f on bEnd5 cell monolayer permeability, using TEER measurements at selected time intervals (mean±SEM; n=4).

		EtOH/0.1% R _f					
Time (hrs)/		24 hrs	48 hrs	72 hrs	96 hrs	120 hrs	144 hrs
Compound	(in mM)						
Ctrl		7.93±1.09	19.25±0.76	23.25±0.56	17.78±0.74	14.20±0.38	12.23±0.85
25		24.10±0.31	17.43±0.98	18.85±0.29	16.08±0.49	14.68±0.42	17.80±0.69
50		26.33±0.81	19.35±0.64	19.70±0.34	16.98±0.47	13.98±0.26	10.43±0.88
100		25.5±0.64	21.93±0.57	18.73±0.39	17.33±0.35	13.78±0.39	11.68±0.89



APPENDIX E

1. Optimization of the TEER across the bEnd5 cell monolayer.

1.1 Effect of acute treatment with HC (500nM) on TEER in the absence or presence of serum.

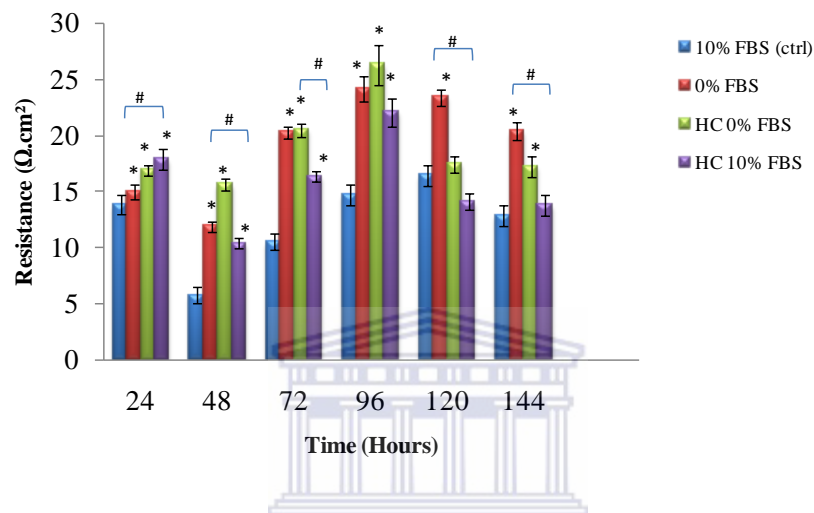


Figure 1. Effect of acute exposure to media supplemented with HC (500nM) in the absence (0%FBS/SFM) and presence (10% FBS) of serum at selected time intervals. The *, denoted statistically significant differences in TEER, between the experimental samples relative to the control (cells+ DMEM supplemented with 10% FBS) and the #, denoted statistically significant differences between media conditions. Data was represented as mean \pm SEM (n=4). Statistical significance was determined at $P < 0.05$ (See Methods).

It appears that between 24-96 hrs a gradual linear progression in TEER was observed across all conditions. At 24 greater TEER readings were reflected in the bEnd5 cell monolayers exposed to 0%FBS DMEM-F12 compared to the 10% supplemented DMEM-F12 (control) with statistical significance only reflected in HC - supplemented treatment conditions, relative to the control ($P < 0.0071$). At 48 hrs a decrease in resistance was observed across all treatment conditions from the 24

hr readings, with statistical significant differences observed, relative to the controls ($P<0.0001$). At 72 hrs the resistance readings began to plateau, reaching an optimal reading of approximately $25\Omega\cdot\text{cm}^2$ significantly greater than control readings ($P<0.0001$). At 96 hrs The SFM and SFM supplemented with HC (500nM) exhibited the significantly TEER readings across the bEnd5 cell monolayer, compared to the DMEM supplemented with 10% FBS (control) and the DMEM supplemented with serum (10% FBS) and HC (500nM) which only managed to reach $20\Omega\cdot\text{cm}^2$ and below ($P<0.0001$). At 120-144 hrs TEER readings begin to regress, however, the SFM and HC-supplemented SFM remained significantly high, relative to the control readings ($P<0.0023$).

1.2 Effect of chronic treatment with HC (500nM) on TEER in the absence or presence of serum.

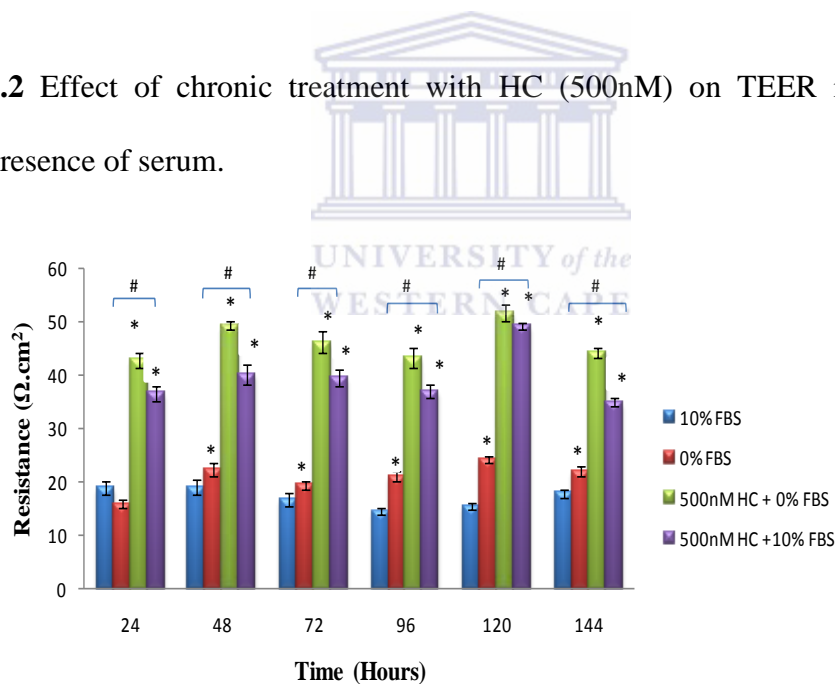


Figure 2. Effect of chronic exposure to media supplemented with HC (500nM) in the absence (0%FBS/SFM) and presence (10% FBS) of serum at selected time intervals. The *, denotes statistically significant differences in TEER, between the experimental samples, relative to the control (cells + DMEM supplemented with 10% FBS) and the #, denoted statistically significant differences between media conditions. Data was represented as mean \pm SEM (n=4). Statistical significance was determined at $P<0.05$ (See Methods).

A visible media effect on TEER across the bEnd5 monolayer was observed between the HC-supplemented media and the media unsupplemented with the HC, across the entire experimental timeframe. Significant increases in TEER occurred in both SFM and DMEM-F12, supplemented with 10% FBS and 500nM HC compared to media conditions unsupplemented with HC. However, between SFM/HC-supplemented media and 10%FBS/HC- supplemented media, 0% FBS/HC showed a significant increase in TEER in comparison to controls at 24 hrs ($P<0.0001$). At 48, 72, 96, 120 and 144 hrs a significant increase in TEER was observed across all treatment conditions compared to controls ($P<0.0001$). However, the greatest TEER readings were generated using the SFM media supplemented with 500nM HC which was consistent across the entire timeline, maintaining approximately $45\Omega\cdot\text{cm}^2$.



APPENDIX F

Cape Times Article

Date: 21 October 2014



Rooibos being processed at the Wuppelila station in the Cederberg.

CAPE TIMES - 21 Oct 2014

UNIVERSITY of the WESTERN CAPE

Cape's rooibos dops pioneer new way to make a drink

Almed Areeff

FANS of rooibos and honeybush tea can anticipate more bite with their antioxidants as the fynbos plants are being used to make alcoholic drinks.

Stellenbosch-based Rod Davies IP Holdings, which is owned by winemakers Aulbea and Kooperalieve Wijnbouwers Vereniging van Zuid-Afrika, announced yesterday that it had patented "a game-changing way" of producing alcoholic drinks using the fynbos.

"Our patent covers the making of all wine, beer and cider products by adding rooibos and honeybush plant material during manufacturing," director Trevor Strydom said.

"We have also trademarked the terms Rooibos Wine, Rooibos Beer and Rooibos Cider, among other marks."

He said the patent was set for an imminent grant. This would mean that no other South African entity could use the indigenous plants, or their derivatives, for alcoholic drink production according to the patented process, unless it was under licence from Rod Davies.

Strydom said the innovation was subject to a further 03 pending patent applications worldwide. "As soon as these are approved, the same restrictions will hold for international production and sales."

One of the aims of the new process of using fynbos was to

alleviate synthetic preservatives usually added to alcoholic drinks. "Scientific research indicates that powerful antioxidants found in these indigenous plant materials may assist in preserving them naturally."

Strydom said this preservation process could potentially mean an entirely new way of making wine and other drinks. "Equally importantly, we have found that the addition of rooibos and honeybush woods in a natural and toasted format improves and enhances aroma, taste and/or mouth feel of wine, beer and cider."

"Consumer feedback on products we have created according to our patented processes thus far has been overwhelmingly positive."

In July, rooibos tea secured geographic indicator status in the long-awaited economic partnership agreement between southern African nations and the EU.

Trade and Industry Minister Rob Davies said at the time: "It will be the rooibos tea manufacturers of South Africa which will have ownership of that particular name and that term will be applicable only to products that come from and are approved by us."

He called the designation significant, given the widespread popularity rooibos had acquired in Europe.

Last year, the SA Rooibos Brand South Africa in a positive and unique way." - Sapa

stop a bid by a French company, the Compagnie de Trucy, to trademark the name, fearing it could secure exclusive use.

Strydom said this designation was significant. "Rooibos and honeybush have historically been cultivated and produced exclusively in South Africa. Their characteristics and properties are the result of unique climate and geography."

"Europe has traditionally used geographical indication protection for products such as French Champagne or Greek Feta. Now we can do the same - our range of rooibos and honeybush alcoholic beverages are at the forefront of marketing Brand South Africa in a positive and unique way." - Sapa